Precipitation-Static Radio-Interference Phenomena Originating on Aircraft

Including Studies of High-Voltage Direct-Current Point Discharges and Accompanying Radio Disturbances, and of Electric and Magnetic Induction

By
E. C. STARR

Bulletin Series, No. 10

June 1939

A Cooperative Research Project by the
Engineering Experiment Station
and the United Air Lines Transport Corporation

Engineering Experiment Station
Oregon State System of Higher Education
Oregon State College

THE Oregon State Engineering Experiment Station was established by act of the Board of Regents of the College on May 4, 1927. It is the purpose of the Station to serve the state in a manner broadly outlined by the following policy:

(1) To stimulate and elevate engineering education by developing the research spirit in faculty and students.

(2) To serve the industries, utilities, professional engineers, public departments, and engineering teachers by making investigations of interest to them.

(3) To publish and distribute by bulletins, circulars, and technical articles in periodicals the results of such studies, surveys, tests, investigations, and researches as will be of greatest benefit to the people of Oregon, and particularly to the state's industries, utilities, and professional engineers.

To make available the results of the investigations conducted by the Station three types of publications are issued. These are:

(1) *Bulletins* covering original investigations.

(2) *Circulars* giving compilations of useful data.

(3) *Reprints* giving more general distribution to scientific papers or reports previously published elsewhere, as for example, in the proceedings of professional societies.

Single copies of publications are sent free on request to residents of Oregon, to libraries, and to other experiment stations exchanging publications. As long as available, additional copies, or copies to others are sent at prices covering cost of printing. The price of this bulletin is 75 cents.

For copies of publications or for other information address

Oregon State Engineering Experiment Station,

Corvallis, Oregon

Precipitation-Static Radio-Interference Phenomena Originating on Aircraft

Including Studies of High-Voltage Direct-Current Point Discharges and Accompanying Radio Disturbances, and of Electric and Magnetic Induction

By

E. C. STARR,
Associate Professor of Electrical Engineering

Bulletin Series, No. 10

June 1939

A Cooperative Research Project by the
Engineering Experiment Station
and the United Air Lines Transport Corporation

Engineering Experiment Station
Oregon State System of Higher Education
Oregon State College

TABLE OF CONTENTS

TABLE OF CONTENTS—*Continued*

Page

FIGURES

TABLE OF CONTENTS—*Continued*

Precipitation-Static Radio-Interference Originating on Aircraft

By

E. C. STARR,
Associate Professor of Electrical Engineering

I. INTRODUCTORY SUMMARY

A dependable system of moderate-range communication is essential to the success of modern, scheduled aerial transportation. The radio telephone, utilizing controlled electromagnetic radiations for the transmission of intelligence, is highly successful under most flight conditions and all airplanes used in regular passenger transportation in the United States are equipped with two-way radio telephone apparatus. This equipment is employed not only for voice communication between the airplanes and ground stations, but also as an aid to navigation when visibility is poor and "contact" flight is not feasible. The navigational aids are of extreme importance when flights are to be made in heavy weather and the compasses, altimeters, air speed indicators, and chronometers alone are not adequate for the positive determination of location or the course of flight.

The radio aids fall in three general classes. Successful voice communication with ground observers enables the pilot to allow for approximate wind errors and to know the limits of visibility from the ground. The radio compass, utilizing the well-known directional properties of the loop antenna, can be used as a "homing" device or to check location by triangulation. The radio range, or beam, can be employed as a continuous course marker, making possible the flight of an exact course between two terminals.

These aids are successful in their operation during normal weather conditions but at times when they are most needed, during heavy weather with low visibility, they may become useless. Flight research has shown that certain precipitation conditions accompanying atmospheric storms cause large, high-speed, all-metal airplanes to become charged electrically and subsequently to discharge to the surrounding atmosphere, producing local radio disturbances of severe intensity. It has been found that these charges are accumulated through a number of different mechanisms, and that the discharge is a process of maintaining the potential of the airplane at a value not greatly different from that of its surroundings.

Tests in flight and on the ground have indicated that these discharges are the same as those which can be created by high, direct voltages impressed upon point electrodes. An extensive study was made of the nature of these discharges and of means available for controlling them.

The nature of the normal-frequency radio interference accompanying point discharges was investigated both experimentally and analytically, and good correlation was obtained between the experimental and predicted results.

The shielded-loop radio receiving antenna was found to exhibit, under

most precipitation-static conditions, a notable property of rejecting interference and accepting desired signals. This characteristic was investigated experimentally and mathematically and again the experimental and theoretical performances checked closely.

It is suggested that a systematic electrical discharging arrangement can be installed on airplanes to control effectively the accumulated charges and to reduce the radio interference resulting from their dissipation to the atmosphere. In a limited form, such discharging equipment has been tested in flight and has been found to give promise of a high degree of success.

As a result of some of the work reported in this bulletin, one of our major airlines has installed on all of its transport airplanes a simple trailing-wire discharging device. This trailing wire is so mounted that it can be projected into its normal position when severe static conditions develop and can be replaced economically when destroyed by contact with the ground during landing operations. Although this device is very simple and somewhat limited in its ability to discharge the airplane, it has, nevertheless, given a good account of itself in a number of different emergencies.

II. ACKNOWLEDGMENTS

An extensive investigation such as that reported in the following pages is made possible only by the cooperation of a number of individuals and agencies. This work was undertaken at the suggestion of, and in cooperation with the Communications Department of the United Air Lines Transport Corporation. All of the flight data, and also the ground data involving the use of an airplane, were taken by means of a modern transport airplane and flight personnel furnished by United Air Lines. Mr. H. M. Hucke, formerly Chief Communications Engineer for the above corporation, who was in direct charge of the flight tests, made it possible to obtain the well-correlated data that were taken during the storm-static flights.

Fundamental work on the nature of point discharges and the accompanying radio interference was carried on in the electrical engineering laboratories of Oregon State College. The experimental and mathematical results obtained were largely due to the tireless cooperation of two graduate students, Mr. Hendrick J. Oorthuys and Mr. William J. Walsh, Jr.

The financial assistance of the Engineering Experiment Station of Oregon State College, and the encouragement of Professor F. O. McMillan, Head of the Department of Electrical Engineering, are gratefully acknowledged. The work carried on locally was under the general supervision of S. H. Graf, Director of Engineering Research, who edited this report and prepared the material for publication. Charts and graphs were drawn by E. H. Moore, senior in mechanical engineering.

The experimental and theoretical material presented was completed in June, 1938. Funds were not available for publication at that time and during the interim further work was carried on to study the instantaneous character of the point discharge currents. This resulted in cathode-ray oscillograms, making possible a more detailed analysis of the interference phenomena.

III. THE RADIO COMPASS

In common with the magnetic and gyroscopic compasses, the radio compass alone is not adequate for successful instrument, or "blind," flying. When it is used as a "homing" device, the nose of the plane will be maintained in such a position as constantly to point toward the radio transmitter. In the presence of a cross wind, however, a rather devious route may be flown, resulting in the airplane arriving at its destination in a direction different from normal. If the magnitude of the cross wind is known, the resultant drift can be compensated and the plane will remain on its normal course. An off-course condition of serious character may arise due to unreported heavy cross winds.

A method has been developed for the combined use of the magnetic or gyro and radio compasses. This method is illustrated in Figure 1. The course is to be flown in such a manner as to maintain a constant angular relationship between the radio compass and the magnetic or gyro compass. This angle is set when the airplane is in some known position

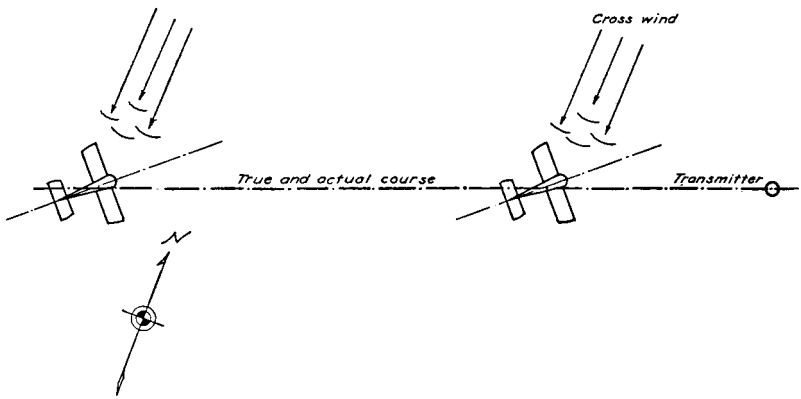

Figure 1. Blind or instrument flying with combined radio and gyro or magnetic compasses.

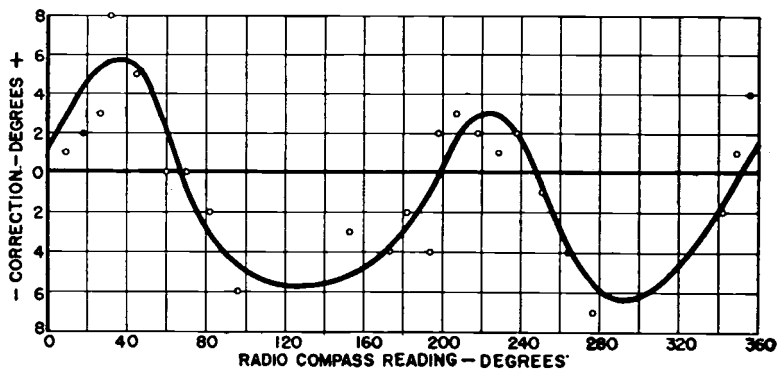

Figure 2. Radio compass calibration on Portland Range at Washougal, Washington.

on the course and held constant throughout the flight. It will be observed that if the actual course of flight deviates to right or left of the true course, the difference angle between the radio and gyro or magnetic compass will change, indicating an off-course condition. This method can be used to best advantage only when the radio compass is being used as a "homing" device; that is, when the airplane is flying directly toward the radio transmitter.

If two or more radio transmitters, located at some distance apart, can be received on the radio compass, it is possible by triangulation to locate the position of the receiver with a fair degree of accuracy. Since the airplane is changing its position rapidly, however, such observations must be taken in rapid succession if they are to give satisfactory results.

Due to reflections from the wings and fuselage of metal airplanes, the radio compass requires a calibration chart showing the errors introduced when receiving from different directions with respect to the axis of the airplane. Such a calibration curve is shown in Figure 2. It is indicated that maximum corrections of the order of six degrees are necessary in certain positions and also that the farthest experimental point from the mean curve is approximately two degrees. This would tend to indicate that the radio compass may be depended on to give indications having maximum error, when corrected for direction with respect to the axis of the airplane, of approximately two degrees.

Several modifications of the radio compass are now available and a few of them are quite highly developed. The simplest compass makes use of the well-known directional properties of the loop antenna. When a bearing is being taken, the loop is so oriented as to give a null reading, this position being considerably more accurate than that for a reading of maximum signal intensity.

IV. THE RADIO RANGE

In the previous section it was indicated that it is possible to employ the combined magnetic or gyro and radio compasses to fly a true course regardless of cross winds. The technique involved, however, is not simple, and the desired radio transmitters upon which "homing" directions can be taken, frequently are not available.

A radio range, or beacon, system has been developed, which to a large extent eliminates these objections. The type of low-frequency range that at present is installed, or is superseding others, on the major

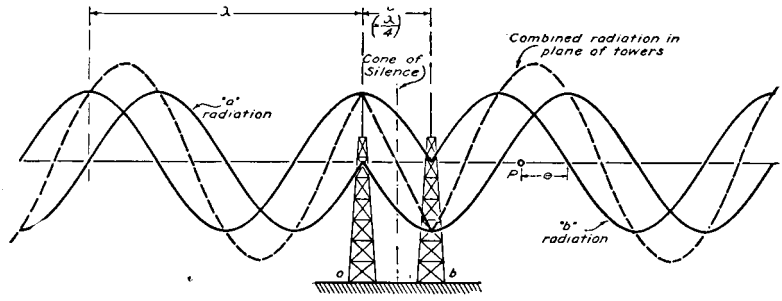

Figure 3. Antenna elevation in plane of towers.

airways of the United States employs vertical-tower radiators so combined into an antenna system as to produce definite directional patterns.

With reference to the diagram of Figure 3, if two vertical radiators, a and b, are spaced apart a distance, d, and driven in phase opposition, a useful radiation pattern is obtained. In the illustration the towers are spaced one-quarter wave length and the maximum resultant radiation is, therefore, 41 per cent greater than that resulting from either radiator independently. It is shown also that at a point midway between the two towers there is zero radiation, and since vertical towers propagate a vertically polarized wave, the area immediately above the pair of towers is devoid of radiation. This point, therefore, may serve as a marker and is known as the "cone of silence."

It will be observed that the waves combine as they do because of two factors. They are, first, the separation between the radiators, and second, the phase difference between the driving voltages of the two radiators. For the condition shown in Figure 3, it is obvious that if both waves were traveling in a direction normal to the plane of the towers, they would have equal distances to travel in arriving at any given point, and hence, would cancel each other completely. The result would be a line of zero radiation intensity.

The field pattern obtained by such a pair of radiators is illustrated by Figure 4. In this case the point, p, is any point on the horizon, the locus of which is a circle with center at the radiators. The radius vector of each of the curves is proportional to the ideal field strength radiated by the antenna in the direction of that vector. It will be noted that for tower separations closer than approximately one-quarter wave length, the field patterns are essentially circular. In every case the radiations in the 90-degree and 270-degree directions are of zero intensity.

If the two radiators are not driven in exact phase opposition, a field pattern such as that of Figure 5 may be obtained. In this case the tower separation is one-quarter wave length and the driving phase difference is 150 degrees. Equal currents are supplied to both radiators. It will be observed that the radiation in the zero-degree direction is now much stronger than that in the 180-degree direction and the axes of zero field strength have been shifted from their former 90-degree and 270-degree positions. As a means of comparison, the dashed circle indicates the relative field strength of one radiator alone drawing the same current as is supplied to each radiator in the combined pattern. These directional patterns are readily analyzed and their equations are developed in Appendix I. It should be noted that these equations apply exactly only when the radiators are operating on a flat, perfectly conducting plane. The presence of buildings, towers, and mountains tends to alter considerably the patterns obtained.

In the United States Department of Commerce Type TL radio range, the above patterns are combined in pairs to obtain the desired courses. Four radiators are erected on the corners of a rectangle in such a position that their normal patterns lie at 90 degrees with respect to each other. The resultant field pattern is that illustrated by Figure 6. In this case, diagonally opposite towers are driven in phase opposition and the driving energy is alternately switched from one pair of radiators to the other. The radio carrier wave is modulated at a frequency of the order of 1,000 cycles per second, and is so keyed ordinarily that one pair of towers radiates an "A" signal and the other radiates an interlocking "N." An

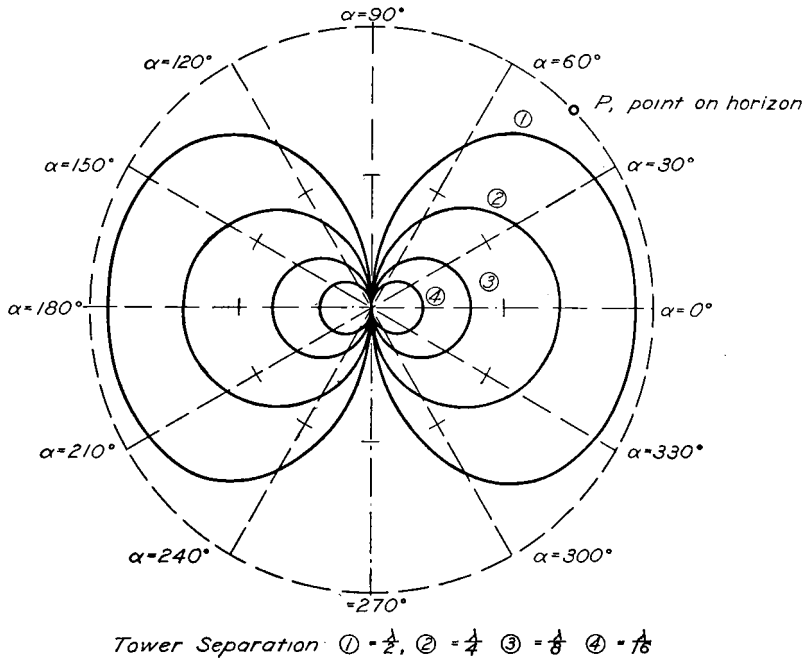

Figure 4. Relative field strength; two-tower, phase-opposition radiators.

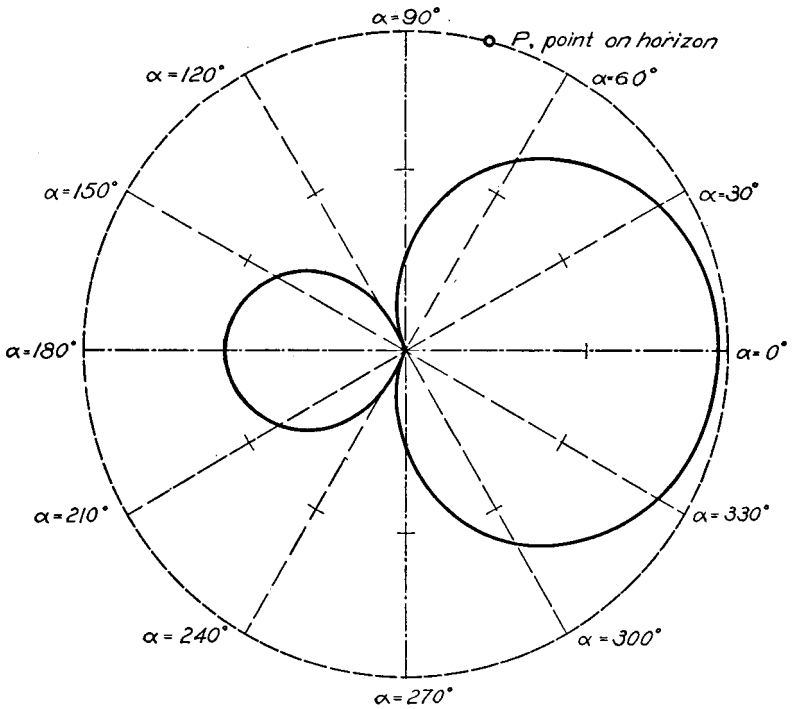

Figure 5. Relative field strength; two-tower, equal-current radiators.

airplane, then, in position 1 would receive a strong signal from the radiators transmitting the "N," and no signal at all from the other pair of radiators. If this airplane were moved around to position 2, it would receive substantially the same signal from the "N" radiators as in the first position and also weak signals from the "A" radiators. When in position 3, the plane would be receiving signals of equal intensity from both sets of radiators. Since the dot and dash of the "A" are interlocked with the dash and dot of "N," the signal received in this position would be essentially a continuous note of modulation frequency. This is the

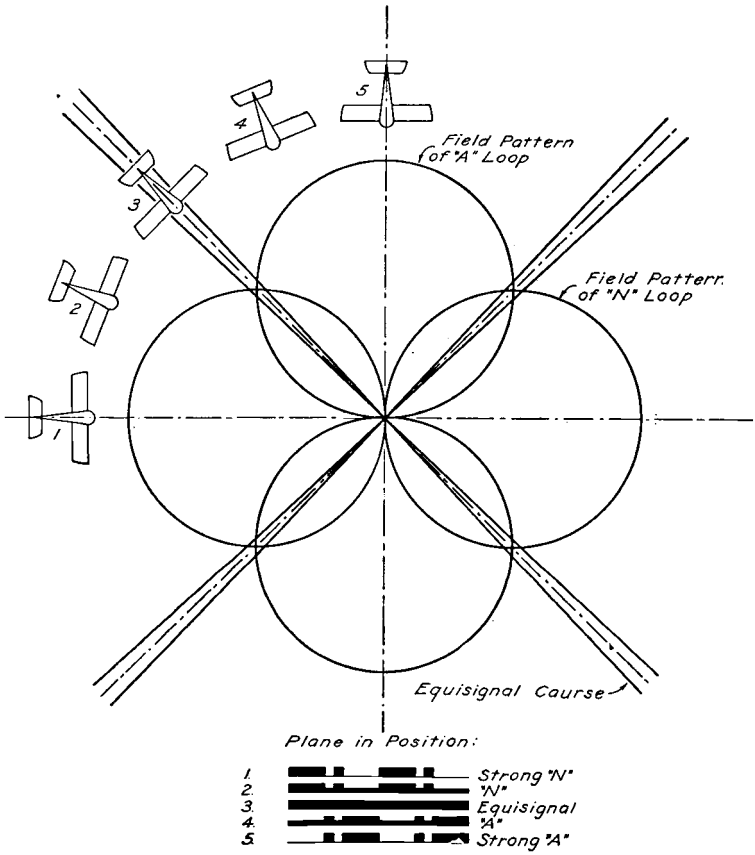

Figure 6. Simple aural radio range.

on-course signal and is easily differentiated from the off-course, predominant "N" on one side changing to the "A" on the other side.

It is obvious that if simple equal-current, phase-opposition radiators were employed for such a radio-range transmitter, the courses would lie at 90 degrees with respect to each other and would, in general, be useful

only in one direction. By driving the opposite towers in some phase difference other than 180 degrees, as indicated in Figure 6, however, and also by changing the signal strength in certain radiators by insertion of resistances, it is possible to shift or bend these equisignal courses to any desired position. In order to make possible the accurate final adjustment of the course position, the energy is usually fed from the transmitter to the radiators through a movable-primary transformer known as a goniometer. This device enables the proper distribution of energy between the two sets of radiators to obtain the exact course position desired.

In the new simultaneous type range a fifth radiator is employed, making it possible simultaneously to transmit the range signals together with weather information. In the elementary type it is necessary to withhold range signals during periods of transmission of weather information.

The above type of radio range is extremely successful over flat terrain and gives a beam width of from 100 to 200 yards per mile of distance from the radiators. Under normal conditions, the range signals with the present amount of power are intelligible over distances of at least 100 miles. The equisignal courses, however, tend at times to bend in mountainous terrain due to reflections and they may even break up into multiple courses. This feature is, of course, highly undesirable, and the major course must be flown enough times in good visibility to enable the differentiation between the main and false courses. Certain weather conditions have been known also to produce perceptible shifts in the range courses.

The Civil Aeronautics Authority is at present carrying on extensive experimental work with ultrahigh-frequency radio ranges. These signals cover line-of-sight distances only but are found to remain very true and to be reasonably free from most of the interference encountered by the low-frequency signals. Valuable developments may be expected in this field.

It is evident that a satisfactorily operating radio range would enable the accurate flight of a given course under conditions of zero visibility. The "cone of silence" markers, together with the low-power localizers, enable the flight personnel to determine their exact position as well as course of flight. The only other equipment then necessary to make complete instrument flying successful is an adequate landing system. These devices are now being developed and will be in general use within the next few years.

V. RADIO INTERFERENCE

In heavy weather, particularly in violent squalls and in air-mass fronts, it is especially important that the airways radio ranges and marker beacons be operative. Under these conditions local cross winds of severe intensity may tend to drive the airplane far from its course unless the range signals can be received satisfactorily. Unfortunately, such weather conditions are usually accompanied by some form of precipitation. There may be snow, rain, dust, or frost crystals in the air. Experience has shown that an airplane, particularly of the all-metal variety, flying into such precipitation at speeds considerably above 100 miles per hour, in general has all but its ultrahigh-frequency radio reception very seriously

impaired. The interference may appear in any one of, or in a combination of, several different forms.

Since the early days of radio communication it has been known that electrical discharges from conductors at either low or high voltage will produce local interference in receiving equipment. The making or breaking of a low-voltage circuit will produce a shock disturbance in the receiver. Low-voltage vibrating-type interruptors and machine commutators may produce such a rapid succession of these shock disturbances as to create a musical note in the receiver. High-voltage corona discharges on conductors and insulators are known to create serious radio interference (14).* On the airplane the high-voltage ignition system of the engine must be shielded very carefully to avoid the introduction of heavy shock interference into the receiving equipment.

In many of the above types of interference, the actual disturbance occupies a relatively small part of the total time. Even though the disturbing impulses may occur in rapid succession, their individual duration is so small as to leave relatively long intervals during which no disturbance occurs. In the case of vibrating interruptors, commutators, and alternating-current corona discharges, the undisturbed interval may be of considerable magnitude relative to the disturbed interval. In such cases, it is possible to build into the receiving equipment a very rapid automatic volume control that will tend to bias the receiver to zero gain during the interval for which the disturbance level is higher than that of the carrier wave of the desired signal (4). The disturbance is thereby caused essentially "to commit suicide" within the receiving set, in that the set is effectively turned off at the moment a noise impulse arrives and is turned back on again during intervals between successive noise impulses. The desired signal, therefore, comes through in an intelligible form.

Some of the radio interference created by an airplane flying at high speed into an area of precipitation is of such a type as to be susceptible to improvement by noise-suppressor circuits. When the airplane is in a light snow of relatively large individual flakes, the interference created is generally of a typical low-frequency vibrator type. Such interference could be removed by noise-suppressor circuits. When the flight is through most forms of precipitation of normal density, however, the interference created is of such a continuous character that no noise-suppressor circuit at present available has any beneficial effect. The interference ranges in nature from a harsh, rasping sound in the headphones to a varying, high-pitched musical note. The intensity frequently becomes so high as to make necessary the reduction of receiver gain to a point where the normal radio range signals, in the absence of interference, could be read only a very short distance from the transmitter.

Such storm-static conditions may exist for only brief periods during the passage through a precipitation area or, in the event of flight along an air-mass front, they may exist for a matter of thirty minutes or more. Under such conditions, the normal-frequency radio range cannot be read, and no reception of voice communication from the ground or other airplanes is possible. The flight personnel must, therefore, resort to dead reckoning to maintain the course at a time when the radio navigational aids are most essential.

*Numbers in parentheses refer to Bibliography.

VI. PRECIPITATION-STATIC FLIGHT RESEARCH

As airplanes became larger and speeds became higher, the precipitation-static interference problem became more acute. A number of accidents were attributable directly to airplanes being off-course due to their having lost the radio range under storm conditions. Having then encountered unreported squalls for which no correction could be made, they were driven unknowingly into dangerous terrain. The hazard was recognized by pilots as well as by administrative personnel and efforts were started to attempt to solve the problem. At first it was thought that the interference was due to charged particles of precipitation impinging upon the exposed radio antennas. In an effort to eliminate this difficulty, the antenna conductors were covered with rubber insulation, but no improvement was obtained.

It was reported by a number of pilots that under certain cold, dry-snow and frost-crystal conditions the airplane windshields had been seen to glow with a brush discharge. At times these brushes were reported to become so severe as to give the appearance of the windshield sparking over completely. Under these same conditions, the rubber deicers on the leading edges of the airplane wings were observed to glow with brush discharges, and at times to appear practically to spark completely across. The tips of the propellers were observed to glow at times with a typical St. Elmo's Fire.

These reports definitely established the existence of an electrical charging mechanism that was causing insulated areas on the airplane to attain very high potentials with respect to the ship itself. If that were the case, it was reasonable to assume that by the same mechanism the entire airplane was being charged to potentials considerably above that of the surrounding atmosphere. It was further evident, since the insulated surfaces, such as windshields and rubber deicers, were being charged to potentials considerably above those of the airplane proper, that the potential of the ship was being held down by some form of discharge mechanism. In other words, it appeared that the windshields and deicers were discharging to the ship, adding to the charge it was receiving by similar action, and the whole was discharging to the atmosphere. If such were the case, at least one source of the observed radio interference was the direct-current brush, or corona, discharge from sharp extremities of the airplane to the atmosphere.

Recognizing this possibility, the United Air Lines Transport Corporation led a cooperative, systematic study of the problem. A regular ten-passenger, two-motor Boeing Type 247-D transport airplane was withdrawn from passenger service and made available as a research ship. A number of the seats were removed and a test bench for scientific instruments was installed in their place. A partial view of the arrangement is shown in Figure 7.

The exterior of the plane was equipped with a number of insulated charge- and discharge-measuring electrodes. Those that gave the most interesting results were as follows:

1. A short rod projecting from the side of the fuselage directly behind the left propeller tips.
2. A sphere supported below the fuselage and behind the pitot stub.
3. A 30-inch pointed rod projecting from the nose of the plane ahead into undisturbed air.

4. An insulated plate in the form of an annular disk, conforming to the streamlined shape of the nose of the plane.
5. Three pointed rods, each approximately 12 inches long, projecting from each wing tip.

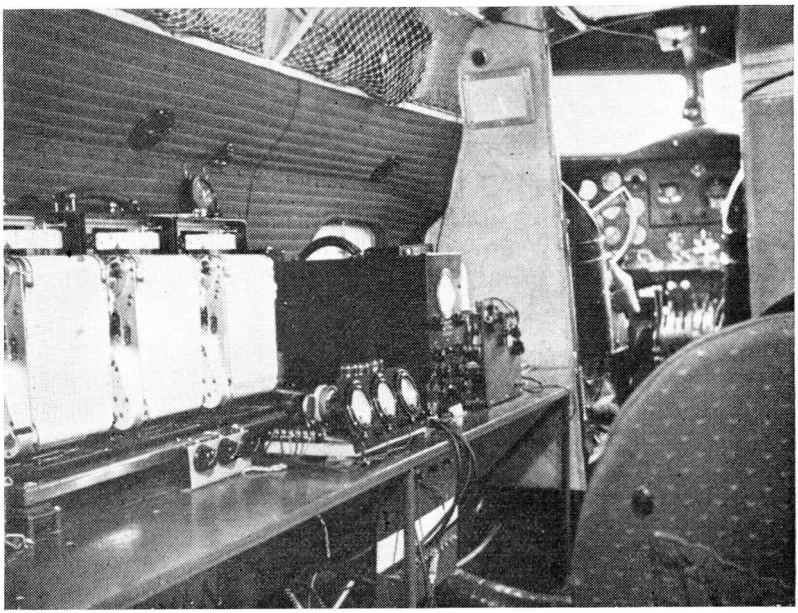

Figure 7. Interior view of precipitation-static research airplane showing synchronized graphic recording milliammeters and current amplifiers.

6. A 30-inch pointed retractable rod extending rearward from the tail of the ship.

The nose electrode and nose plate, wing-tip electrodes, and tail electrode are illustrated in Figures 8, 9, and 10. Each of the various electrodes was well insulated from the airplane and was connected through conductors to a terminal board beneath the test bench inside the cabin.

The instruments used in determining the currents of charge and discharge, and the polarity and character of these qualities were as follows:

1. Two highly sensitive vacuum-tube electrometers.
2. A cathode-ray oscillograph.
3. Three synchronized graphic-recording milliammeters, driven by a three-element vacuum-tube ammeter.
4. A standard air-transport beacon receiver.
5. A special Bell Telephone Laboratories receiver equipped with noise-suppressing circuit.
6. Various microammeters and auxiliary equipment.

The graphic recording instruments from which the most orderly data were obtained, together with their driving vacuum-tube ammeter, are shown in Figure 7.

The airplane was also equipped with an intercommunication telephone system that could be connected to the output of a radio receiving set being driven by any one of the following antennas:

1. The standard "Belly V" beacon receiver antenna.
2. The short-wave transmitting antenna.
3. A shielded loop projecting beneath the fuselage of the plane and located approximately on a line between the two engines.
4. A shielded loop in a streamlined housing above the nose of the airplane.
5. A diagonal antenna extending from the end of horizontal fin to a position approximately midway of the fuselage of the ship.
6. An interchangeable shielded loop or crossed dipole projecting forward from the nose of the ship.

Neither of the last-named antennas could be employed at the time the nose electrode and nose plate were in use. Most of these antennas are illustrated in Figures 8 and 19. For a time a straight-wire antenna enclosed in a nonconducting tube coated with a high-resistance conducting compound was installed beneath and parallel to the fuselage of the airplane.

In the early work an attempt was made to observe the charge and discharge currents on indicating instruments and to correlate these currents with the radio interference observed on the different antennas. It was soon learned, however, that the conditions change so rapidly that it was not possible to take notes fast enough to obtain an accurate record.

Before many tests had been made it was observed that all of the wire antennas gave approximately similar results. The one exception was the antenna extending toward the rear of the ship and this one was found to have a consistently higher noise-pick-up property than the others. It was also observed that the shielded-loop antennas, in agreement with previous tests, gave a noticeably higher signal-to-noise-pick-up ratio than any of the wire antennas.

Since the standard "Belly V" beacon receiver antenna gave results essentially as good as any of the wire antennas, it was used as the comparison standard throughout most of the tests. It was found that the interference picked up by this antenna became severe as soon as any of the pointed electrodes began to pass an appreciable current. When the electrode currents exceeded the order of 5 to 15 microamperes, the interference in the "Belly V" became so intense as to make impossible the reception of radio range signals even when relatively near the range transmitter.

The discharge interference picked up by the shielded-loop antennas was noticeably much less than that picked up by the "Belly V," but when the electrode currents approached orders of magnitude of 50 microamperes or more, the loop interference became excessive.

VII. ELECTRIC CHARGE AND DISCHARGE RECORDS

In order to determine something of the mechanism of the airplane charge and discharge phenomena, the graphic-recording milliammeters were so connected as to obtain simultaneous records of three currents. For some of the tests, the nose plate and nose and tail electrodes were used, and for other tests the wing-tip and tail electrodes were employed.

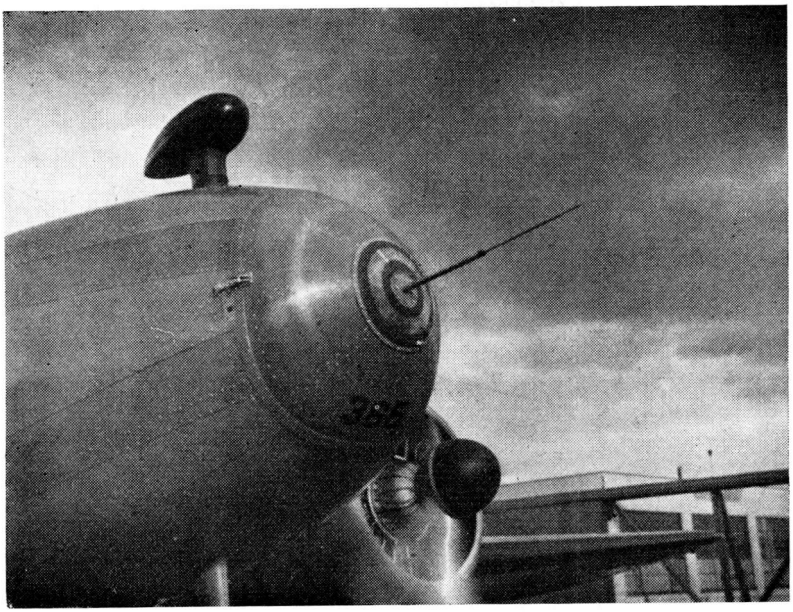

Figure 8. Nose electrode and nose plate installed on Boeing Type 247-D airplane for precipitation-static research.

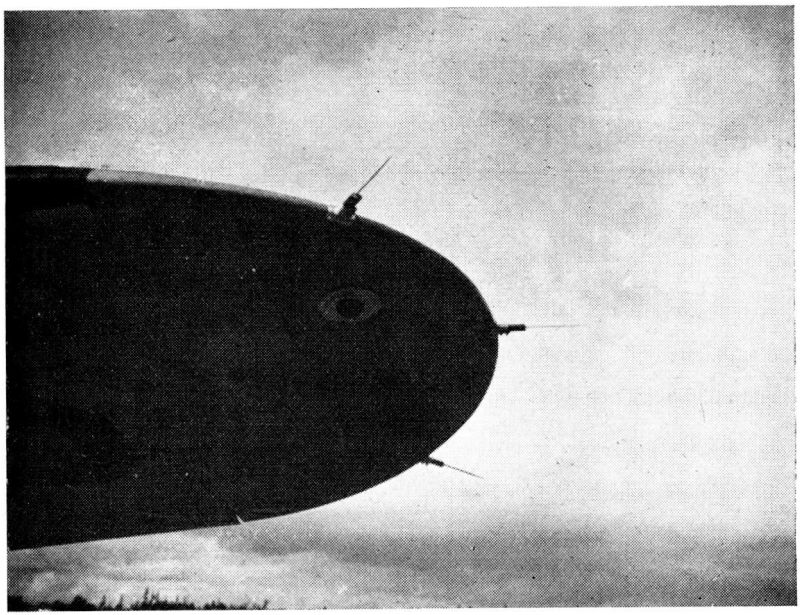

Figure 9. Left wing-tip electrodes installed on Boeing Type 247-D airplane for precipitation static research.

A great number of records were obtained by flights in different types of precipitation in various cloud formations, and examples of these records are given in Figures 11 to 16, inclusive. The record of Figure 11 is low in intensity, but is typical of those obtained under dry-snow con-

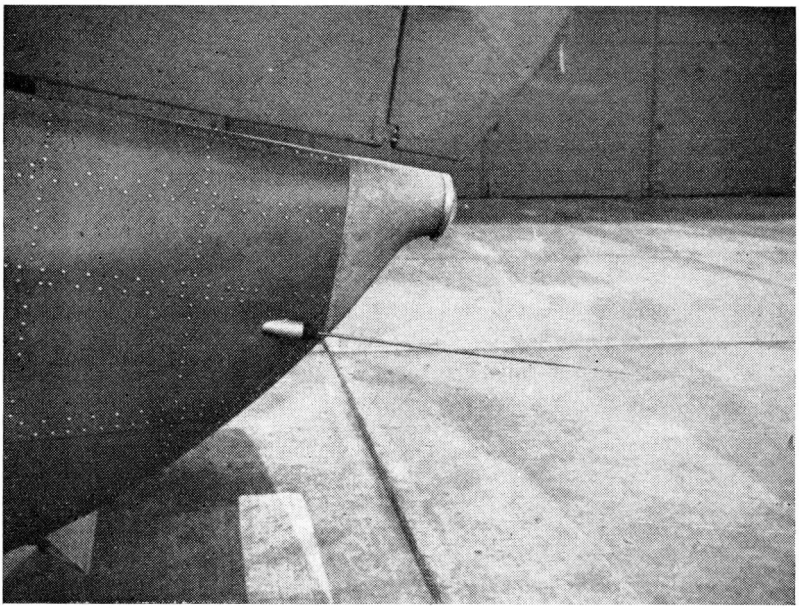

Figure 10. Retractable, pointed tail electrode installed on Boeing Type 247-D airplane for precipitation-static research.

ditions. It is indicated that the nose plate charged negatively, whereas the nose and tail pointed electrodes discharged positively; that is, in the case of the nose-plate record, the airplane was positive with respect to the plate, while in the case of the nose and tail electrodes, the ship was negative with respect to the points. Since no appreciable ionization could be taking place from the nose plate, it was obvious that this surface was charged negatively by the precipitation in which the airplane was flying. The points, however, since they would readily admit of ionization, were discharging this negative electricity into the atmosphere. This was a typical mechanism frequently observed in relatively stable dry-snow and frost-crystal areas.

A somewhat similar record in Figure 12, giving only the nose and tail electrode currents, shows the airplane discharging negative electricity to the atmosphere. In this case the airplane was in a condition of moderate snow that was not particularly dry.

An interesting condition is indicated by the record in Figure 13. The airplane was flying in moderate snow and then suddenly entered a region of heavy snow toward the center of a cumulus cloud. The tail electrode began discharging negative electricity rather heavily and the nose elec-

trode inverted its polarity, indicating that negative electricity was flowing from the region ahead of the ship, through the longitudinal conductors, and out the tail of the airplane. This condition would indicate the presence of a high electrical voltage gradient within the cloud. It will be observed that the airplane very suddenly emerged from that region into one of reversed gradient, that is, the nose electrode was in a positive region and the tail electrode in a relatively negative region. Another slight reversal followed this condition and then the airplane settled down to a discharge of negative electricity from both nose and tail electrodes. These rapidly changing gradient conditions were experienced frequently in all of the work, particularly in cumulus or heat clouds. The radio interference accompanying high cloud-gradient conditions was always of such a character as to give the effect in the head phones of running through the entire musical scale. In the background there usually would be an additional harsh, rasping type of interference.

A typical case of the airplane discharging heavily from all electrodes on which measurements were being taken is recorded in Figure 14. The very consistent character of the negative-electricity discharge from both wing tips and from tail electrode is shown. It will be noted that the

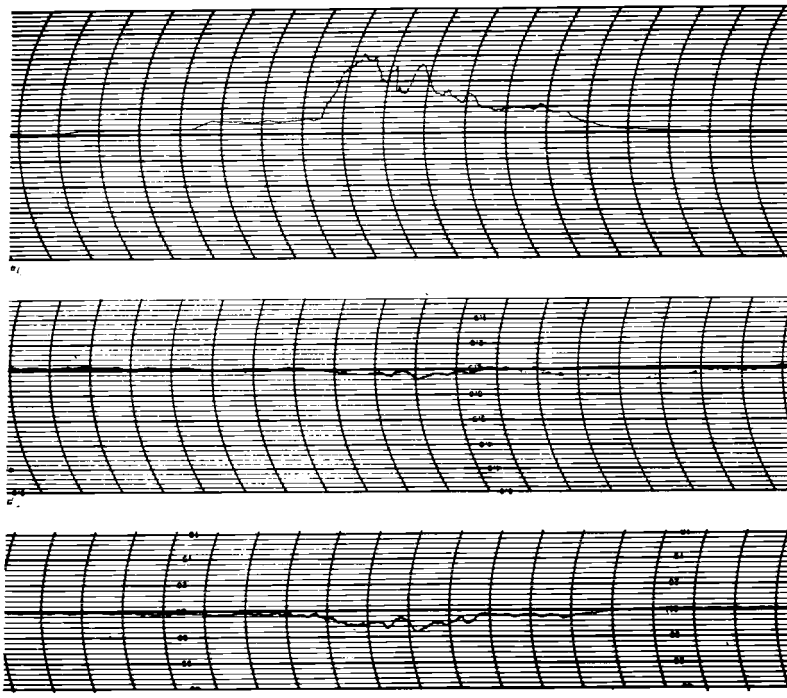

Figure 11. Airplane discharge currents: Nose plate, nose and tail electrodes. Upper, nose plate; center, nose electrode; lower, tail. Precipitation: dry snow.

Scales: Upper, 0.1; others, 10 microamperes per major division, 8 units per minute. Airplane negative for negative deflections. Boeing 247-D plane.

change of intensity of the discharge from any one electrode was accompanied by a similar change in the discharges from the other two electrodes. It is obvious that the ship was being charged negatively very strongly by some action of the precipitation in which it was flying. In this case the precipitation was heavy snow. The uniform vertical deflections present at periodic intervals in each graph were created by a special timing device and represent one-minute intervals. The radio interference accompanying the discharge in this case was very severe and of harsh character.

An interesting condition of high transverse gradients is illustrated in the record of Figure 15. In this case the right wing was in an area that was very strongly negative with respect to the area surrounding the end of the left wing. Transverse currents of considerable magnitude were flowing from wing tip to wing tip as a result of this short-circuiting action. Near the end of the record a slight reversal of the gradient oc-

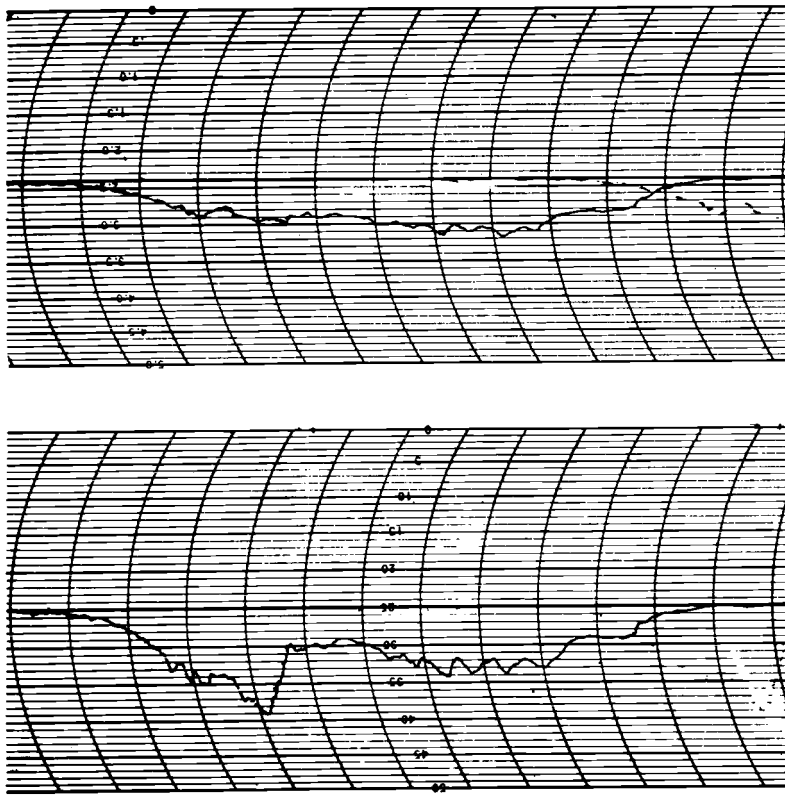

Figure 12. Airplane discharge currents: nose and tail electrodes. Above, nose; below, tail. Precipitation: moderate snow.

Scales: 4 microamperes per major division, 8 units per minute. Plane negative for negative deflection. Boeing 247-D plane.

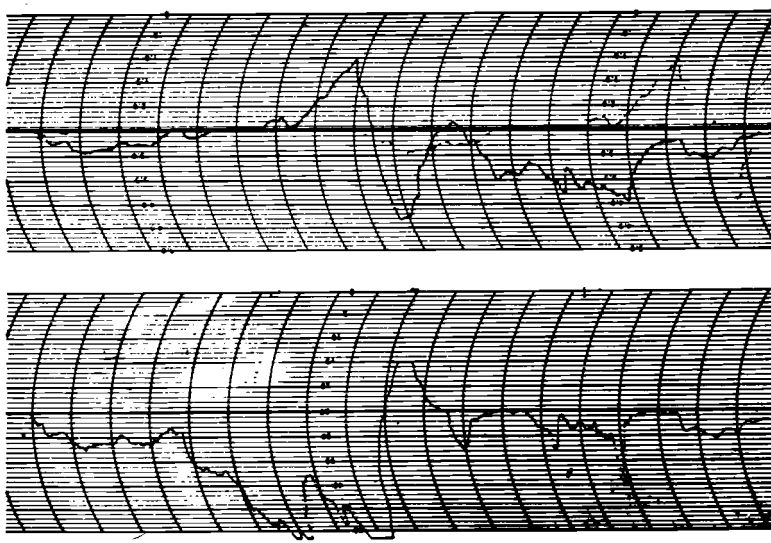

Figure 13. Airplane discharge currents: Nose and tail electrodes. Above, nose; below, tail. Precipitation: heavy snow, center of cloud.

Scales: 4 microamperes per major division, 8 units per minute. Plane negative for negative deflection. Boeing 247-D plane.

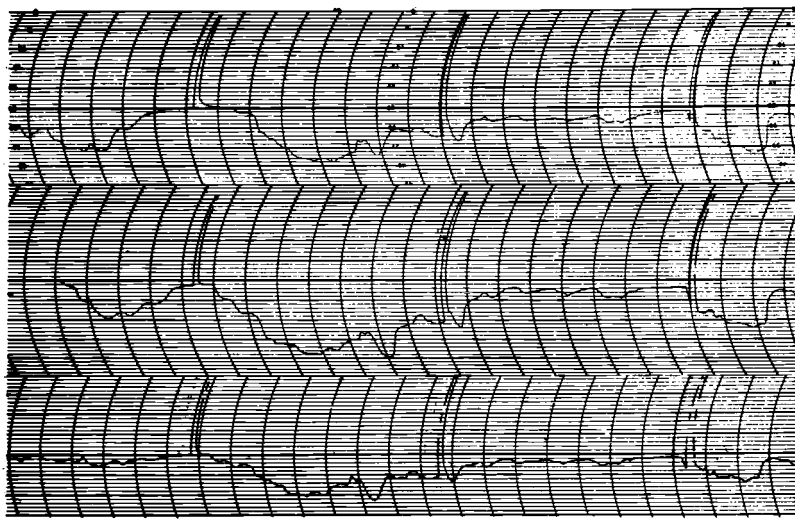

Figure 14. Airplane discharge currents: wing-tip and tail electrodes. Upper, right wing; center, left wing; lower, tail. Precipitation: wet snow.

Scales: 10 microamperes per major division, 8 units per minute. Plane negative for negative deflections. Boeing 247-D plane.

curred. It is interesting also that in this case the tail electrode was relatively inactive. Its tendency was to alternate somewhat between negative and positive discharges of relatively weak magnitude.

A condition different from any other so far discussed is brought out in the record of Figure 16. In this case the nose plate was receiving positive electricity at a time when both the nose and tail electrodes were discharging negatively. A period of longitudinal gradient reversals affecting only the ionization points also is brought out in this record. The most interesting feature, however, is that the ionization electrodes were indicating heavy negative discharges at a time when exposed surfaces, represented by the nose plate, were receiving positive electricity. This indicated charging mechanisms that were apparently considerably different from those in the other records. The precipitation into which the airplane was flying was evidently either neutral or positively charged, or the impact of the air foils upon this precipitation resulted in a positive

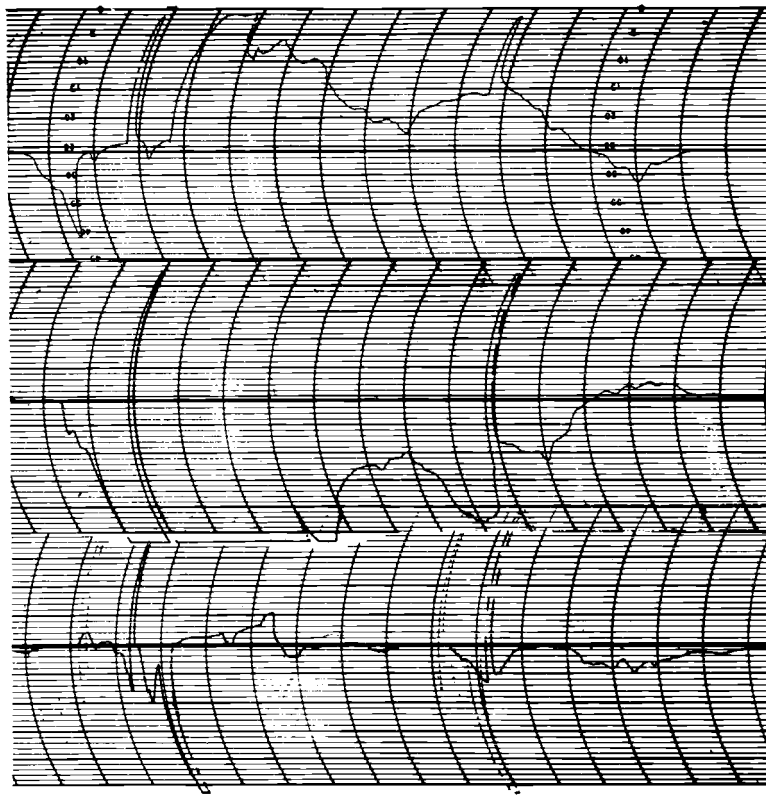

Figure 15. Airplane discharge currents: wing-tip and tail electrodes. Upper, right wing; center, left wing; lower, tail. Precipitation: dry, light snow.

Scales: 10 microamperes per major division, 8 units per minute. Plane negative for negative deflections. Boeing 247-D plane.

charge. The ship, however, was being charged negatively as indicated by the negative discharges. This leads to the belief that the propeller action in breaking up the heavy snowflakes was such as to create a resultant negative charge on the airplane even though some positive charge was being accumulated by contact of the air foils with the charged snowflakes.

A careful study of the discharge records leads to several rather definite and other somewhat obscure conclusions. It is well known that cloud masses can become heavily charged by some type of thermal activity similar to that described by Simpson (5). When an airplane flies into one of these charged areas it must gradually attain the potential of that area, first by electric induction and later by actual contact with the charged precipitation. A potential gained in such a manner would place the ship at the same potential as the region in which it is flying, and hence would result in no localized voltage gradients that would product corona discharges.

It has been shown that the airplane can become charged either positively or negatively with respect to its surrounding medium, the negative, however, being predominant. This phenomenon indicates that the contact with and breaking up of particles of precipitation by the air foils and propellers result in charging the plane to a potential different from that of the particles themselves. The extreme windshield and deicer potentials observed at times indicate that contact with and breaking up of dry-snow and frost-crystal particles result in extremely high charge accumulations. The record in Figure 16 indicates that the action of the air foils of the propellers may be such as to produce negative charges on the airplane from positively charged or neutral precipitation.

In large storm areas, where the precipitation is rather general and

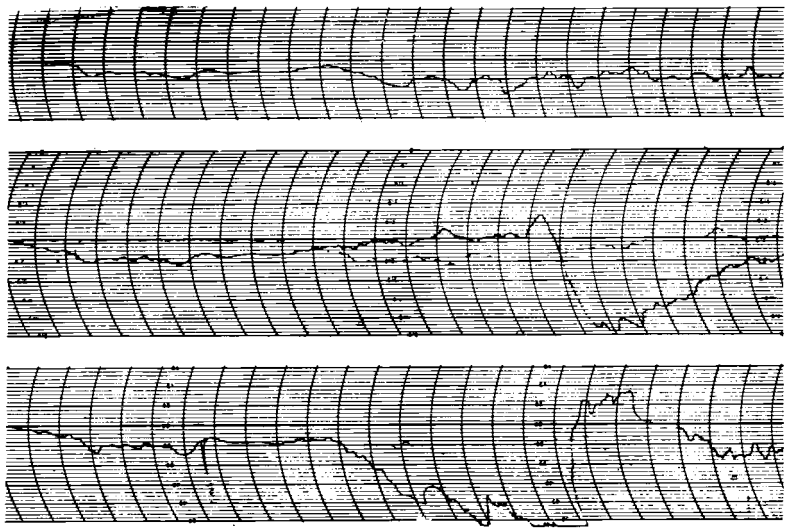

Figure 16. Airplane discharge currents: nose plate, nose and tail electrodes. Upper, nose plate; center, nose electrode; lower, tail. Precipitation: heavy snow, center of cloud.

Scales: Upper, 0.1; others, 4 microamperes per major division, 8 units per minute. Plane negative for negative deflections. Boeing 247-D plane.

where the vertical air currents are not pronounced, a reasonably uniform charging condition may exist. At such times the airplane will attain a high negative potential with respect to the surrounding atmosphere and will discharge continuously. In squally conditions, notably in heat clouds, however, the charged areas are not at all uniform. The airplane may, therefore, fly from an area of low charge to one of much higher potential in a very brief period of time and, in so doing, the ship must be brought to the potential of the new region. This change will result in heavy corona discharges of short duration between the plane and the higher-potential region into which it is flying. Subsequently, as the ship leaves this high-potential region and enters one of lower potential, the reverse operation will take place; that is, the ship will discharge its higher voltage to the lower potential region. Most of the high longitudinal gradients illustrated in the records were due to conditions of this character. The so-called "crying" or musical-note static in the radio receivers was observed to accompany these particular conditions, and it will be shown in the section, "High-Voltage Direct-Current Point Discharges," that positive corona discharges under many conditions characteristically produce this type of interference. Under certain rather critical conditions, the negative discharges also will produce the musical-note interference.

In order to determine the ability of the propellers to produce electrical charges by breaking up water particles, the test airplane was subjected to a spray test on the ground. The left motor was allowed to operate at approximately normal speed and a stream of water from the Portland, Oregon, city supply was directed into the propeller. It was observed that the electrode mounted behind the propeller indicated the accumulation of a positive charge. When the same test was made at Cheyenne, Wyoming, the electrode indicated a charge but this time of reversed polarity. This characteristic indicates that the breaking up of water particles by propeller action may produce charges in a manner similar to that observed when drops of water are allowed to fall into a vertically rising air current.

A number of years ago some experiments were performed in the Electrical Engineering laboratories of Oregon State College which indicated that if the salt content of the water that was allowed to drop into the rising air current were less than approximately two parts per million, the spray that was blown from the water drops during their fall through the air current would be negatively charged. The droplets themselves attained a positive charge. When the salt content was increased, a point was reached at which no charging action took place. If the salt content were further increased the polarities were reversed; that is, the spray would attain a positive charge and the water droplets a negative charge. This experience lends strength to the belief that the propellers, in breaking up certain types of precipitation, are largely responsible for the charges accumulated on airplanes. Further substantiation of this belief is brought out by the fact that a large, all-metal airplane in a "power stall" is reported to give heavy radio interference when in bad static regions, whereas a "dead stall" in the same region results in a marked reduction of the radio interference.

It was found that the discharge currents under practically all flight conditions fluctuate very rapidly. Some of the observations indicated transverse currents as great as one milliampere, and discharges from the

tail electrode approaching the same order of magnitude were recorded on a few rather extreme occasions.

The characteristic Saint Elmo's Fire discharge, so frequently reported as being observed during the hours of darkness at the propeller tips, is undoubtedly due to two elements. The first is that these propeller tips are very sharp, and since they extend out a considerable distance from the shielding influence of the fuselage and wings, they constitute excellent discharge points. The second is that due to the very high peripheral speeds of these propellers, as well as their pitch, a low-pressure region exists near the tips. Since ionization occurs much more readily at low absolute pressures than in the normal atmosphere, the discharges would take place in these regions at reduced potentials.

Two of the general types of cloud formations in which flight tests were made are shown in Figures 17 and 18. The cumulo-nimbus, or heat cloud, of Figure 17 was of the violently agitated type, resulting in rapid changes from one type of charging action to another. Practically every type of charge is represented in such a cloud when tests are flown at various levels. The heavy rain and snow near the lower edge of the cloud is predominantly positive, while the light, drier snow in the upper part of the cloud usually releases negative charges upon contact with the frontal surfaces of the airplane.

The photograph in Figure 18 illustrates a condition frequently encountered in cross-country flight. The airplane is in a clear region be-

Figure 17. Moderately charged cumulo-nimbus cloud, Lower Willamette Valley, Oregon.

tween two moderately heavy overcasts. In this position the range signals can be received clearly because there is no precipitation, and hence no static other than the occasional crash variety due to localized atmospheric discharges more or less distant from the plane. In both the lower and upper overcasts, however, there was a moderate amount of snow and frost and the accompanying radio interference was considerable.

The influence of size and speed of aircraft on the charging action observed in precipitation areas and hence the influence of these same factors on the radio interference created is pronounced. The larger and faster craft, since their frontal areas are larger and their speeds are greater, make contact with more particles of precipitation per unit of time than do the smaller ships. The result is a definitely higher charge and discharge rate, together with a greater volume of interference. The broad wing spans and great axial lengths of the larger ships cause them to span greater areas and hence to create greater disturbances in the regions of high-voltage gradients.

Since various areas on the airplanes experience such pronounced charging actions under certain storm conditions, it is evident that very thorough bonding should be practiced between all parts of the airplane. Occasions have arisen in which the cowling about the engines has become disconnected electrically from the nacelle. Under this condition, radio interference of severe character is produced when the ship is flown through precipitation areas. The cowling repeatedly charges up and then discharges through sparks to nearby bonded metal parts.

Figure 18. Between two moderately heavy overcasts, Siskiyou Mountains, California. Altitude 12,000 feet.

Any exposed insulating surfaces, such as the windshields, the deicers, insulating housings over radio loops, and the exposed landing wheel tires, will, under certain conditions as outlined previously, accumulate electric charges that will dissipate themselves in the form of sparks to nearby metal supports. This condition can be alleviated only by causing the surfaces of the offending elements to provide a leakage path to nearby bonded metal parts. It is interesting to observe that the ice caps, which under certain precipitation conditions will form on the leading edges of the air foils, can have charges developed on their exposed surfaces. Since the ice accumulated at high altitude forms a very excellent insulator, the ice cap creates, in effect, a localized insulated area similar to the windshields and plain rubber deicer boots.

VIII. HIGH-VOLTAGE DIRECT-CURRENT GROUND TESTS

The rapidly fluctuating character of the voltages encountered in the flight tests indicated the desirability of making tests on the airplane with more accurately controlled voltages. It was felt that flight conditions might be simulated by mounting the plane on insulators and charging it to a sufficiently high direct potential to cause exposed points to go into corona. Information had been obtained on the magnitudes of discharge currents to be expected under storm conditions and the type of radio interference created had been observed carefully. It was felt that if these same conditions could be developed on the ground under accurately controlled conditions, much more consistent results could be obtained.

In line with these thoughts, the research airplane was taken to Oakland, California, and mounted on high-voltage insulating supports in one of the large hangars at the Oakland Airport. Figure 19 illustrates the ship set up on insulators for the high-voltage direct-current tests. Adequate insulation was provided to prevent the appearance of any brush discharges from the landing gear and wheels toward the concrete floor.

An improvised high-voltage rectifier, Figure 20, utilizing X-ray equipment, was assembled and adjusted to give a maximum potential of approximately 100,000 volts to ground. The circuit employed for this rectifier is given in Figure 21. It will be observed that with this arrangement it is possible to obtain from a transformer developing 50 kv peak, an output voltage, either positive or negative with respect to ground, of 100 kv dc. The principal advantage of this circuit is that the maximum inverse potential applied to either high-vacuum tube is the same as the output potential, and furthermore, it is necessary to use a transformer having a rating of only 50,000 volts, line to ground.

With a potential of the order of 50,000 volts applied to the airplane, conducting surfaces connected to ground were brought up into close proximity to the various discharge points mounted on the airplane. Observers inside the cabin noted that currents of the same order of magnitude could be drawn from these points by this arrangement as were obtained in flight. They observed, furthermore, that the radio interference created by such discharges was of exactly the same character as that which had been noted during the flight tests.

Following these preliminary tests, arrangements were made to suspend conducting points from the tail electrode of the ship toward the concrete floor for a series of discharge tests. It was felt that if the

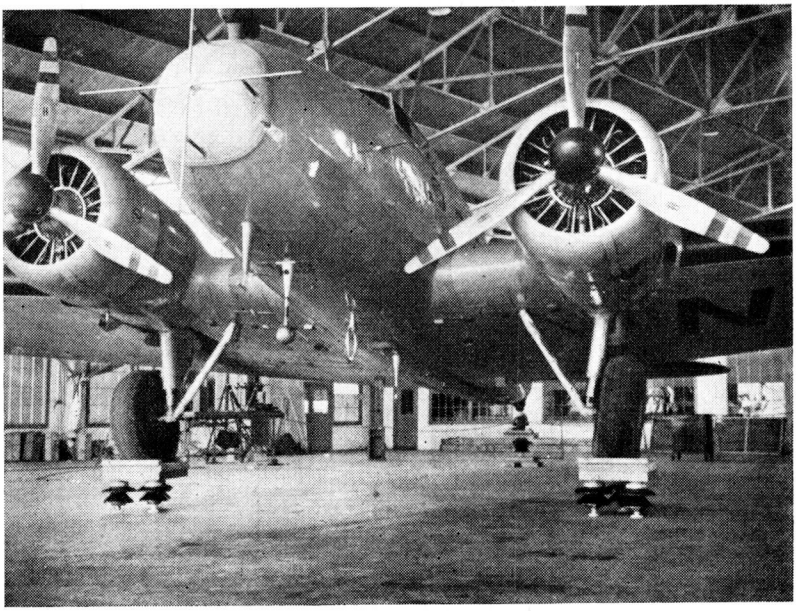

Figure 19. Boeing Type 247-D research airplane on insulating supports for high-voltage direct-current corona discharge tests.

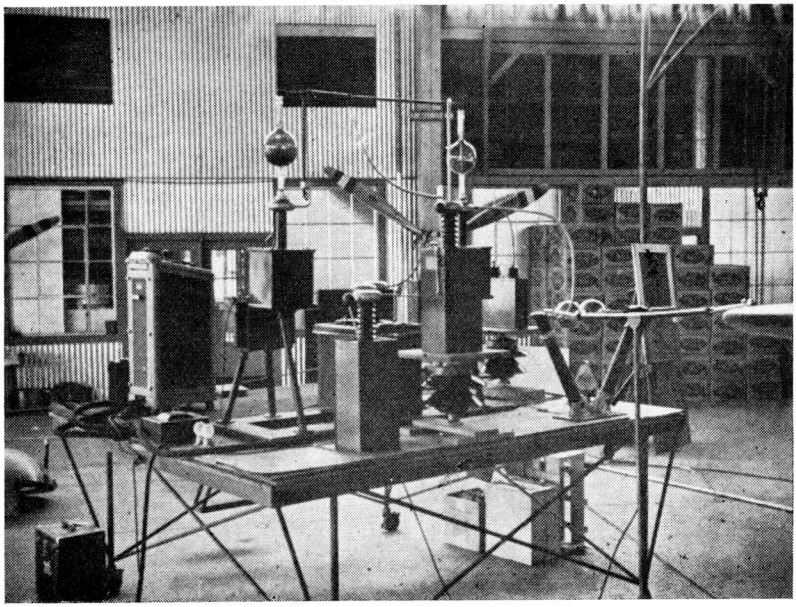

Figure 20. High-voltage rectifier for energizing airplane in corona discharge tests. Capacity: 100,000 volts, line to ground.

concrete floor were used as the ground plane, the currents would distribute so widely and return to the generator through such a broad conducting medium as to prevent the creation of disturbances in the radio antennas due to these currents.

For the first series of tests, a 0.25-inch steel rod was sharpened with a rather long taper and was suspended 11 inches from the concrete floor. High-voltage ignition conductor was used for the support in order to eliminate the possibility of corona discharges from the conductor itself. The tail electrode was well-covered with rubber insulating tape to prevent

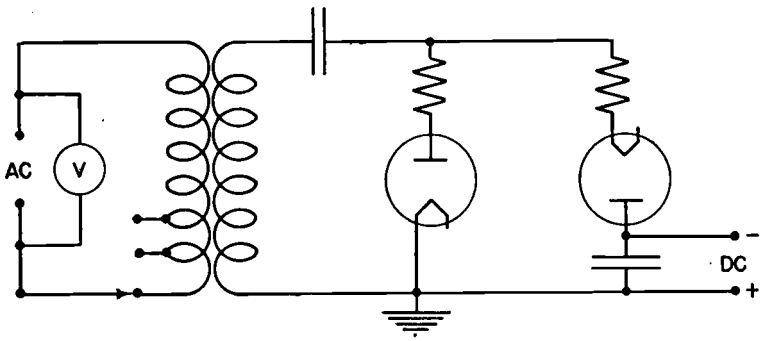

Figure 21. Rectifier circuit used in airplane ground tests.

it from going into corona. Observations made during the hours of darkness indicated that no visible discharges were taking place from any part of the plane other than the point where the discharge was desired. For the first tests, no resistance was placed in the discharge lead and the radio beacon receiver was connected to the "Belly V" antenna.

A local signal generator was employed to create a background carrier wave, for which the beacon receiver was tuned, which was modulated at a frequency of approximately 1,000 cycles per second. It was so located, together with the gain setting of the radio receiver, as to produce a rectified output in the headphone circuit of 0.5 microampere. For all tests, the receiver gain setting was kept at approximately the same point and a signal of 0.5 microampere was obtained by so locating the local signal generator as to produce the desired output.

Since most of the flight work had indicated that the ship was discharging negative electricity, the first ground tests were made with the point negative with respect to the concrete floor. The results of the tests with this arrangement are given in Appendix V, Table 2, and are illustrated by the curves in Figures 22 and 23. These curves indicate that the maximum discharge current obtained was 110 microamperes and that the accompanying radio noise was severe only in the lower regions. This characteristic was checked many times and it was found that even though considerable current was being discharged, no appreciable interference was produced except at the highest values of current and again for currents of the order of less than 20 microamperes. At approximately 13 microamperes the radio interference was extremely severe. The character of the noise produced in the headphones was very similar to that observed in flight tests.

The radio receiver was then connected to the lower shielded-loop antenna and another set of data taken. These data are given in Table 2 and it will be observed that no interference was created except at the low-current point referred to above. The interference at this point was not of a severe magnitude although it was definitely noticeable. This result again checked the flight-test data very accurately. It had been observed in storm flying that the shielded loop had much better signal-to-noise ratio pick-up characteristics than the open antennas, and here again exactly the same characteristics were exhibited. It was now thought that the ground tests were probably a very good check on the flight tests because the same orders of magnitude of currents, the same type of interference, and the same selectivity of the shielded loop over the open antennas were observed.

It was felt that the rather large backing of the rod point was producing a shielding action that was influencing the characteristics at the higher voltages. Accordingly, a 7.5-inch length of tungsten wire with a diameter of 0.007 inch was suspended from the same support with the

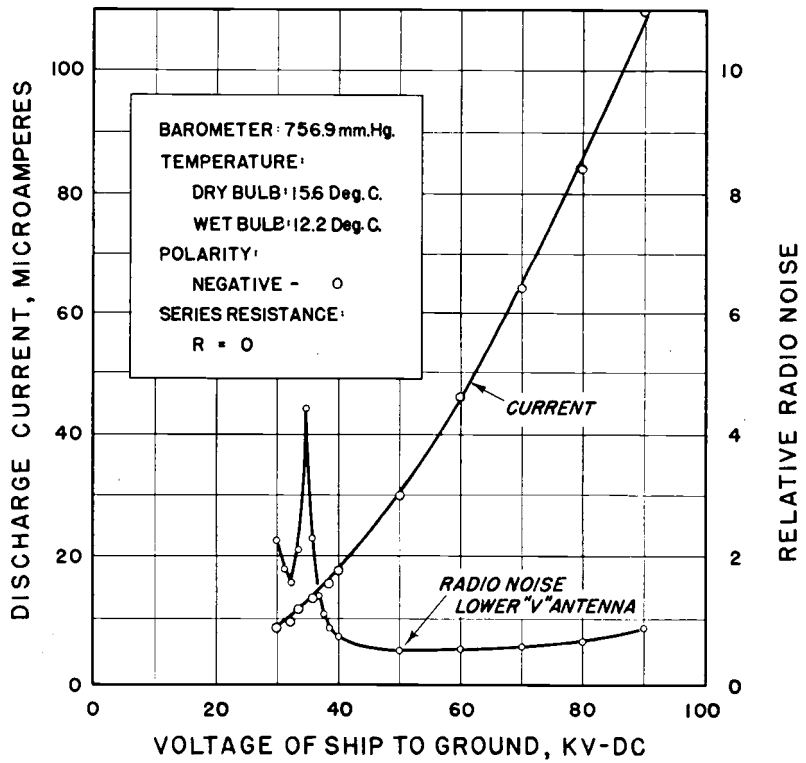

Figure 22. Airplane discharge characteristics for rod electrode. Potential vs. current and radio noise. Discharge electrode: vertical rod, 0.25 in. diameter, pointed, 11 in. from concrete floor.

spacing reduced to three inches. The polarity of the ship remained negative and the same local signal generator output was maintained as previously. The results of the tests on this electrode are given in Tables 3 and 4. It will be observed that the maximum currents were of the order of 580 microamperes and the radio interference as obtained from the lower, or "Belly V," antenna was severe throughout the entire voltage range. The shielded loop in this case also gave considerable interference for the higher current values, tapering down to relatively low interference at the lower voltages. The curves in Figures 24 and 25 illustrate these data graphically. Again it will be noted that the shielded loop provides a very favorable signal-to-noise ratio over the open antennas.

By charging the airplane to a relatively high potential, and then cutting off the rectifier, it was possible to allow the charge to leak down slowly and thereby to obtain a number of points for currents lower than those obtained for the lowest voltage setting of the rectifier. These points are presented graphically in Figure 25, and it will be noted that below 50 microamperes the interference on the open antenna decays to zero with no characteristic high peaks as were observed in the case of the pointed rod.

A resistance of 28 megohms was then connected in series with the discharge point and further tests were made. The data obtained with

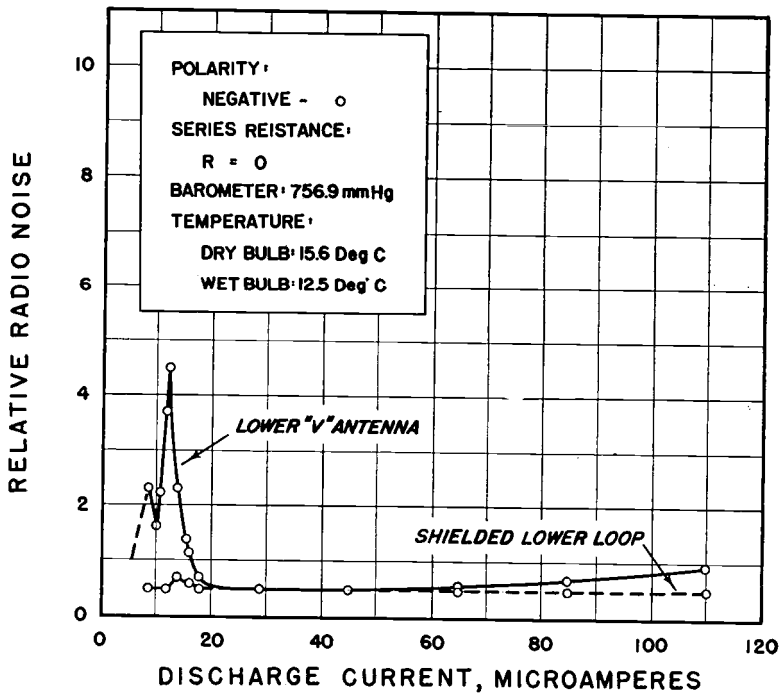

Figure 23. Airplane discharge characteristics for rod electrode. Current vs. relative radio noise.

this arrangement are presented in Tables 3 and 4, Appendix V, and in the curve of Figure 25. It will be observed that the insertion of resistance reduced the interference for a given discharge current to a marked degree. The interference pick-up of the shielded loop was actually reduced to zero throughout the entire range of currents observed. Although some interference was still obtained from the open antenna, a marked improvement in its performance was produced.

These results immediately suggested the possibility of using in flight some type of trailing discharge conductor. The flight tests had indicated that the interference problem could be solved only by preventing the charging of the airplane to potentials greatly different from those of the surrounding atmosphere, or by dissipating these charges without disturbing the radio receiver. It was obvious that if the potential of the aircraft, by means of some discharging device, could be maintained at a value near that of the surrounding atmosphere, then no corona discharges could take place except in the event of passing through high-gradient regions where the airplane effectively is short-circuiting high differences of poten-

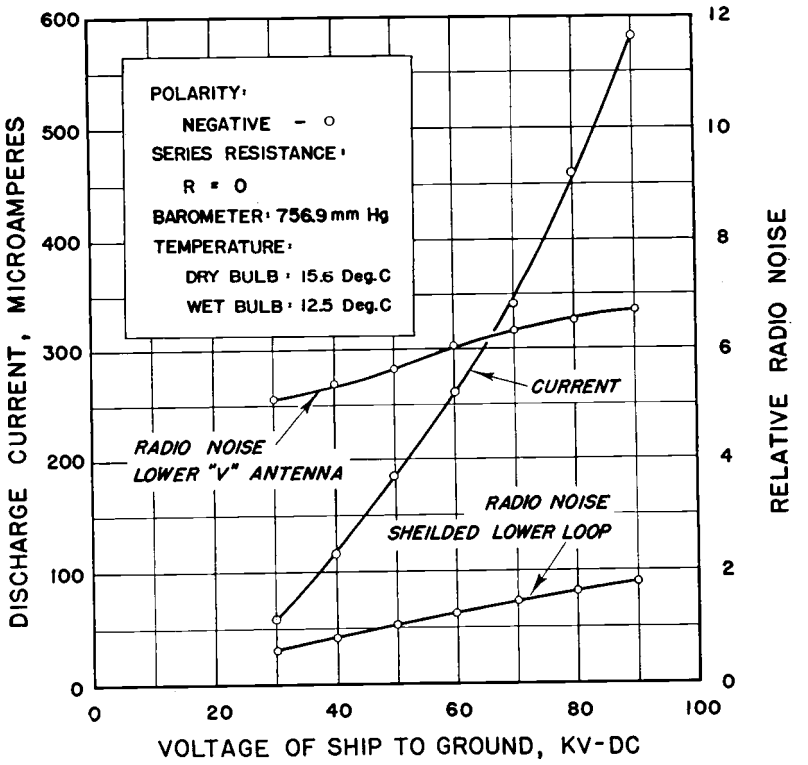

Figure 24. Airplane discharge characteristics for wire electrode. Potential vs. current and radio noise. Discharge electrode: vertical wire 7.5 in. long, 0.007 in. diameter, 3 in. from concrete floor.

tial. Since these latter conditions are only transient in their character, they are not particularly objectionable. This trailing-wire discharger, with high-resistance impulse suppressors, has been tried in flight and found to be very beneficial under certain conditions.

At least one large air transport corporation has installed such trailing-wire devices on all of its transport airplanes and has found them to be of material assistance in combating the precipitation-static problem. In this case, the trailing wires are contained in small cartridges and can be released from the tail of the airplane when severe static conditions arise. Normally, they are totally enclosed and hence are not subject to mechanical fatigue and failure when not in use.

After a satisfactory amount of negative-polarity data had been obtained, the rectifier was reversed and provisions were made for obtaining positive-discharge data. Because of the very much greater sparking distance of point-to-plane electrodes with point positive than with point negative, it was necessary to increase the spacing between the end of the fine tungsten wire and the concrete floor from 3 inches to 7.5 inches. Otherwise, the set-up employed was exactly the same as for the negative

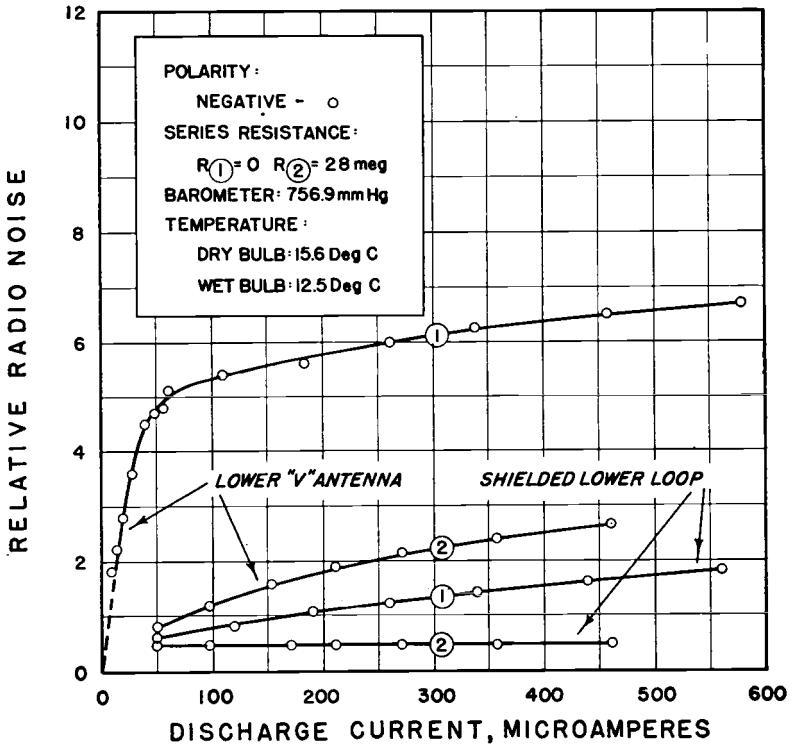

Figure 25. Airplane discharge characteristics for wire electrode. Current vs. relative radio noise.

tests. The data obtained from these tests are given in Tables 5 and 6, Appendix V. Some very peculiar characteristics were noted. Reference to the curves of Figure 26 will show that as the potential of the ship was raised slowly from 30 kv to 75 kv, the interference received by the open antennas, regardless of the fact that the current had risen to over 120 microamperes, was practically zero. Then, very suddenly the interference jumped to a high value, and as the voltage was further increased, continued on to still higher values. Observations of the discharge point indicated that prior to the sudden burst of interference the discharge was in the form of a very fine point of localized ionization. At the instant the interference started, a long ionized streamer was observed to burst out from the end of the discharge electrode.

Again, the shielded loop gave results similar to its previous performance in that its noise pick-up was vastly less than that of the open antennas. No positive-polarity data were taken on the pointed-rod electrode.

A different analysis of the positive-discharge data is given by the curves of Figure 27. It is shown that in this case the interference picked up by the open-wire antenna jumped from practically nothing at all to a very high value at approximately 110 microamperes. As the current was further increased to 190 microamperes, the interference followed a rather devious but increasing path. When the current was allowed to die out, by reducing the voltage on the ship, the interference remained fairly high on down to low values of discharge current. These characteristics brought

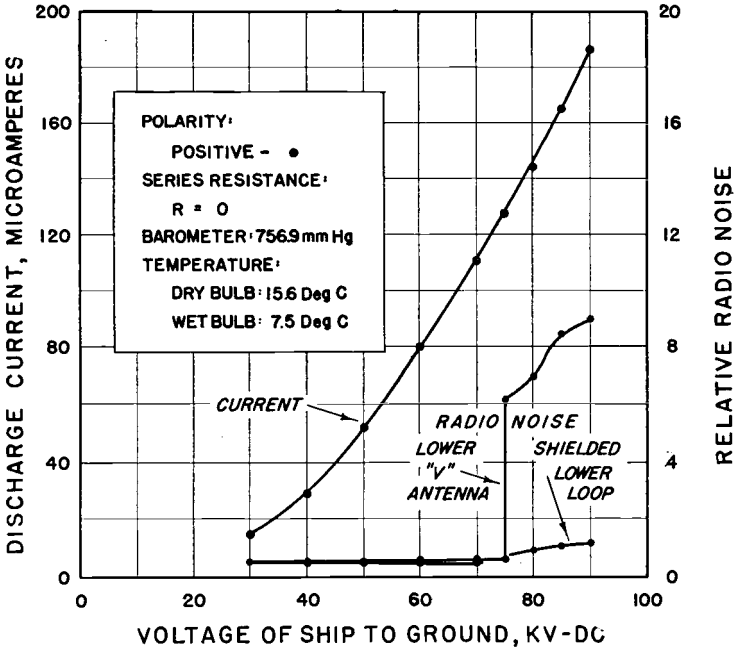

Figure 26. Airplane discharge characteristics for wire electrode 7.5 in. from concrete floor.

out the fact that the presence of ionization streamers was responsible to a considerable extent for the radio interference produced by the positive corona discharges. This phase of the subject is treated in detail in the section, "High-Voltage Direct-Current Point Discharges."

Again the insertion of a discharge resistance of 28 megohms resulted in a marked improvement in the radio noise characteristics. Curve 2 (solid) of Figure 27 illustrates the improvement obtained by the use of resistance. This curve is for decaying currents and represents ionized-streamer discharges from the highest to the lowest values. Again, it will be observed from Curve 2 (dotted) of Figure 27 that the resistance completely eliminated the noise pick-up of the shielded loop.

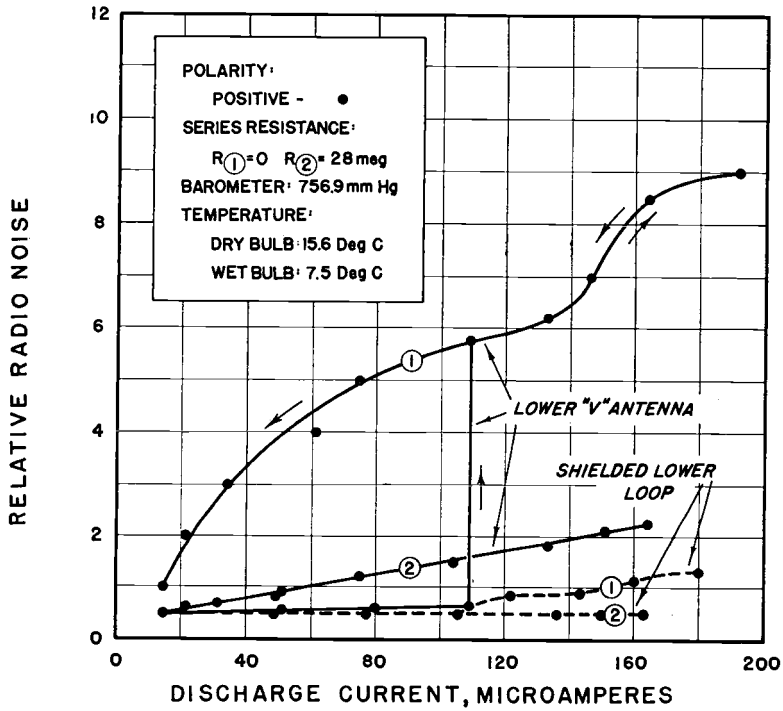

Figure 27. Airplane discharge characteristics for wire electrode 7.5 in. from concrete floor.

IX. COORDINATED LABORATORY AND ANALYTICAL STUDIES

The data obtained from the ground tests on the research airplane emphasized the necessity for additional basic studies in three different fields. The first subject requiring investigation was that of the character of high-voltage direct-current point discharges. The data so far obtained had indicated an erratic behavior of the interference produced by point discharges. It was felt that a comprehensive study of the subject should

be made in order to understand better the nature of the controlling factors in this type of discharge.

The second subject requiring intensive study was the mechanism of the radio interference produced by corona discharges from point electrodes and the nature of the noise-suppressing influence of resistors and inductors in discharge circuits.

The third subject was an extensive study of the characteristics of antennas, particularly the shielded loop, with a view to determining the reason for its noise-rejecting properties and further improving this property if possible. These subjects were taken up in the above order and they will be discussed in subsequent sections.

X. HIGH-VOLTAGE DIRECT-CURRENT POINT DISCHARGES

The point-discharge study was undertaken in considerable detail. It was soon learned that the type of discharge obtained was dependent very largely on the geometry of the point employed, and that the radio interference accompanying the ionization was very definitely a function of the discharge characteristics. The maximum potentials required were of the order of 50 kv dc and it was essential that the voltage ripple be reduced to a minimum. The currents involved were of the order of microamperes and, since it was desired to record by means of the Duddell oscillograph both the discharge current and the accompanying radio interference, it was necessary that a current amplifier be employed. In recording the radio interference on this oscillograph, it was necessary to provide only an impedance-matching transformer between the low-frequency output of the radio set and the vibrator circuit.

The general test circuit employed is given in Figure 28. A full-wave, high-vacuum rectifier was employed for the high-voltage generator, and a loading capacitance of one microfarad was used to reduce the voltage ripple. The output voltage of the rectifier was determined by sphere gaps used within their proper polarity range and correlated with the voltmeter-coil instrument, designated as V on the diagram. A high-voltage vacuum-tube voltmeter also was employed for voltage measurements.

A two-stage linear vacuum-tube amplifier employing a Type 57 and a GE Type FP 110 tube was constructed. This is a resistance-coupled amplifier, and by means of a proper setting of the bias voltage, E_c it was possible to utilize the amplifier over its entire range for either positive or negative polarities on the point, P. It was convenient, by connecting the deflector-plates of a cathode-ray oscillograph across R_1, R_2, or R_3, to obtain wave-form checks against the indications of the Duddell oscillograph. These checks, as summarized in Table 15, indicated that this latter oscillograph was responding with a satisfactory degree of accuracy. In the case of steep-front impulses of current or radio output, this oscillograph gave somewhat erroneous peak indications, and the vibrators displayed a minor tendency to fall into damped oscillations at their natural period. These characteristics, however, were not at all confusing.

The capacitance C_2 was necessary to prevent feed-back oscillations in the amplifier circuit.

To examine the radio interference created by discharges from the point P to a plane, the conductor connecting this plane to the short-circuiting switch around A_1 and R_1 was carried once around the loop an-

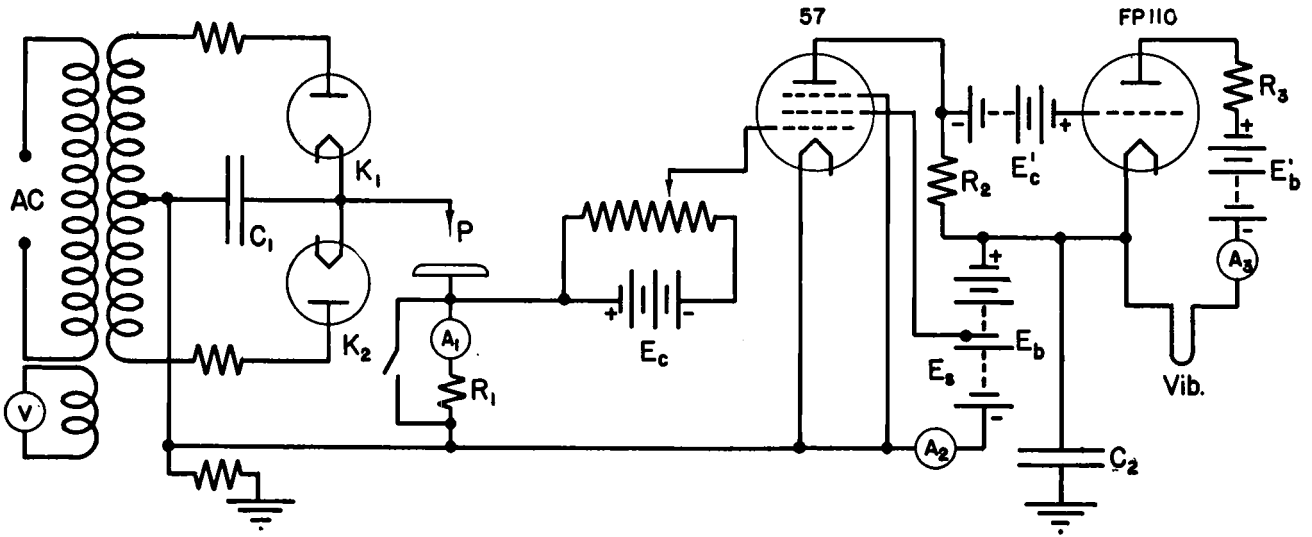

A_1 = 150 μa	E_b = 315 v	R_1 = 5000-25000 Ω
A_2 = 5 ma	E'_b = 125 v	R_2 = 0.5 meg.
A_3 = 250 ma	E_c = 6 v	R_3 = 200 Ω
C_1 = 1.0 μf	E'_c = 90 v	C_2 = 0.25 μf
	E_s = 113 v	

Figure 28. Resistance-coupled linear amplifier for oscillographic study of high-voltage d-c point discharges.

tenna of a Western Electric radio field-strength measuring set tuned for approximately 900 kilocycles. (7) The position of this coupling loop was so adjusted that no difference in radio output was observed when R_1 was introduced or short circuited. The coupling was sufficiently loose to prevent the oscillations set up in the antenna circuit of the field-strength set from feeding back into the current amplifier and giving erroneous indications in the amplifier output.

1. **Types of discharges.** As the point-discharge studies progressed, it was observed that when the point is positive with respect to the ground plane, there are three distinct types of discharges to be obtained. These discharge types are dependent on the geometry of the point employed and are illustrated in Figure 29. Type 1 is characteristic of the discharge obtained throughout the range of voltages available, from a sharp, slender point. In total darkness a small bead of ionization is visible at the end of the point and a tapering sheath of ionization extends for a short distance back from the point. An extremely interesting characteristic of this type of discharge is that no normal-frequency radio interference accompanies it.

The discharge indicated as Type 2 is characteristic of that obtained from points that have a rather acute angle of backing; that is, in general, if the angle made by the surface of the point with its center line is approximately 30 degrees or less and the point is carefully polished, this type of discharge will nearly always occur. It may be described as a long, sharp, ionized needle extending a considerable distance out from the point, and the current accompanying it for a given voltage is characteristically high. The radio interference produced by this type of discharge is severe and is characteristically harsh.

The type of discharge practically always obtained from a rough point or one that has a rather blunt backing, such as a conical point with sides making an angle of 60 degrees with the center line, is that illustrated as Type 3 in Figure 29. In this case there is a typical bead of ionization adjacent to the point proper, and then a rather slender stem extending below the bead for a short distance before the discharge blossoms into a broad plume. The current drawn by this type of discharge is in general the lowest of the three and the radio interference produced has a characteristic musical note. The pitch of this note may run from the order of several thousand cycles per second down to less than 100 cycles per second and is exactly similar to that described as being observed under certain conditions in airplane flight tests. It would appear, then, that at least Type 2 and Type 3 discharges occur from airplanes in flight under certain storm conditions.

2. **Oscillograms.** Oscillographic records of point-discharge currents and the accompanying radio disturbances bring out a number of interesting and fundamental characteristics. The oscillogram of Figure 30 shows the discharge-current and radio-noise characteristics of a 60-degree positive point, spaced 10.2 centimeters from the ground plane and operating at a potential of 15.2 kv. The average current, as indicated by a D'Arsonval instrument, was 2.0 microamperes. The scales were such that the current zero line blends in with the actual current wave between the impulse peaks. The timing wave employed was 1,000 cycles per

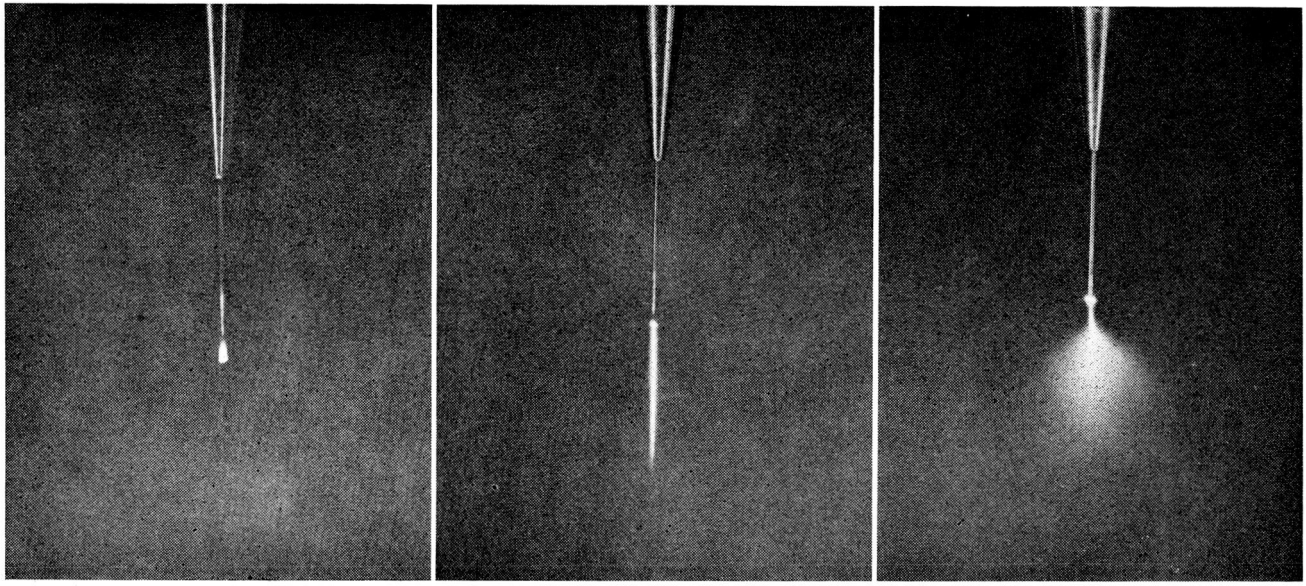

TYPE 1
Point: Sharp, slender.
Current: 42.5 MUA

TYPE 2
Point: No.0 steel needle.
Current: 48.0 MUA

TYPE 3
Point: Sixty-degree conical.
Current: 41.5 MUA

Figure 29. Direct-current corona discharges. Electrodes: point to plane. Polarity: positive. Spacing: 10.2 cm. Voltage: 44.0 kv.

second, and it will be observed that the average frequency of the current impulses was approximately 500 cycles per second.

It is important to note that the radio-noise surges occur exactly in synchronism with the current impulses, there being no radio output during the intervals of steady current flow. These current impulses, when viewed on the screen of a cathode-ray oscillograph employing a high-speed sweep, are very similar to those of an impulse generator. Figure 40 contains typical cathode-ray oscillograms of both the positive and the negative discharges. The individual steep-front impulses superimposed upon a steady direct current are shown in detail. Curve 1 of Figure 49 is typical of the individual impulses. It is evident that these impulses create the interference response in the radio receiving equipment. This subject will be treated further in the section "Nature of Radio Interference Arising from Corona Discharges." The actual positive discharges used for the above oscillograms were of Type 3.

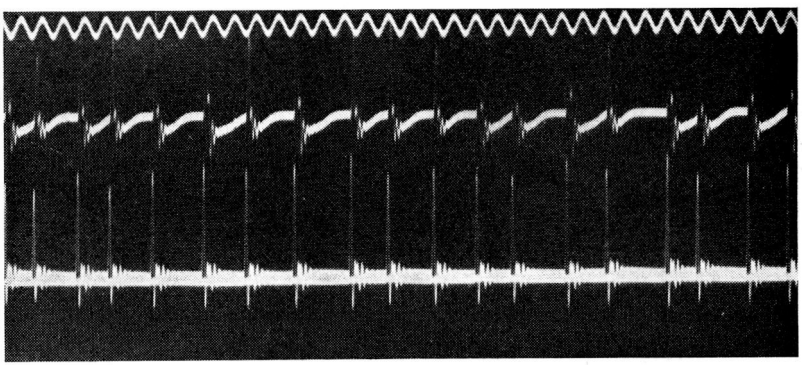

Figure 30. Direct-current corona discharge characteristics. Electrodes 60° point to plane; spacing, 10.2 cm. Point positive, plane grounded; E = 15.2 kv., I = 2.0 microamp. Upper, radio noise; lower, current with zero line. Timing wave: 1,000 cycles.

When the voltage on the same point was increased to 38 kv, the current increased to 28.3 microamperes, and the radio noise and current appeared as is shown in the oscillogram of Figure 31. The individual impulse character is still present in the current wave, but the impulses are spaced much more closely, the frequency now being of the order of 2,200 cycles per second. The radio interference, although somewhat irregular in character, has the same general frequency as the impulses in the discharge current. The slightly wavy zero line was due to a parasitic voltage picked up by the highly sensitive amplifier employed in the work.

Throughout the investigation, it was observed that the periodicity of the current impulses was a function not only of the current being discharged from the point, but also of the type of point employed. In general, increased currents were accompanied by higher impulse frequencies, but occasions were observed when the impulse frequency actually decreased as the current was raised to higher values. Atmospheric conditions were also observed to have a definite influence on this characteristic.

When the electrode was changed from a 60-degree to a 45-degree point, the discharges obtained were somewhat unstable in that they would occasionally shift back and forth from Type 2 to Type 3. The 45-degree point is on the border line between the geometry which consistently gives the Type 3 discharge and that which gives Type 2. The oscillogram of Figure 32 was taken with this point operating at 43.5 kv to the ground plane. The moment the exposure was made, an observer reported that

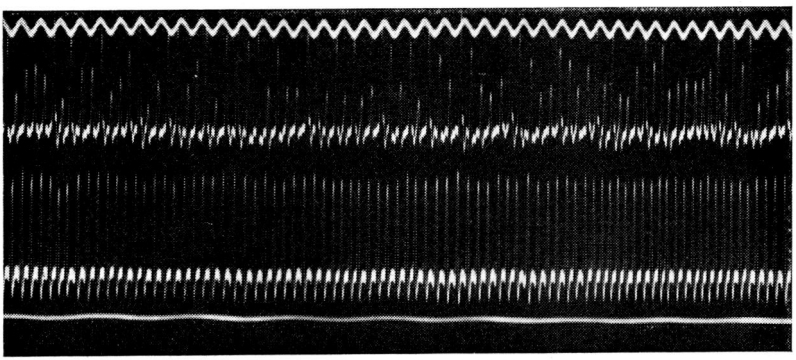

Figure 31. Direct-current corona discharge characteristics. Electrodes: 60° point to plane; spacing, 10.2 cm. Point positive, plane grounded; E = 38.0 kv., I = 28.3 microamp. Upper, radio noise; lower, current with zero line. Timing wave: 1,000 cycles.

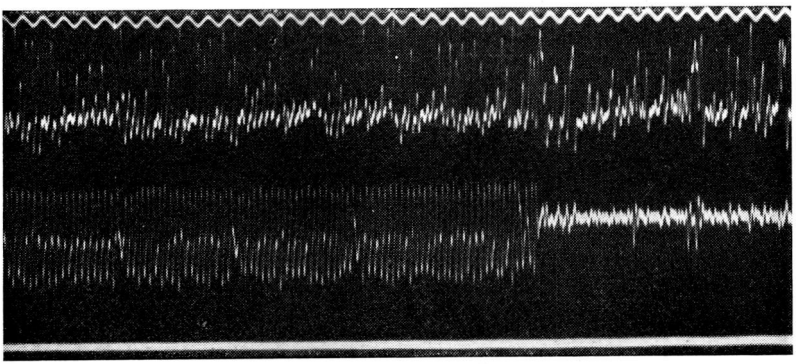

Figure 32. Direct-current corona discharge characteristics. Electrodes: 45° point to plane; spacing, 10.2 cm. Point positive, plane grounded; E = 43.5 kv., I = 42-47 microamp. Upper, radio noise; lower, current with zero line. Timing wave: 1,000 cycles.

the discharges changed from Type 3 to Type 2, and the record of this change is given on the oscillogram. The typical high-frequency succession of current impulses produced by the Type 3 discharge is indicated in the first part of the oscillogram. On three occasions, however, there were breaks indicating that a change in discharge type was about to occur. Near the end of the oscillogram this change did occur, and the irregular current wave and associated radio interference typical of the Type 2

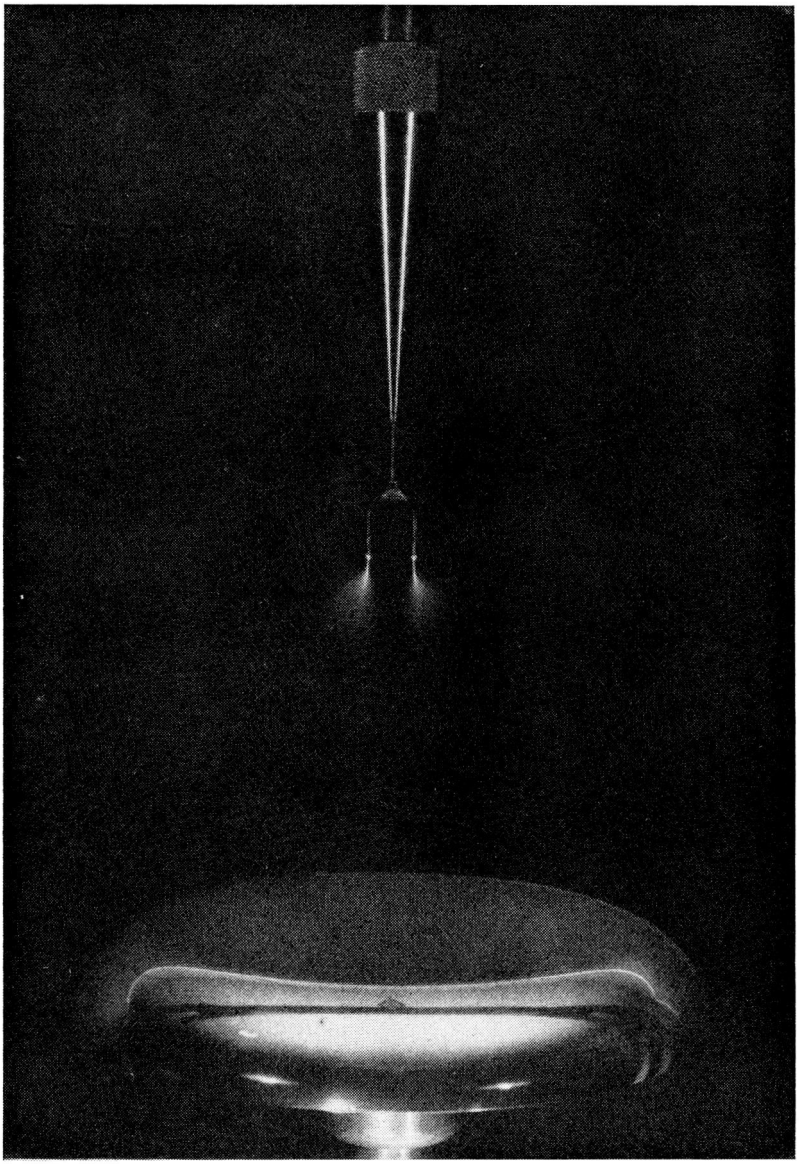

Figure 33. Direct-current corona discharges. Electrodes: double, 60° point to plane; spacing, 10.2 cm. Polarity: positive. Current: 48.3 microamp. Voltage: 44.0 kv.

discharge are shown in the last one-third of the record. It is indicated that there was a distinct change in the character of the radio interference in that the definite periodicity of the output impulses was largely gone. It is also of interest that the current increased from 42 microamperes during the Type 3 discharge to 47 microamperes during the Type 2 discharge. For this type of discharge also, the cathode-ray oscillograph indicated that the current was made up of a steady ion-migration component plus superimposed impulses. In this case, however, these impulses do not occur periodically, but appear at random and sometimes are actually superimposed upon each other.

At this point in the work, some question arose as to whether or not the high-frequency pulsation character of the currents indicated by the oscillograms, for particular types of discharges, actually had occurred in the discharges themselves or were a characteristic of the circuit used in the measurements. In order to answer this question, a double, 60-degree point was made up in the form shown in Figure 33. The two points were similar, although not exactly the same, and were sufficiently close together to create a certain amount of mutual interference between their individual discharges. It was felt that if the circuit were responsible for the definite periodicity of the current impulses, then this type of double discharge would give the same result as a single individual discharge. The oscillogram of Figure 34, however, which shows a very definite beat or heterodyne action in the current ripple, indicates that each point had its own individual impulse frequency and that the two were sufficiently different to produce a pronounced beat in the resultant current ripple. The circuit thus was shown to be responding with a good degree of accuracy.

It has been stated that the Type 1 discharge that is obtained from sharp, slender positive points is free from radio interference. This characteristic is illustrated by the oscillogram of Figure 35. The radio output is shown to have contained no interference whatever, while the current wave shows a number of very small impulses. These disturbances were evidently not sufficiently great to create any interference in the radio receiving set when tuned for normal frequencies.

After the earliest types of points had been subjected to a rather complete study under positive polarity conditions, the high-voltage generator was reversed and the studies were repeated for negative polarities. It was soon learned that all types of points, when of negative polarity, give discharges having essentially the same visual appearance. They seem similar to the type obtained for a positive sharp, slender point. A comparison between the Type 1′ discharge obtained on negative polarity and the Type 3 obtained when positive, for the same identical point, is given in Figure 36. It will be noted that the glow at the point of the electrode is very intense and restricted in the negative case, and that the current is approximately 20 per cent higher than for the same voltage when positive. Microscopically, the Type 1′ discharge negative is different from the Type 1 positive when the negative discharge is obtained on anything but the sharp, slender point. On the bluntly backed point, the negative discharge appears to be a very small but intense, localized plume of ionization in contrast to the very much larger but less intense Type 3 discharge obtained when the same type of point is of positive polarity. As brought out later, there is a very fundamental difference between the negative

discharges from sharp, slender points and those from the bluntly backed type of points.

The radio interference produced by the negative discharges was very erratic in its character for all types of points except the sharp, slender one illustrated in Figure 29. In this case, again, no perceptible interference was produced within the range of voltages available for the test.

The oscillogram of Figure 37 compares with that of Figure 30, with the difference that the former is negative and the latter is positive. The currents and voltages were of the same order of magnitude and identical points were used for both. It is shown that the negative discharge current, in common with the positive as illustrated in Figure 30, is made up of a continuous value with a superimposed high-frequency series of small impulses. The frequency of these impulses is of the order of 2,000 cycles

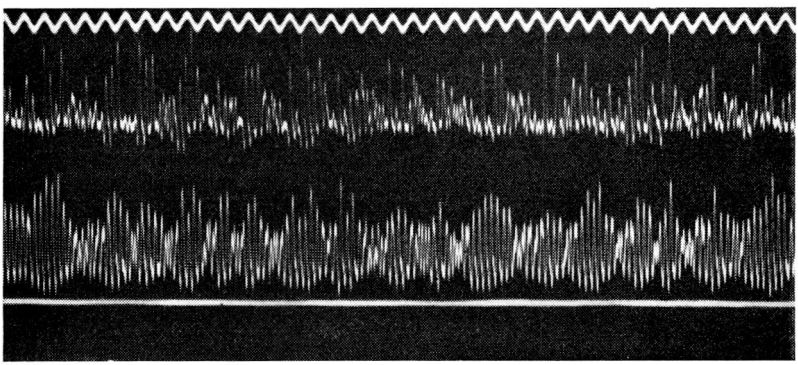

Figure 34. Direct-current corona discharge characteristics. Electrodes: double 60° point to plane; spacing, 10.2 cm. Point positive, plane grounded; E = 33.0 kv., I = 26.0 microamp. Upper, radio noise; lower, current with zero line. Timing wave: 1,000 cycles.

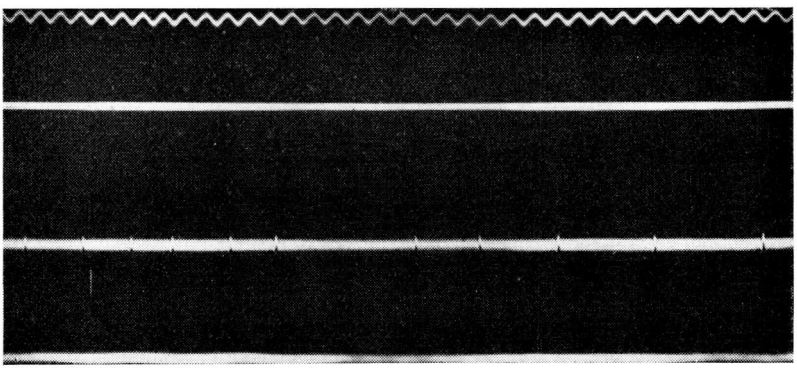

Figure 35. Direct-current corona discharge characteristics. Electrodes: slender, sharp point to plane; spacing, 10.2 cm. Point positive, plane grounded; E = 43.2 kv., I = 40 microamp. Upper, radio noise; lower, current with zero line. Timing wave: 1,000 cycles.

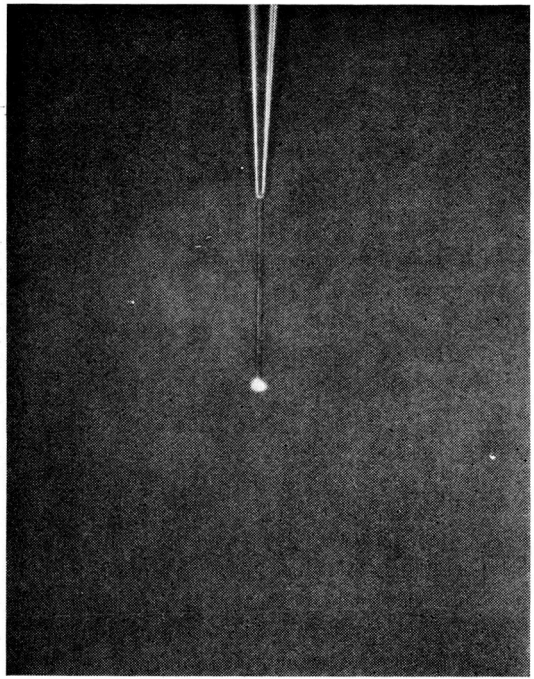

TYPE 1'

Polarity: Negative.

Current: 49.6 MUA

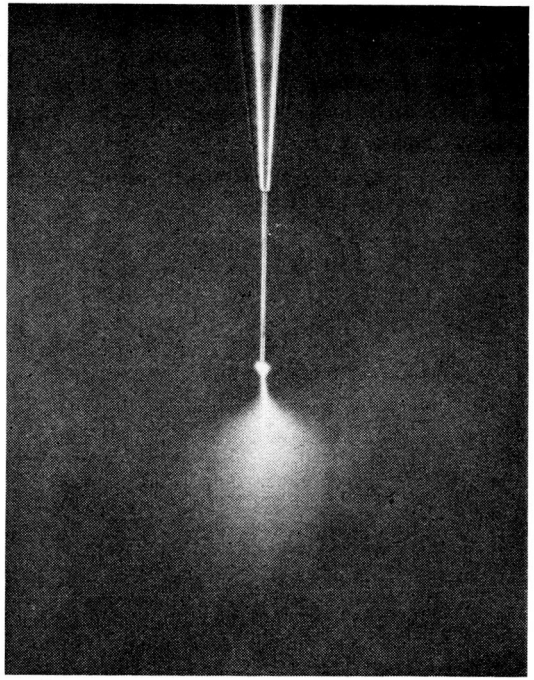

TYPE 3

Polarity: Positive.

Current: 41.5 MUA

Figure 36. Direct-current corona discharges. Electrodes: 60° point to plane; spacing: 10.2 cm. Voltage: 44.0 kv.

per second as compared with approximately 500 cycles per second in the positive case. The amplitude of the negative impulses is considerably less than that of the positive. Again, the radio interference is well synchronized with the current impulses although somewhat less regularly so than in the positive case.

For the very low discharge currents, it was observed occasionally that in the negative case also a tendency toward the musical note is produced by the interference in the radio receiver. When the voltage is

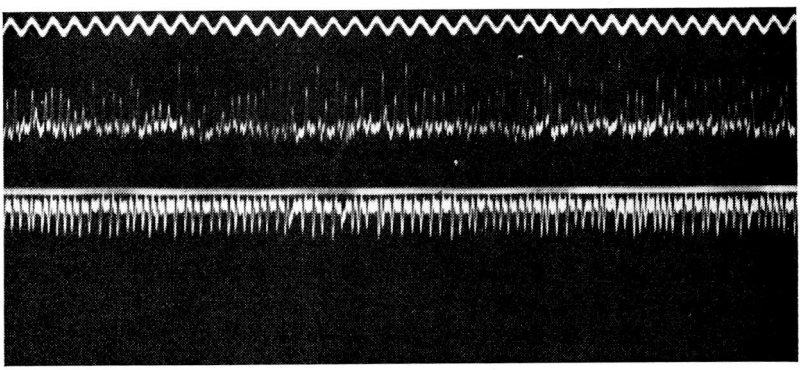

Figure 37. Direct-current corona discharge characteristics. Electrodes: 60° point to plane; spacing, 10.2 cm. Point negative, plane grounded; E = 16.6 kv., I = 3.0 microamp. Upper, radio noise; lower, current with zero line. Timing wave: 1,000 cycles.

increased to higher values, the negative impulses lose their individual distinction. In the case of most types of points, the interference becomes very erratic, sometimes rising to high values and then dropping off to practically nothing only to rise again, perhaps to intermediate values, as the voltage is slowly changed.

The oscillogram of Figure 38 compares with that of Figure 31 in that the points and discharge currents were identical, with polarities reversed. In the positive case, the radio-interference peaks were much higher than in the negative case although the latter condition seemed to give the more irregular interference. Close observation will bring out the fact that the current wave in the negative case is made up of a continuous value plus a heterogeneous succession of current impulses. A great many of these impulses will be observed to start in the positive direction. In other words, the average current is negative, but many of the impulses are in such a direction as momentarily to reduce the current rather than increase it as is practically always the case with positive polarity. This reversal phenomenon was particularly evident for the larger values of discharge current when the oscillograph screens were observed visually. The cathode-ray oscillogram of Figure 40-C indicates the erratic character of the negative discharges for currents well above the threshold value.

In the experimental work with negative discharges, the 60-degree point was practically the only one that could be depended on to give finite radio-interference characteristics of any regularity whatever. Furthermore, points that were made of steel or copper were rapidly al-

tered in their characteristics by oxidation and positive ion bombardment. Points constructed of tungsten gave much better results for operation over long periods of time.

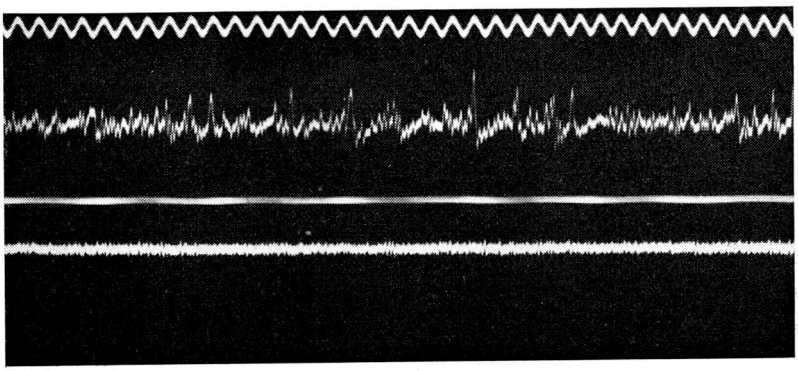

Figure 38. Direct-current corona discharge characteristics. Electrodes: 60° point to plane; spacing, 10.2 cm. Point negative, plane grounded; E = 36.2 kv., I = 28.3 microamp. Upper, radio noise; lower, current with zero line. Timing wave: 1,000 cycles.

An oscillogram of the sharp, slender point operating at 39 microamperes negative is shown in Figure 39. This oscillogram compares with that shown in Figure 35, the difference being only in polarity. Again, there is no perceptible radio interference and the current contains no apparent ripple. It should be explained that the slight appearance of radio interference was due to an extraneous disturbing factor, foreign to the test set-up.

3. **Cathode-ray oscillograms.** For the purpose of studying the instantaneous character of the point-discharge currents, a 2,000-volt cathode-ray oscillograph having a 5-inch blue fluorescent screen was connected across the resistor R_2 in the circuit of Figure 28. In this case, the power output tube and its circuit were disconnected. A circuit producing a single logarithmic sweep of the electron beam was provided, and the vertical deflector plates were connected directly across R_2. A biasing potential having the lowest possible capacitance to ground was provided for centering the image on the screen.

In order to make possible an analysis of the individual impulses occurring in the discharge current, it was necessary to employ a sweeping speed great enough to carry the image completely across the screen in approximately 200 microseconds. The image of the trace was consequently extremely faint, but by employing a camera having a lens opening of F/1.5, together with Eastman Super XX panchromatic film, it was possible to obtain weak photographic records of these traces. Figure 40 contains four cathode-ray oscillograms taken with this equipment. A 60-degree point spaced 10.2 cm from a grounded plane was used for each of the records.

Figure 40-A shows an individual positive impulse together with the steady ion-migration component of the discharge when the average current flowing from the point was 8 microamperes. The time scale given

under Figure 40-B is common to all of the oscillograms shown. Careful measurements made on the positive impulse of Figure 40-A indicate that the current increased from its steady value to the peak of the impulse in approximately 0.8 microsecond. The time to decay to one-half value was 7.4 microseconds. The crest of the impulse represents approximately 45.5 microamperes total, of which 37.5 microamperes were in the impulsive component. Figure 40-B shows the effect of placing a resistance of 10 megohms in the discharge circuit as near the point as possible. In this case, the current required approximately 3 microseconds to rise to the crest of the weaker impulse, and 13.5 microseconds to return to one-half value.

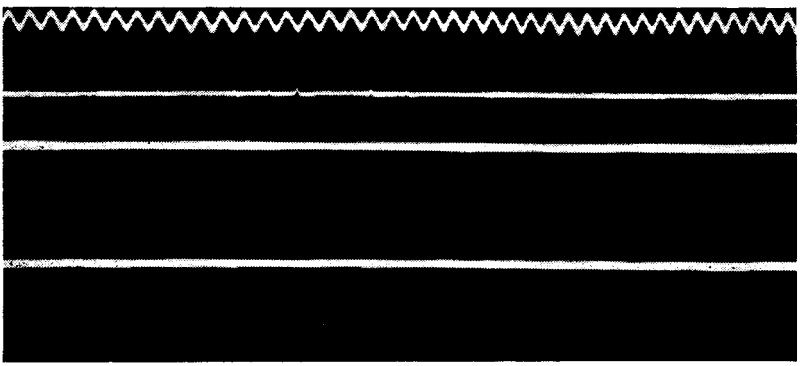

Figure 39. Direct-current corona discharge characteristics. Electrodes: slender, sharp point to plane; spacing, 10.2 cm. Point negative, plane grounded; E = 38.5 kv., I = 39.0 microamp. Upper, radio noise; lower, current with zero line. Timing wave: 1,000 cycles.

It is indicated that the resistor not only reduced the crest value of the impulse and increased its time of duration, but also reduced the rate of propagation of the ionization streamer that produced the impulse, thus reducing the steepness of the front of the wave. It is shown later in Section XII "Nature of Radio Interference Arising from Corona Discharges" that this resistance, because of the reduction in the rate of rise of the front of the impulses, results in a material decrease in the radio interference produced by the discharge.

Figure 40-C illustrates the erratic but impulsive character of the negative discharge from the same point, in this case producing a current flow of 10 microamperes. The greatest impulse attained its crest value in approximately 0.5 microsecond and returned to half value in 5 microseconds. The rate of rise of the negative impulses is accordingly shown to be extremely great, even exceeding that of the positive impulses. The erratic behavior of the negative discharge, in that the impulses may actually overlap, is clearly shown.

Figure 40-D shows that the 10-megohm resistor practically completely removed the impulsive character of the negative discharge. The oscillographic trace has now become merely a wavy line, showing, however, a few somewhat abrupt breaks. As would be expected, the radio inter-

ference produced by this discharge was a great deal less than that created by the discharge of Figure 40-C.

It is shown that in every case, both positive and negative, even with no external resistance in the discharge circuit, the impulses were critically damped, that is, there were no oscillations produced in the discharge circuit due to the current impulses. The Duddell oscillograph, accordingly, is shown to have given a reasonably good qualitative record, although the quantitative indications were not so good as might be desired due to the frequency limitations of this type of oscillograph.

4. **Characteristic Curves.** A series of discharge-current and radio-interference data was taken on each of several different types of elec-

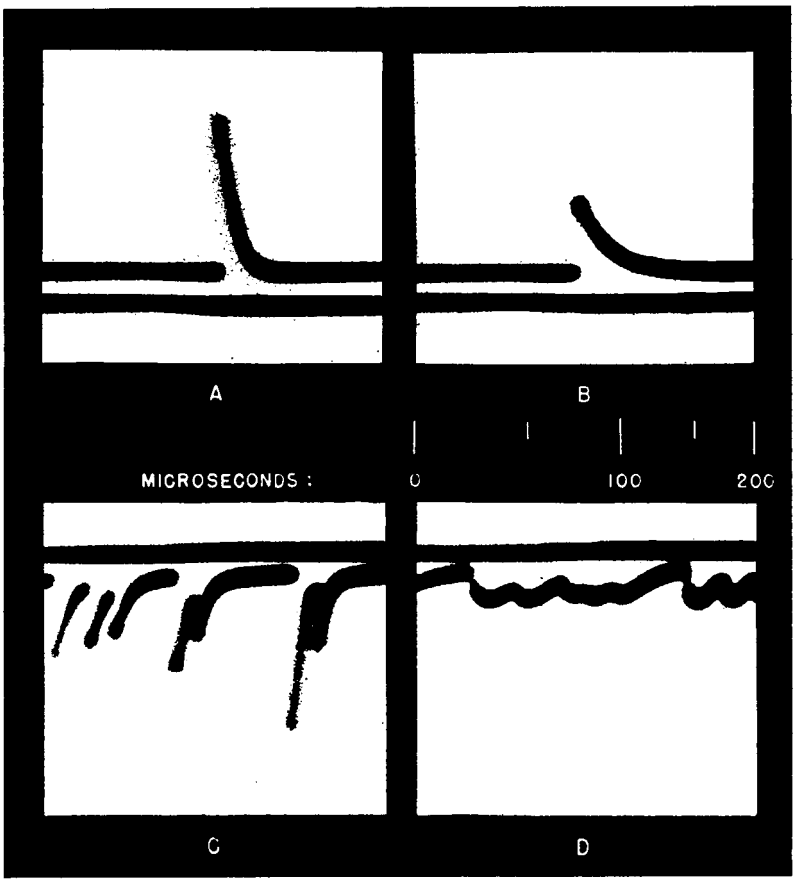

Figure 40. Cathode-ray oscillograms of point discharge currents. Electrodes: 60° point to plane; spacing, 10.2 cm. Polarity: A and B, point positive; C and D, point negative. Current (average): A and B, 8 microamp; C and D, 10 microamp. Discharge resistance: A and C, zero; B and D, 10 megohms.

trodes. These data are given in Tables 7, 8, 9, 10, 11, 12, 13, 14, Appendix V. The discharge characteristics of a 30-degree conical point-to-plane are shown in Figure 41. It is indicated that the negative currents were considerably higher throughout the entire range than the positive, and that the negative radio interference was very erratic. The character of the discharge occurring during this test was Type 1′ for the negative and Type 2′ for the positive. Type 2′, it should be explained, is somewhat a combination of Types 2 and 3, the long ionization needle of the Type 2 discharge being somewhat shortened and surrounded by a halo approaching the Type 3 characteristic. This type occurs frequently in the transitional period between the Type 3 and Type 2 discharge. The radio interference produced by the Type 2′ positive corona is of consistent character and, in general, is much more severe than that obtained from the same point operating at the same voltage but of negative polarity.

The performance of the 45-degree point is shown graphically in Figure 42. It is similar in most every respect to the 30-degree point. The discharge is again Type 2′ throughout most of the range, although at the lower voltages a Type 3′ appeared. This type of discharge is somewhat a combination

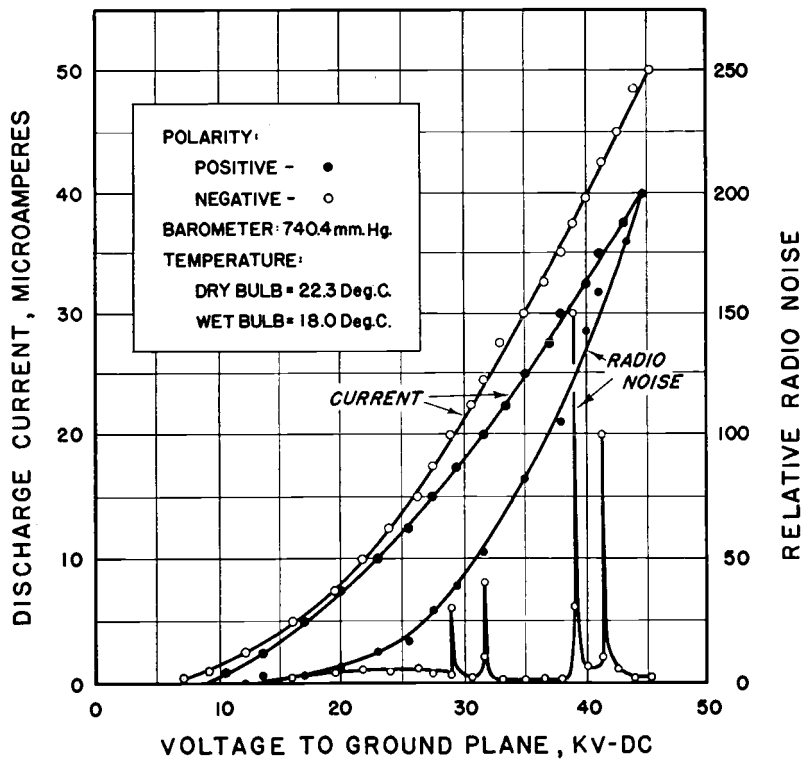

Figure 41. Direct-current point discharge characteristics. Electrodes: 30° conical point to plane. Spacing: 10.2 cm.

of the Type 1 and the Type 3 discharges in that the plume forms very close to the point, there being only a very short, concentrated streamer connecting the point to the diminutive plume.

The discharge characteristics of the 60-degree point are shown in Figure 43. The currents and positive noise were somewhat similar to those given by the sharper points, but the negative radio noise in this case was reasonably consistent, although considerably less severe than the positive. The discharges for this point were a pure Type 3 for the positive and a Type 1', with diminutive negative plume, for the negative.

The very interesting and useful discharge characteristics of the sharp, slender point are given in Figure 44. It is shown that the currents for this electrode were the highest of all the different points tested, but the radio interference, with the exception of one very weak disturbance at a relatively low voltage, was zero throughout the entire range. During practically all of the tests with this particular point, no interference was obtained on either polarity over the entire voltage range. The data indicating a small amount of interference were included on this particular

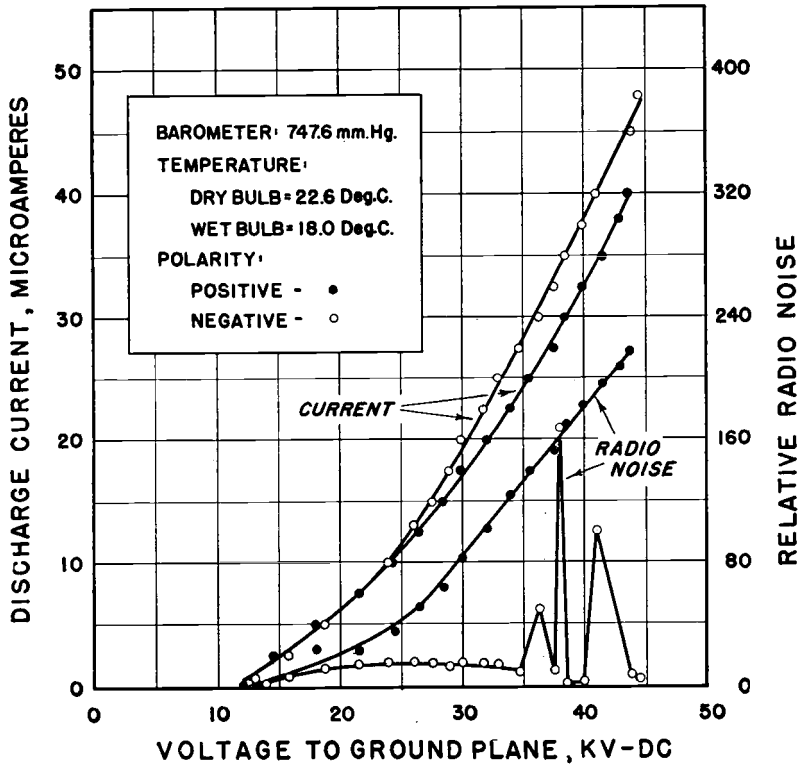

Figure 42. Direct-current point discharge characteristics. Electrodes: 45° conical point to plane. Spacing: 10.2 cm.

curve because on one occasion a minor disturbance did occur in that region.

No attempt was made to formulate a mathematical law of the discharge current as a function of voltage, spacing, and point configuration. Such a study is sufficiently involved to warrant special consideration.

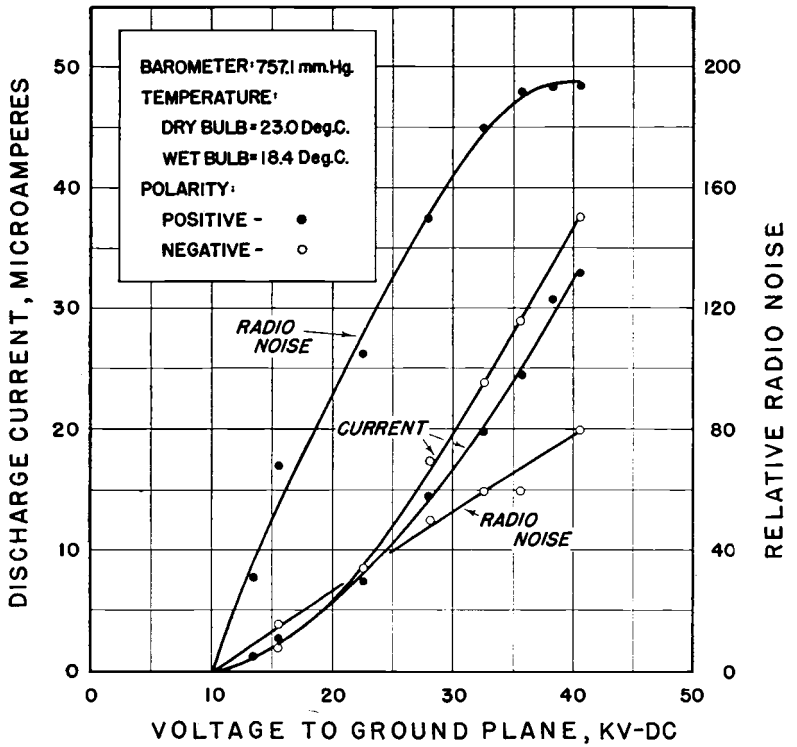

Figure 43. Direct-current point discharge characteristics. Electrodes: 60° conical point to plane. Spacing: 10.2 cm.

For both polarities and for all of the different types of points, it is indicated, however, that the discharge currents in the region near the threshold voltages are an approximate parabolic function of the voltage above the critical disruptive value. For the higher voltages, these currents approach a linear function of the point potential. It is indicated also that the sharpness of the point as well as the type of discharge has a definite bearing on the currents. As the points are made sharper; that is, as the included angle becomes less, the discharge current for both polarities becomes greater. For all of the conditions employed in these tests, the negative currents were observed consistently to be higher than the positive.

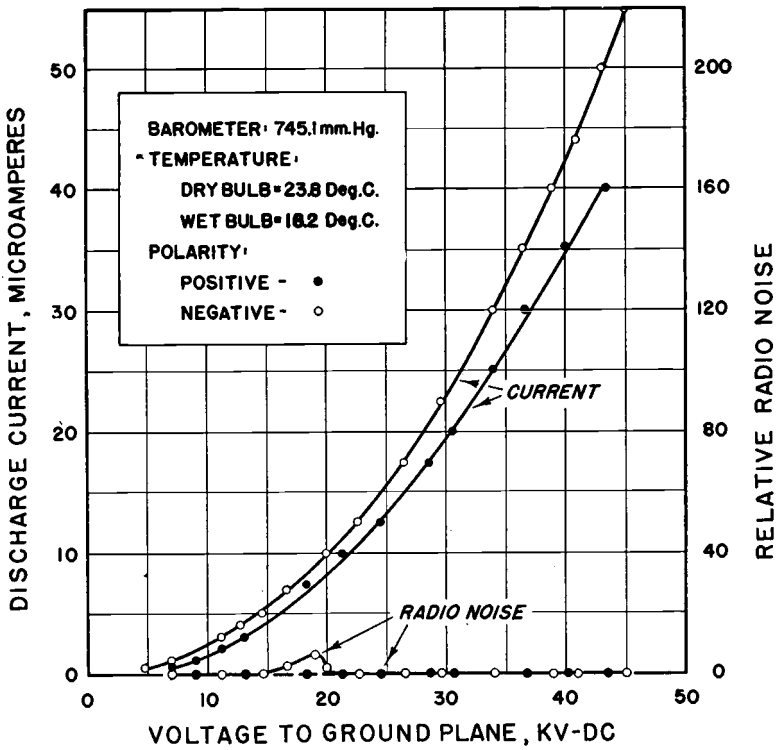

Figure 44. Direct-current point discharge characteristics. Electrodes: sharp, slender point to plane. Spacing: 10.2 cm.

XI. MECHANISM OF DISCHARGE

The foregoing curves and oscillograms point clearly to the nature and mechanism of high-voltage, direct-current discharges from points. Again, as in the case of alternating-current corona discharges from conductors, space-charge phenomena are controlling factors in the point-discharge mechanism (8), (9), (13).

When the discharge electrode is positive, and of a blunt-backed type such as the 60-degree conical point, a general ion migration seems to account for a continuous flow of current between the point and the ground plane. Positive streamers composed of electron avalanches periodically project into space from the point, creating relatively immobile positive-ion space charges which momentarily reduce the gradients and block further ionization until they have become reduced in intensity to the point where succeeding streamers can develop. Since the entire point is somewhat symmetrical, creating a localized region of high electric field concentration surrounded by a relatively large background shield, the phenomena repeat with definite regularity. The frequency of repetition as

well as the intensity of the streamers depends largely on the voltage and, therefore, on the current being discharged from the point. These individual positive streamers are responsible for the current impulses superimposed upon the otherwise relatively steady flow of current.

In the case of the sharper points with a less effective backing, the space charges do not build up with such definite regularity, and the positive streamers are of a more random character. The orderly repetition of current impulses does not, therefore, occur.

Surrounding the end of the extremely sharp point having a long slender shank, the positive space charge seems to build up to a stable equilibrium and remain there over a wide range of discharge currents. This space charge, with its internal gradient falling off rapidly from the point outward, blocks off the development of any positive streamers, and, hence, no current impulses occur.

In the case of the negative polarity, the positive-ion space charges are established in the region of high potential gradients and tend to move in toward the point of discharge. As they approach it closely, the voltage gradients build up to the point where further impulsive discharges occur. This mechanism results in the extraction of large numbers of electrons from the electrode and its vicinity. For low values of negative discharge currents, these electrons move outward with relatively low velocities and create, momentarily, a neutral or even negative space surrounding the point. As more remote ions move in, the positive space charge is again established, and the process is repeated. These phenomena result in the negative current impulses appearing in the circuit between the plane and ground (see Figure 40-C). At the higher voltages, however, the clouds of electrons are projected with much higher velocities and result in the rapid creation of high positive space charges that actually block off, momentarily, the passage of more electrons out into the interelectrode space. Hence, the current appearing in the ground circuit tends to drop off abruptly as each of these high positive space charges is created, thus resulting in apparent positive impulses on the negative current flow. As these positive space charges move in toward the ionization point, breakdown occurs with great abruptness, and hence the fronts of the current impulses are exceedingly steep although the impulses themselves are not always large in magnitude. Professor Loeb and his associates have done considerable work upon the physical nature of these ionization phenomena and have studied certain phases of the subject in great detail (13).

Two of the most interesting characteristics brought out by the above tests are as follows:

1. A sharp, slender point can be caused to discharge positive or negative electricity in amounts up to at least 40 or 50 microamperes per point without creating any appreciable radio interference at frequencies up to several megacycles.
2. Rough points, which microscopically are sharp points with rather blunt backing, produce the most severe negative radio interference and also produce the musical-note type of positive interference.

It is proposed to carry on more extended studies of the high-voltage point-discharge phenomena. It is particularly important that the radio-interference characteristics in the ultrahigh-frequency region be examined.

XII. NATURE OF RADIO INTERFERENCE ARISING FROM CORONA DISCHARGES

The nature of direct-current point discharges, as brought out by the oscillographic study outlined in the previous section, gave a very definite clue to the mechanism of the radio interference produced by such discharges. It was evident that the disturbances were created by the steep-wave-front current impulses. Particularly in the low-current, positive discharge studies, it was obvious that each impulse was accompanied by a heavy shock in the radio.

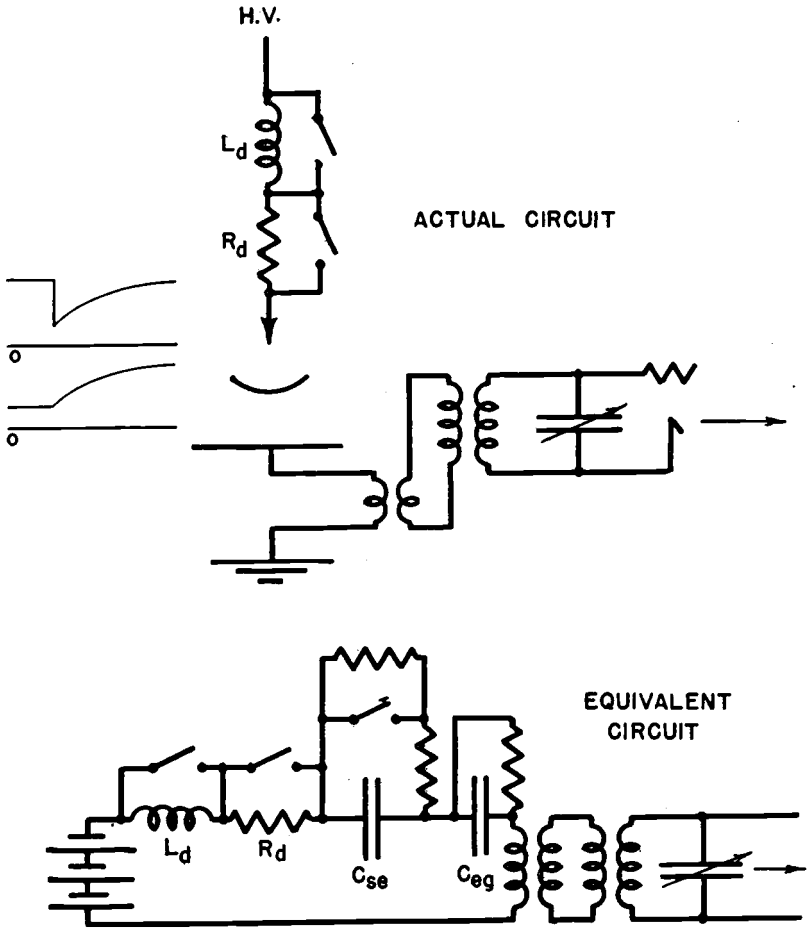

Figure 45. Test circuit with loop pick-up.

The essentials of the circuit employed in these tests, so far as the coupling to the radio field-strength set was concerned, are given in the diagram of Figure 45. The electrical equivalent of this circuit as it might be set up for a deliberate low-frequency study is shown in the same figure. In the actual circuit the input to the radio receiver is through an inductive coupling between the circuit carrying point-discharge current and the parallel-resonant antenna circuit of the radio receiver. The waves at the left of the discharge point indicate what might be expected of the voltage appearing on the point and also on the space charge surrounding the point, indicated in the diagram by the arc of a circle, as the recurrent impulses develop.

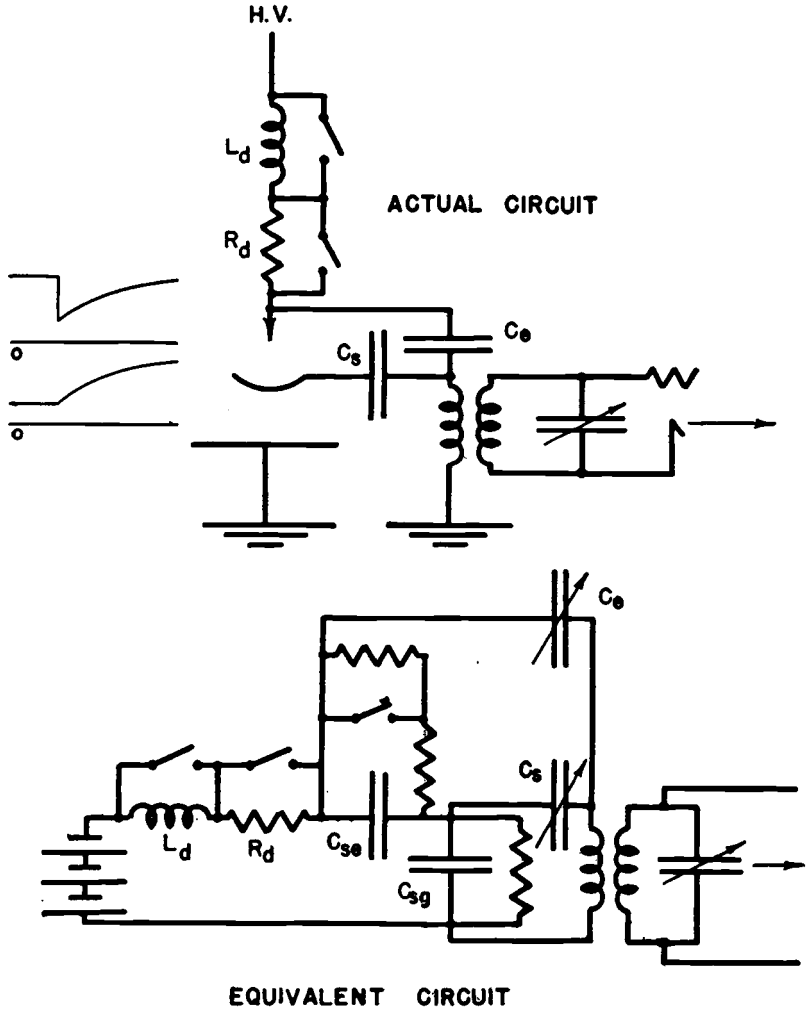

Figure 46. Antenna to discharge-point pick-up.

The impulsive currents, in flowing to ground through such an inductively coupled system, induce transient voltages in the antenna circuit of the radio receiver. These voltages drive the tuned antenna circuit into oscillation at its natural period, and since each resultant oscillation has a definite decrement due to circuit losses, the high-frequency disturbance carried into the radio-frequency amplifiers is effectively modulated and appears in the output circuit as a surge of energy. The intensity of this surge depends on the amplitude of the oscillation induced in the antenna circuit

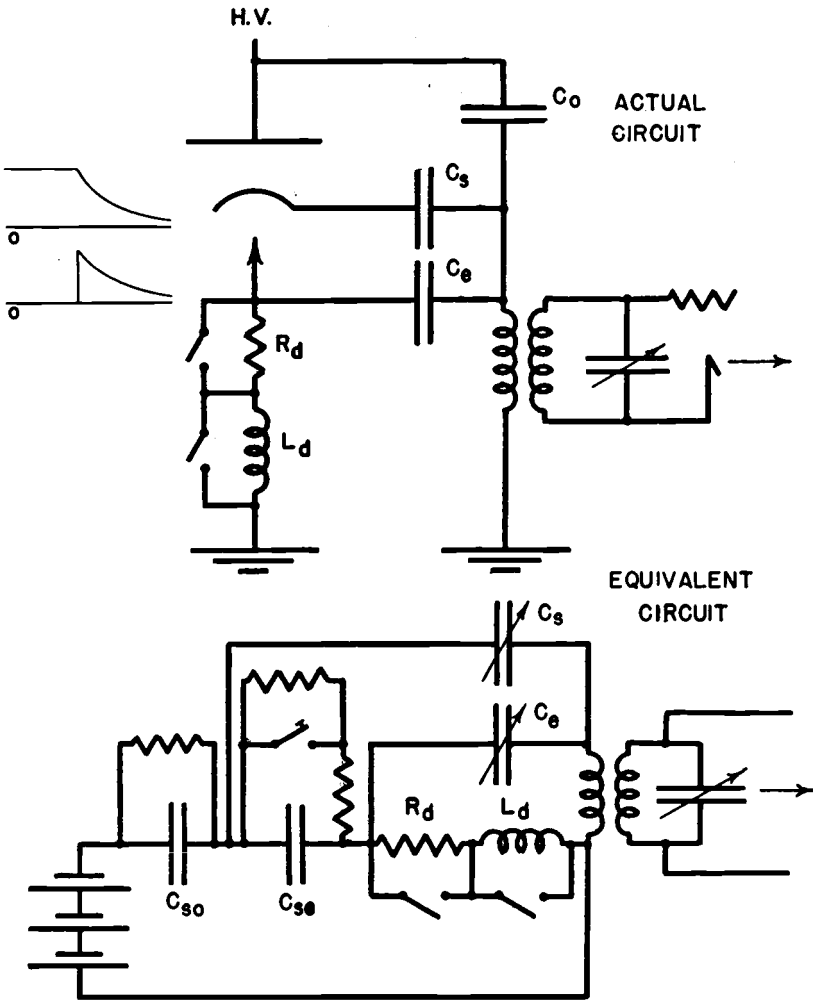

Figure 47. Antenna to grounded-point pick-up.

by the steep-wave-front current impulse. Since the induced voltage is equal to $M \cdot di/dt$, the steepness of wave front of the current impulse, as well as its magnitude, influences this voltage. A current impulse of high amplitude and steep wave front, therefore, would be expected to induce a severe oscillation in the tuned antenna circuit of the radio receiver and a resultant heavy surge in the output.

In many cases of radio disturbances produced by point discharges, the coupling of the discharge point and of the space charge surrounding that point to the radio antenna is capacitive. This type of circuit is illustrated in Figure 46. Here again the individual current impulses occurring in the discharge circuit produce similar, although much smaller, current impulses in the primary of the antenna-circuit coupling coil. The same mechanism, therefore, applies in this case as in the former with respect to the transient excitation of the tuned radio-frequency circuits. The equivalent circuit for low-frequency studies of this type of interference pick-up is given in the same figure.

In case the discharge occurs from a grounded point, or from one at the same potential as the radio receiving equipment, toward a high-voltage space or plane, the circuit of Figure 47 applies. Again, the current impulses have their counterpart, due to capacitive coupling, in the primary of the antenna coil. This is the condition most frequently encountered in aircraft precipitation-static radio interference.

1. **Impulse excitation of oscillatory circuits.** It is evident that in every practical case, the coupling of the radio receiver to the discharge circuit is such as to cause steep-wave-front currents to pass through the primary of the antenna-coupling transformer when similar currents appear in the corona-discharge circuit. The subject resolves, therefore, into a study of the impulse excitation of oscillatory circuits.

An equivalent circuit for such a study is given in Figure 48. In this case the quantities R, L, and C are the constants of the circuit of an impulse generator. The mutual inductance M, coupling the impulse generator to the oscillatory circuit, is assumed to be very small relative to L, and hence a negligible amount of the disturbance created in the oscillatory circuit is fed back into the exciting circuit. The quantities R′, L′, and C′ are the constants of the oscillatory circuit.

If the key in the exciting circuit is raised to the upper position, the capacitor C is charged by means of the battery to a certain voltage. If this key is then depressed, the capacitor will discharge through the circuit composed of R, L, and M, and if R is greater than the critical value, this discharge will be impulsive in character. Such an impulse will cause the same type of voltage to be induced in the oscillatory circuit as the discharge impulses in the high-voltage point-discharge circuits cause to be induced in the tuned antenna circuit of the radio receiver. The oscillatory circuit should, therefore, respond to the impulse excitation in a manner exactly similar to that in which the high-frequency circuits of the radio receiver respond to the impulses in the antenna circuit.

The complete circuit of Figure 48 has been treated mathematically in Appendix II and curves derived from equation (1) are given in Figure 49. These curves indicate the wave shape of the currents created in the exciting circuit of Figure 48 for different values of the quantities R and L. The capacitance C and battery voltage remain constant. Solid curve number 1 is the result of relatively low inductance and low resistance.

Solid curve number 2 is the result of the same inductance as was used for number 1 but with R increased by a factor of four. Solid curve number 3 is the result of the same resistance as was employed for number 2, but with the inductance multiplied by eight.

The dotted curves show the voltages that the respective current waves would inject into the oscillatory circuit through the mutual inductance M. It will be observed that waves number 1 and number 2 induce the same maximum voltages but have much different times of duration,

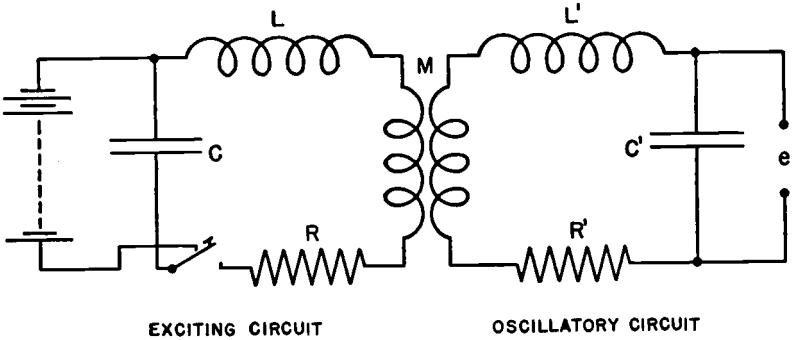

Figure 48. Impulse excitation of oscillatory circuit.

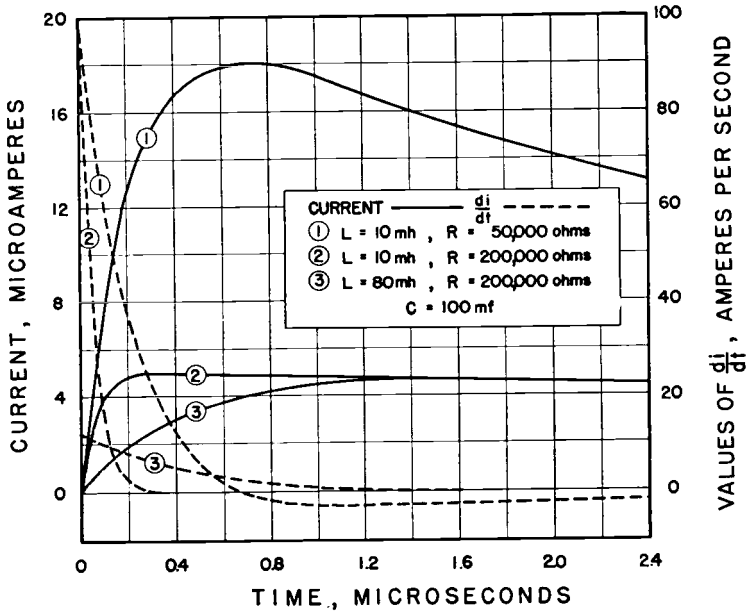

Figure 49. Impulse current waves. Influence of resistance and inductance in discharge circuit.

number 2 being the shorter. Wave number 3 induces a very much lower voltage with a relatively long time of duration. The general equation of these voltages is 2, Appendix II.

When such voltages are induced into the oscillatory circuit, the potentials resulting at e are given by equation (7). As long as the resistance R' is kept below the critical value, these potentials will be oscillatory in character. The amplitude of the oscillation will be determined very largely by the character of the voltage induced in the oscillatory circuit by the mutual inductance, M.

The waves of Figure 15 were calculated by means of equation (7), Appendix II, and illustrate the types of oscillatory voltages appearing at e when the three different impulsive currents of Figure 49 are caused to flow in the exciting circuit. The amplitude of the voltage produced by impulse wave number 1 is relatively large. Wave number 2 results in a somewhat smaller voltage at e while exciting wave number 3 produces an oscillation of the lowest amplitude of all. Of particular interest is the fact that the introduction of higher resistance in the exciting circuit, resulting in impulse current waves of lower amplitude, produces correspondingly lower amplitudes of oscillation at e.

Of further interest is the effect of increased inductance in the exciting circuit. The introduction of this higher inductance at L, together with the same resistance at R as was employed for impulse wave number 2, results in a current wave of essentially the same maximum amplitude but of greatly reduced steepness of front. The relative amplitudes of oscillatory waves number 2 and number 3, Figure 50, illustrate the effectiveness of this reduced steepness of front of the exciting impulses in producing lower amplitudes of oscillation at e (Figure 48).

These results can be summarized briefly as follows:

1. The steepness of front and amplitude of the impinging impulse have a direct influence on the magnitude of the oscillation induced in the tuned circuit.
2. The steepness of descent of the tail of the impulse, if it occurs at approximately one-half period of the resonant circuit, has a direct influence on the amplitude of the oscillation.
3. The area under the impulse-current wave for the first one-fourth period of the oscillatory circuit has a direct bearing on the magnitude of the induced oscillation.
4. Resistance in the discharge circuit, since it cuts down the amplitude of the current impulse and therefore the average rate of rise of the wave from zero to crest, reduces the amplitude of the induced oscillation. Figure 40 illustrates this property oscillographically. Since resistance does not change the initial rate of rise of the front of the impulse, its effect is most pronounced for the lower oscillation frequencies.
5. Inductance in the discharge circuit, since it reduces the steepness of front of the current impulse, tends to cut down the amplitude of the induced oscillation.

The above analysis and summary indicate that not only resistance but also inductance in the high-voltage point-discharge circuits should be effective in reducing the impulse excitation of the tuned antenna circuit of the radio receiver. This analysis again indicates that the type of radio interference produced by these high-voltage discharges is of impulse excitation character, the only high-frequency oscillations appearing in general

being those set up in the antenna circuit of the radio receiver, at the frequency for which it is tuned, by the impinging impulse.* It is evident, therefore, that any operation upon the interfering circuit that will eliminate or will lessen the amplitude and reduce the steepness of wave front of the individual current impulses will result in improved radio interference characteristics. (See also Section XVI) It is also evident that as the resonant frequency of the tuned input circuit of the radio receiver is increased to the high and ultrahigh-frequency regions, the amplitude of the induced oscillations created by the current impulses will decrease to a marked degree. For a given radio-receiver sensitivity, then, much less interference would be expected from the high-voltage point discharges in the high and ultrahigh-frequency regions than in the normal and low-frequency bands. Recent experience with ultra-high-frequency equipment has borne out this prediction.

The influence of discharge resistors and inductors on the radio-interference characteristics of point discharges was examined experimentally and typical results are given in Table 16. The same data are presented graphically in Figure 51. A 50-degree conical point was employed, and the series resistance changed from zero to two megohms and the series inductance from zero to 37.2 millihenrys. A reduction of more than 50 per cent in the radio interference was produced by the two-megohm

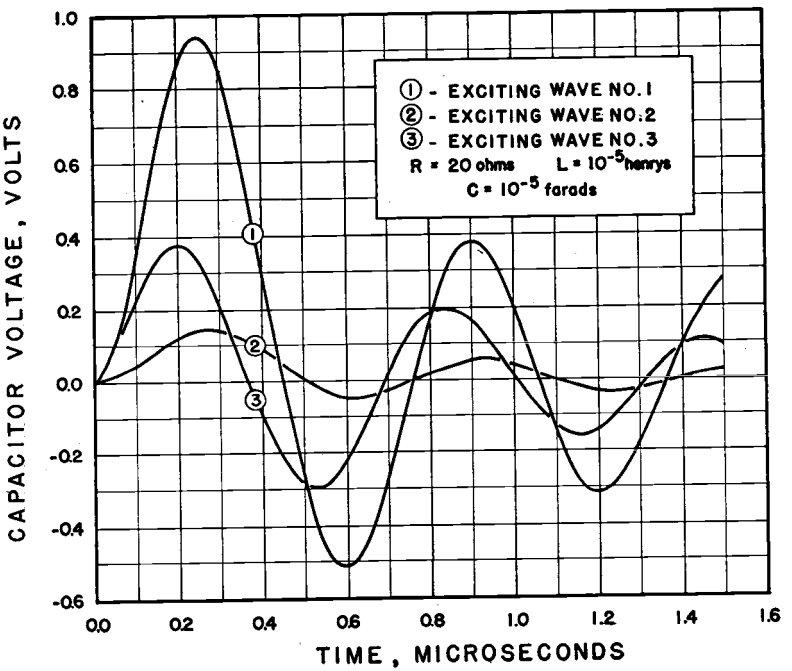

Figure 50. Impulse excitation of oscillatory circuit.

*In certain cases parts of the circuit carrying the discharge currents are driven into complex, damped high-frequency oscillations and interfering energy is radiated directly. This mechanism, however, is believed to be the exception rather than the rule, particularly in direct-current corona phenomena.

resistor. A further 50-per-cent decrease followed the introduction of the inductance. The inductor employed was not of a particularly good radio-frequency type, but it did verify the analysis and result in a definite improvement in the radio-interference characteristics.

It is evident that the introduction of large amounts of resistance and inductance, with a minimum of distributed or shunt capacitance, in the high-voltage circuit as close as possible to the discharge point will result in minimized radio disturbances. Certain precautions, however, must be employed in using these resistors and inductors. Reference to the circuit of Figures 45, 46, and 47 will show that the voltage of the point may be expected to change abruptly with each impulsive discharge when resistors and inductors are incorporated in the discharge circuit. To prevent these sudden changes of voltage from inducing current impulses in the radio antennas, some form of shielding about the point might be necessary.

XIII. RADIO RECEIVING ANTENNAS

Energy-abstracting devices for radio-receiving equipment fall into three general classes:

1. The extended-conductor or open-wire antenna.
2. The simple-loop antenna.
3. The shielded-loop antenna.

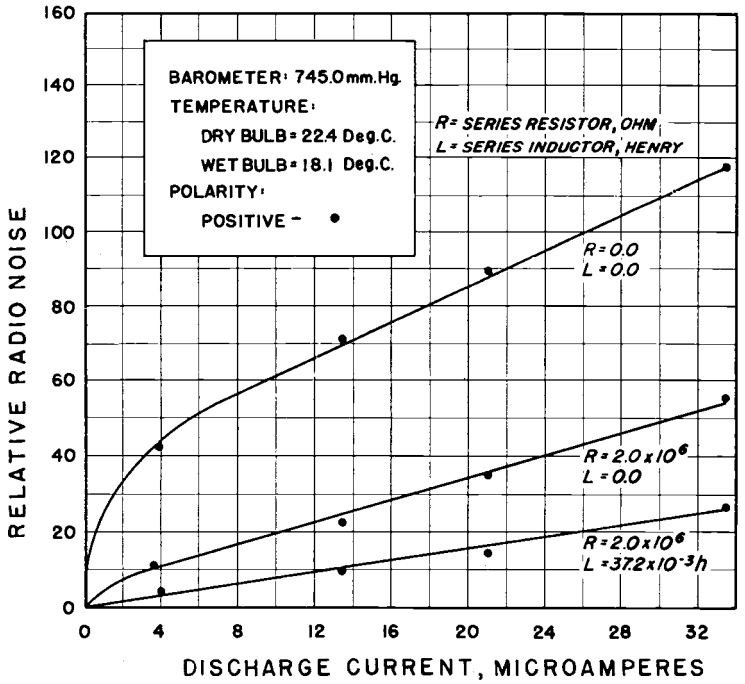

Figure 51. Direct-current point discharge characteristics. Influence of series resistance and inductance on induced radio interference. Electrodes: 50° conical point to plane. Spacing: 10.2 cm.

The extended-wire type responds to the traveling electromagnetic wave and is also sensitive to any electric field in its vicinity. The true wave of electromagnetic radiation is composed of equal electric and magnetic components, and the voltage induced in the open antenna is essentially the same as that created in space by the passage of the wave. Induction fields, preponderantly electric or magnetic, can be caused to exist, however, but their space coverage is relatively very limited. An extended-wire antenna in the presence of these induction fields will respond to both types (Appendix III).

The unshielded-loop antenna may be either a balanced or an unbalanced type. In the latter case, the loop will respond to both magnetic and electric radiation and induction fields. The magnetic response is essentially by transformer action. The electric-induction response is due principally to charging currents flowing through the loop circuit to ground.

The balanced loop responds well to magnetic excitation, again by transformer action, but is very insensitive to electric excitation. In this case, the charging currents due to electric fields flow to ground equally in both directions through the loop, thus effectively cancelling any pick-up that might result. If the midpoint of this balanced loop is grounded, a similar cancelling of electric-field pick-up will occur.

The shielded radio loop, when shielding, is composed of a broken, metallic tube surrounding the turns of the loop and is balanced to ground, is responsive only to the magnetic field. In this case, any changing electric field terminating on the loop produces currents that are conducted to ground in practically equal magnitudes and in opposite directions around the two parts of the shield. Consequently, no potential is induced in the loop proper due to these charging currents flowing to ground. Any improvement in the shielding design that will tend to maintain a balance between the charging currents flowing to ground through the two sides of the shield will be beneficial in its results. The cross-section of the shield itself seems to present a short-circuited area to the impinging electromagnetic signal waves and has some undesirable attenuating effects on the received signal. This condition undoubtedly could be improved considerably by properly laminating the shield in a direction parallel to its minor axis.

XIV. THE SHIELDED-LOOP ANTENNA

It was brought out very definitely in the sections on flight research and ground tests that the shielded loop possessed marked advantages over the extended-wire antenna in its ability to discriminate between the desirable signal and undesirable "static" interference. This feature has been known for several years, particularly as regards effectiveness with certain types of static, and it has been employed advantageously in a number of fields. Its effectiveness in the attenuation of precipitation static on aircraft is due to the fact that this static interference originates fundamentally as a high-voltage low-current discharge phenomenon. The electric fields associated with these discharges are necessarily intense while the magnetic fields, due to the relatively feeble character of the currents, are very weak.

It has been shown that the discharge currents are composed of steady

values with superimposed double-exponential impulses. Such currents may be represented by a complex series of multiple-frequency waves. These waves will produce true electromagnetic radiations. Since the alternating current components are very small, however, the radiation fields, which are functions of the currents, necessarily will be weak. The electric induction fields, on the other hand, are relatively intense because the voltages involved are of the order of several thousand, and the distances from the source of the interference to the antennas are not great. As a matter of fact, for the normal radio frequencies these distances are only of the order of a small fraction of a wave length. An open antenna should, therefore, respond strongly to the electric fields in the vicinity of the corona discharges, and weakly to the magnetic fields accompanying these discharges (Appendix III).

The properly shielded loop, on the other hand, as has been shown in the previous section, rejects the electric induction interference and accepts only the magnetic field. This magnetic excitation has essentially two components (Appendix IV). The first is that of induction, which varies directly with the current and inversely as the square of the distance from the source. The second is that of radiation, which not only varies directly with the current but also with frequency, and inversely as the first power of the distance. The well-known radiation and induction equations indicate that these two components of the field are of equal intensity at a distance from the radiator equal to the radiated wave length divided by 2π (Appendix IV).

In the case of the normal beacon receivers, the wave length is of the order of 1,000 meters and the distance of equality between the magnetic components of the induction and radiation fields is approximately 159 meters. At distances of the order of 10 to 50 feet from the source of interference, the radiation component of the magnetic field would then be expected to have a value of the order of 2 to 10 per cent of that of the induction component. The shielded loop will respond to this resultant magnetic field even though it is weak, and at short distances the response to the induction component will predominate. The strength of interference pick-up in the shielded loop should then vary almost exactly as the inverse square of these short distances from the interference source. This law has been found to apply in some tests conducted in their Chicago Laboratories by the Communications Staff of the United Air Lines (10).

The interference pick-up of the open antenna due to its exposure to the intense electric fields, should be expected to be great. It is shown in Appendix III-A that the electric pick-up of such an open antenna from an essentially localized source should be a function of the voltage of the source, and for the intermediate distances chosen, should be a function of the approximate inverse cube of the distance from this source. This prediction is also borne out by the results of the United Air Lines tests referred to above.

1. **Improvement of shielded loop.** The problem of reducing the interference pick-up of the shielded loop is primarily one of removing the source of disturbance as far as possible from the loop, taking advantage of the inverse-square law, and of reducing as much as possible the amplitude and wave front of the individual current impulses in the discharges.

The relative sensitivities of the shielded loop and open antenna to corona-discharge static suggest a possible means of further improvement

in the loop characteristics. The charging current flowing in the antenna or loop shield due to electric induction is proportional to and, at that point, is in phase with the magnetic field emanating from the conductor inducing the electric field. Hence, the voltage-inducing capacity:

$$M \frac{di}{dt} = K \frac{d\phi}{dt}.$$

If an arrangement were established whereby a small amount of this charging current were caused, by mutual induction, to inject a voltage into the shielded-loop circuit equal to and in phase opposition to the loop output due to the corresponding magnetic field, a complete cancelling action would result.

A small, open antenna, such as an isolated area in the extremity of the loop shield, could be connected through a shielded lead-in and a variable, reversible mutual inductor to the loop output circuit. Such an antenna could be made to have a very weak signal response while retaining its sensitivity to the interfering electric field. By proper adjustments of the mutual inductor, the small magnetic induction voltages of the loop could be cancelled in the output circuit by the voltages obtained from the charging current.

Since the loop has a definite directional sense to interference as well as to signals, the above arrangement would be most effective if the source of the principal interference could be localized in a definite plane.

The use of this device in connection with crossed loops seems to offer good possibilities.

It would probably be necessary to control the coupling inductor from the receiver control panel in order to obtain the proper balance for different conditions.

Experimental work has shown that the corona-discharge-static response of an unshielded, unbalanced loop, with one end of the loop grounded, may be less, for certain loop positions, than that of a completely shielded loop (10).

This characteristic is probably a demonstration of the cancelling action described above. The charging current flowing to ground through the loop conductors induces a voltage in phase opposition to that of normal loop pick-up when this loop has a certain orientation with respect to the interfering source. If the loop is rotated 180 degrees, the two voltages are placed in phase conjunction and increased interference intensity results.

If the electric and magnetic components of the fields impinging upon the loop and antenna arrangement described above produce voltages of equal magnitudes, as in the case of electromagnetic waves, the cancelling action would remove not only the interference but also the signal. It will be shown, however, in the next section, "Electric and Magnetic Induction," that at short distances from high-voltage interfering sources, the electric component may be much greater than the magnetic and hence only a relatively weak open-antenna response will be required.

XV. ELECTRIC AND MAGNETIC INDUCTION

The subject of voltage and energy abstraction by electric and magnetic induction, in the case of conducting elements of simple geometries,

is one that lends itself rather readily to a mathematical analysis. In Appendix III such an analysis has been made. The simple geometries of a straight, overhead conductor inducing voltage and power in loops and conductors parallel to the first element were chosen. These conditions simulate, to a limited extent, the case of a loop antenna receiving voltage and energy by magnetic induction from a radiating conductor, as well as the case of an extended antenna receiving voltage and energy by electric induction from the same conductor. In the final analysis, examples were chosen in which the only current flowing in the inducing conductor was that due to its voltage, frequency, and capacitance to ground. The open-circuit voltage and maximum energy obtainable from the inductively coupled circuits were then computed.

In the case of a radio receiver, the antenna circuit is one of parallel resonance, and since the grid circuit of the first stage of the radio-frequency amplifier is of extremely high impedance, the over-all impedance of the input circuit is high. Although it takes energy to drive this circuit, the response is more a matter of the voltage induced in the input circuit than of the maximum energy available at that point.

For a pick-up loop of the same length as the inducing conductor, Equation 45, Appendix III, gives the open-circuit voltage of magnetic induction. It will be observed that this voltage is a function of the square of the frequency. For loops of shorter length than the inducing conductor, but located near the driving end, Equation 51, Appendix III, applies. Again, the voltage is a function of the square of the frequency.

The open-circuit voltage induced electrically on an extended, parallel conductor by the potential on an inducing conductor, is given in Equation 24, Appendix III. This equation indicates that the induced voltage is independent of frequency and is dependent only upon the voltage of the inducing conductor and upon the interconductor and ground capacitances.

The maximum power that can be obtained by magnetic induction from the full-length loop illustrated in Figure 52 is given by Equation

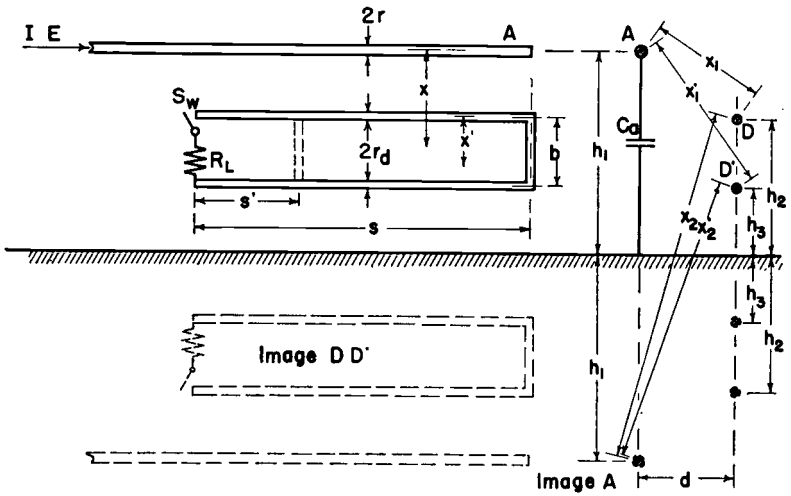

Figure 52. Magnetic induction.

47, Appendix III. This equation is complex but contains factors indicating that the power varies with the cube of the frequency and the square of the voltage. For loops of fractional length located near the driven end of the conductor, this equation becomes 53, the power being still a function of the cube of the frequency and the square of the voltage.

In the case of electric induction employing the circuit of Figure 53, the maximum power available is given by Equation 40, Appendix III. This equation indicates that again the power is proportional to the square of the voltage, but this time to only the first power of the frequency. From the above equations, it is evident that at relatively low frequencies the voltage and power induced electrically may be much higher than that induced magnetically, whereas at high frequencies the exact reverse of these conditions may be obtained.

In Appendix III, examples are worked out for the purpose of determining the voltages and powers to be obtained from certain conductor arrangements and frequencies. The conditions of the examples are given in Appendix III. For the full-length loop, magnetic pick-up at 100 cycles per second, the open-circuit voltage is only 4.33×10^{-5} volts, whereas the electric open-circuit voltage is 2.18×10^{3} volts. With the frequency raised to one megacycle, the magnetic voltage becomes 4.33×10^{3} volts, and there is no change in the electric potential. It is shown that the induced open-circuit voltages are identical at a frequency of 7.08×10^{5} cycles per second.

If the pick-up loop only is reduced in length to 1 per cent of its former value, the magnetic voltage at 100 cycles per second is 8.59×10^{-7} volts. At 1 megacycle this voltage becomes 85.9 volts. Under this condition, to obtain the same voltages from both electric and magnetic inductions the frequency must be raised to 5.03 megacycles.

The maximum power obtainable from the full-length loop by magnetic induction at 100 cycles per second is shown to be 9.4×10^{-9} watts, whereas this power becomes 9.4×10^{3} watts when the frequency is raised to 1

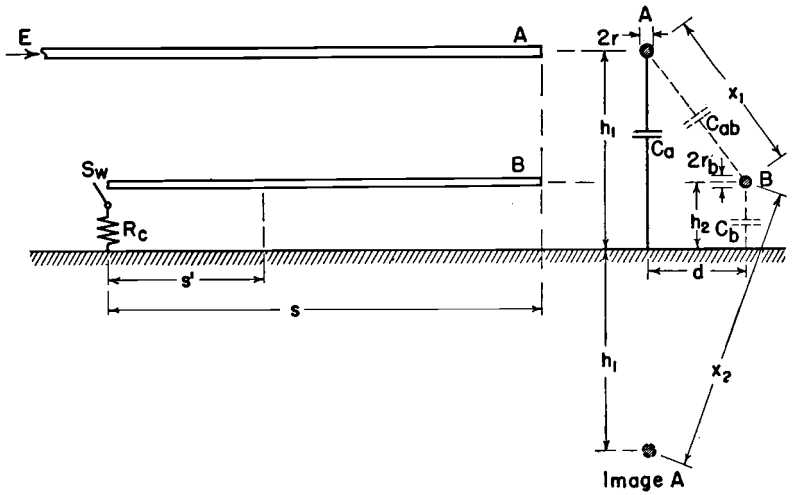

Figure 53. Electric induction.

megacycle. The maximum power obtainable by electric induction from the full-length conductors at 100 cycles per second is 2.69×10^{-2} watts, and if the frequency is raised to 1 megacycle this power becomes 269 watts. The frequency for equal maximum powers by both types of induction becomes 1.69×10^{5} cycles per second. For the short pick-up conductor and loop, but with full-length inducing conductor, the maximum powers become equal at 1.09×10^{5} cycles per second.

If the short pick-up loop is retained, but the inducing conductor is reduced to 4 per cent of its original length, namely to four meters, the frequency for equal power by both types of induction becomes 3.11×10^{6} cycles per second. The induction voltages become equal at 26.8×10^{6} cycles per second (Appendix III, Equation 81). It is thus necessary, for this condition, to raise the frequency to relatively very high values to bring about voltage and power equalities by the two types of induction. These results indicate further that in the ultrahigh-frequency field the high-voltage corona-discharge disturbances should be a great deal less severe. It is even questionable if the shielded loop will show its great noise-suppressing property in the ultrahigh zones.

The foregoing analyses indicate that electrical disturbances that are fundamentally of a high-voltage character may be expected to create a much greater response in a nearby radio receiver driven by an open antenna than in one that is driven by a shielded or balanced loop. As has been noted previously, these conclusions are in exact accord with those obtained experimentally.

XVI. CONTROL OF ELECTRICAL DISCHARGES FROM AIRCRAFT

Since at present it appears impossible to prevent the accumulation of electric charges during flight through certain storm conditions, corona discharges from extremities of the aircraft of necessity must occur when the potential differences between these extremities and the surrounding atmosphere become sufficiently high. It has been shown that these discharges will produce interference in the normal-frequency radio receiving equipment on board the aircraft unless they are so controlled as to prevent the appearance of random, steep-wave-front current impulses.

It is probable that some discharging action is obtained through the medium of the ionized exhaust gas from the engines. It has been suggested that further discharging could be produced by projecting an ionized solution into the atmosphere from the charged airplane. Such methods at present seem inadequate, however, and apparently it is necessary to resort to some ionization device to maintain the proper potential equilibrium.

A conductor trailing from the tail of the airplane and terminating in one or more sharp, slender points would be expected to discharge considerable energy to the region immediately surrounding the points. It has been shown that such sharp, slender points produce discharges, regardless of polarity, which for low and intermediate values of current are free from the disturbing current impulses. To guard against interference from other types of discharges that might form in the vicinity of these points, it would be well to supply the trailing or projecting conductors with resistive and inductive wave-front suppressors.

There are many conditions of flight through severe storm areas where a single trailing conductor on a very large airplane would not provide adequate discharging capacity. In those cases it would be desirable to have point dischargers of the sharp, slender variety, with resistive and inductive wave-front suppressors, on the wing tips and probably also on the nose of the airplane. The wing-tip electrodes, and possibly also other discharge points at the extremities of the vertical and horizontal fins, might be of either a trailing or projecting type. Other sharp projecting edges and points on exposed parts of the airplane then should be carefully removed.

Discharge electrodes of other than the sharp, slender type can, under certain conditions of operation, be made to function satisfactorily. Continuous, heavy ionization at these discharge points, such as can be produced for example by the projection of an ionized liquid, by relatively low-voltage direct-current arcs or by high-voltage, radio-frequency arcs, will result in the elimination of current impulses and their accompanying radio disturbances. The performance of such rather complicated devices under high-velocity air movement conditions is uncertain.

It is probable that under some conditions of heavy charging, the radio transmitting antenna may go into corona. To avoid such a possibility in a final clean-up this antenna might be equipped with a moderately heavy rubber insulation. Such insulation would have the effect of reducing the potential gradient at the surface of the conductor and would thereby increase the voltage required for ionization.

The end to be worked toward is that of allowing sufficient energy to be discharged from the controlled points to keep the potential of the plane low enough, with respect to the surrounding atmosphere, to prevent discharges from occurring elsewhere.

The propellers may be found to be serious offenders. In that event, it might be necessary to ground the engines to the fuselage of the ship only through high-resistance and inductance suppressors. It would not be impossible to connect the propeller blades to the hub electrically only through similar suppressors.

Exposed, normally insulating surfaces such as windshields and deicer boots can be made electrically conducting and thus the accumulation of sufficient charge on such surfaces to cause sparking over to metal supports can be prevented.

It has been suggested that it might be beneficial to excite all of the controlled discharge points on the airplane by means of a high-voltage oscillator, thus causing the discharge to occur periodically, permitting radio reception to be effective during the dead periods. The actual development of this scheme seems physically difficult, but it might be expected to give positive results.

XVII. BIBLIOGRAPHY

1. Cohen, L. Calculation of Alternating-Current Problems; McGraw-Hill Book Co.
2. Henny, K. Radio Engineering Handbook, 2nd ed., p. 93; McGraw-Hill Book Co.
3. Peek, F. W., Jr. Dielectric Phenomena in High Voltage Engineering, 3rd ed., Chaps. II and XI; McGraw-Hill Book Co.
4. Lamb, J. J. A Noise Silencing I. F. Circuit for Superheterodyne Receivers, QST, February, 1936, Vol. XX, No. 2.

5. Simpson, G. C. Philosophical Transaction, Royal Society, A-209, 1909.
6. Ford, L. R. Differential Equations, pp. 75-78; McGraw-Hill Book Co.
7. Jensen, Axel. Portable Receiving Sets for Measuring Field Strength, Proceedings of Institute of Radio Engineers, Vol. 14, pp. 333-334, June, 1936.
8. Peek, F. W., Jr. The Law of Corona and the Dielectric Strength of Air -IV; Transactions, A. I. E. E., Vol. XLVI, 1927, pp. 1009-1024.
9. McMillan, F. O. Some Characteristics of a-c Conductor Corona; Transactions, A. I. E. E., Vol. 54, 1935, pp. 282-292; Reprint No. 4, Eng. Exp. Sta., O. S. C.
10. Hucke, H. M., and Moore, C. Study of Discharge Static; Unpublished report of laboratory work by United Air Lines Transport Corporation.
11. Pierce, G. W. Electric Oscillations and Electric Waves; McGraw-Hill Book Co.
12. Hucke, H. M. Precipitation Static Interference on Aircraft and at Ground Stations; Proceedings of the IRE, May, 1939, Vol. 27, No. 5, pp. 301-316.
13. Love, L. B., and Kip, A. F. Electric Discharges in Air at Atmospheric Pressure; Journal of Applied Physics, March, 1939, Vol. 10, No. 3, pp. 142-160.
14. McMillan, F. O. Radio Interference from Insulator Corona; Transactions, A. I. E. E., Vol. 51, January, 1932.

XVIII. APPENDIX I

Elementary Directive Radio Antennas

The following discussion applies to an antenna composed of two equal-height vertical radiators driven at the same frequency.

With reference to the diagram of Figure 3, the relative instantaneous radiation field strength at point P on the horizon under conditions of perfect transmission is:

$$f_p = b \sin \theta + a \sin \left(\theta + \beta - \frac{l}{\lambda} 360\right)$$

$$= b \sin \theta + a \sin \left(\theta + \beta - 360 \frac{d}{\lambda} \cos \alpha\right) \qquad (1)$$

Where:

f_p = relative instantaneous field strength.
b = relative field strength at P from vertical radiator "b".
a = relative field strength at P from vertical radiator "a".
θ = angle of progression of last positive wave front past P ("b" radiation), degrees.
β = phase angle between driving voltages of "a" and "b", degrees.
d = distance between radiators, meters.
l = d cos α
λ = wave length of radiation, meters.
α = angle which radius vector joining P and center point of line between radiators makes with plane of towers; counter-clockwise rotation.

Equation 1 applies accurately only when the distance from radiators to point P is great relative to d, the tower separation.

The value of θ for maximum instantaneous resultant radiation at P can be obtained by differentiating Equation 1 with respect to θ and equating to zero.

$$\frac{df_p}{d\theta} = b \cos \theta + a \cos \left(\theta + \beta - \frac{l}{\lambda} 360\right)$$

$$= b \cos \theta + a \left[\cos \theta \cos \left(\beta - \frac{l}{\lambda} 360\right) - \sin \theta \sin \left(\beta - \frac{l}{\lambda} 360\right) \right] = 0 \qquad (2)$$

Equation (2) divided by cos θ gives:

$$b + a \cos \left(\beta - \frac{l}{\lambda} 360\right) - a \tan \theta \sin \left(\beta - \frac{l}{\lambda} 360\right) = 0 \qquad (3)$$

Then:

$$\tan \theta_m = \frac{b + a \cos \left(\beta - \frac{l}{\lambda} 360\right)}{a \sin \left(\beta - \frac{l}{\lambda} 360\right)}$$

$$= \frac{b + a \cos \left(\beta - 360 \frac{d}{\lambda} \cos \alpha\right)}{a \sin \left(\beta - 360 \frac{d}{\lambda} \cos \alpha\right)} \qquad (4)$$

Where:

$\theta_m = \theta$ for maximum resultant radiation.

For equal values of a and b:

$$\theta_m = \tfrac{1}{2} \left(180 - \beta + 360 \frac{d}{\lambda} \cos \alpha\right) \qquad (5)$$

and:

$$f_{pm} = 2 b \sin \theta_m \qquad (6)$$

= relative maximum instantaneous radiation (total) at "P."

XIX. APPENDIX II

Impulse Excitation of Oscillatory Circuits

With reference to the diagram of Figure 48, the current flowing in the exciting circuit is a double exponential of the form:

$$i_1 = \frac{E}{2bL} \epsilon^{(b-a)t} - \epsilon^{-(b+a)t} \text{ amperes} \qquad (1)$$

The voltage e_g introduced by induction into the oscillatory circuit is of the form:

$$e_g = M \frac{di_1}{dt} = \frac{ME}{2bL} (b-a)\, \epsilon^{(b-a)t} + (b+a)\, \epsilon^{-(b+a)t} \qquad (2)$$

Where:

E = impulse-generator excitation voltage

$\epsilon = 2.718$

$a = \frac{R}{2L}$

$b = (\frac{R^2}{4L^2} - \frac{1}{LC})^{\frac{1}{2}}$ $\qquad \left(\text{when } \frac{R^2}{4L^2} > \frac{1}{LC}\right)$

$L \gg M$

The quantities R, L, and C are the constants of the exciting circuit in ohms, henrys, and farads, respectively.

Since the sum of the voltages around the oscillatory circuit must equal the applied voltage:

$$e'_R + e'_L + e'_C = e_g$$

or

$$R'i + L' \frac{di}{dt} + \frac{1}{C'} \int idt = e_g \qquad (3)$$

in which R', L', and C' are the constants of the oscillatory circuit in ohms, henrys, and farads, respectively.

Equation 2 substituted in 3 and differentiated gives:

$$L' \frac{d^2i}{dt^2} + R' \frac{di}{dt} + \frac{i}{C'}$$

$$= \frac{ME}{2bL} \left[(b-a)^2\, \epsilon^{(b-a)t} - (b+a)^2\, \epsilon^{-(b+a)t} \right] \qquad (4)$$

This equation can be solved by methods given in any standard textbook on differential equations (6).

The solution of the above differential equation is

$$i = \frac{ME}{2bLL'} \left[\frac{(b-a)^2\, \epsilon^{(b-a)t}}{(b-a+a)^2 + b'^2} - \frac{(b+a)^2\, \epsilon^{-(b+a)t}}{(b+a-a')^2 + b'^2} \right]$$

$$+ (K_1^2 + K_2^2)^{\frac{1}{2}}\, \epsilon^{-a't} \sin \left[b't + \tan^{-1} \frac{K_2}{K_1} \right] \qquad (5)$$

in which

$$a' = \frac{R'}{2L'}$$

$$b' = \left(\frac{1}{L'C'} - \frac{R'^2}{4L'^2}\right)^{\frac{1}{2}} \qquad \left(\text{when } \frac{1}{L'C'} > \frac{R'^2}{4L'^2}\right)$$

$L' \gg M$

K_1 and K_2 = constants of integration.

The voltage appearing across the capacitance of the oscillatory circuit (which is usually the voltage applied to the grid of the first detector or radio-frequency amplifier in a radio receiving set) may be found from an integration of Equation 5 thus:

$$e_c' = \frac{1}{C'}\int_0 i\,dt \tag{6}$$

The result of this integration between the limits indicated, since at $t = \infty$, $e_c' = 0$, is:

$$e_c' = \frac{ME}{2bLL'C'}\left[\frac{(b-a)\,\epsilon^{(b-a)t}}{(b-a+a')^2 + b'^2} + \frac{(b+a)\,\epsilon^{-(b+a)t}}{(b+a-a')^2 + b'^2}\right]$$
$$+\left[\frac{1}{C'}\left(\frac{K_1^2 + K_2^2}{a'^2 + b'^2}\right)^{\frac{1}{2}}\epsilon^{-a't}\right.$$
$$\left.\sin\left[b't - \tan^{-1}\left(\frac{b'K_1 + a'K_2}{b'K_2 - a'K_1}\right)\right]\right] \tag{7}$$

From the condition that at $t = 0$, $i = 0$, from Equation 5 the following expression for the integration constant K_2 can be obtained:

$$K_2 = \frac{2ME\,[a'\,(b^2-a^2) + a\,(b'^2 + a'^2)]}{LL'\,[(b-a+a')^2 + b'^2]\,[(b+a-a')^2 + b'^2]} \tag{8}$$

Further, from the condition that at $t = \infty$, $e_c' = 0$, the relation is obtained:

$$\frac{b'K_1 + a'K_2}{a'^2 + b'^2}$$
$$= \frac{ME}{LL'}\left[\frac{(b^2-a^2) + (a'^2+b'^2)}{[(b-a+a')^2 + b'^2]\,[(b+a-a')^2 + b'^2]}\right] \tag{9}$$

From these last two relations, K_1 and K_2 can be computed.

It can be shown by manipulation of Equations 8 and 9 that

$$\tan^{-1}\left(\frac{b'K_1 + a'K_2}{b'K_2 - a'K_1}\right)$$

$$= \tan^{-1}\frac{b'\,[(b^2-a^2) + (a'^2+b'^2)]}{[a'(b^2-a^2) + (a'^2+b'^2)(2a-a')]}$$

$$= \alpha \tag{10}$$

and that

$$\left[\frac{K_1^2+K_2^2}{a'^2+b'^2}\right]^{\frac{1}{2}} = \frac{b'K_1 + a'K_2}{a'^2+b'^2}\csc\alpha \tag{11}$$

Hence the constant in the expression for the capacitor voltage e_c' in Equation 7 may be computed by using Equations 10 and 11.

XX. APPENDIX III

Voltage and Energy Abstraction by Induction

In the analytical study of certain interference-rejecting properties of the shielded-loop radio receiving antenna, it is helpful to analyze the general phenomena of magnetic and electric induction. The same analysis is also helpful in the study of inductive coordination between power and telephone circuits.

To a very large extent in the case of radio receiving equipment and to a lesser degree in telephone circuits, the output response is a function of the voltage induced in the input circuit. A certain amount of input power is also necessary. In the case of radio receivers, however, the input circuit is one of parallel resonance, which approaches infinite impedance and zero power. The output of this resonant circuit is to the high impedance grid of a vacuum tube, leaving the over-all input impedance very high in its order of magnitude.

In the following analysis the inducing conductor is assumed to be parallel to the pick-up conductors. Equations 3, 10, 23, 24, 44, 45, and 51 give induction voltages. It will be noted that in the case of magnetic induction the voltage is a function of frequency, current in the inducing conductor, spacing, and length. The magnetically induced voltage due to charging current in the inducing conductor is a function of the frequency squared, the voltage and length of the inducing conductor, the length of the pick-up loop, and the spacings. This latter condition similates, in a way, the case of a radio receiving loop in the field of a high-frequency conductor.

In the case of electric induction, the open-circuit voltage is independent of frequency and length (where the length is not too short) and is a function of effective interconductor capacitances and of the voltage on the inducing conductor. These capacitances can be expressed in terms of spacings and conductor sizes as in Equations 32 and 34.

The maximum power that can be obtained by induction is given in Equations 20, 21, 22, 39, 40, 46, 47, 52, and 53. It will be noted that the maximum power of magnetic induction is a function of the frequency, the

square of the length of the pick-up loop, the square of the current in the inducing conductor, the square of a spacing factor, and is a reciprocal function of the self-inductance of the pick-up loop.

In the case of electric induction the maximum power is a function of the frequency, the voltage of the inducing conductor squared, the effective capacitance between the two conductors squared, and is a reciprocal function of twice the sum of the effective interconductor capacitance plus the effective ground capacitance of the pick-up conductor.

The maximum power of magnetic induction due to charging current in the inducing conductor is given by Equation 53. In this case, which again simulates in a way the case of a radio receiving loop in the field of a high-frequency conductor, the power is a function of the cube of the frequency, the square of the length of the loop, the square of the voltage and length of the inducing conductor, the square of a spacing factor, and is a reciprocal function of the self-inductance of the loop.

It will be noted that the power of electric induction varies *directly* with frequency, whereas that of magnetic induction due to charging current varies as the *cube* of the frequency.

1. **Magnetic induction.** Consider the circuit of Figure 52. The flux in the loop D-D′ due to the uniform current i in the long, straight conductor A is (neglecting ground reflections):

$$\phi_d = S \int_{X_1}^{X'_1} \frac{0.2i}{X}\, dX = 0.2i\, S\, ln\, X \Big|_{X_1}^{X'_1}$$

$$= 0.2i\, S\, ln \frac{X'_1}{X_1} \qquad (1)$$

Where length of loop is S and induction intensity at point X is:

$$H = \frac{0.2i}{X}$$

In air:

$$B = \frac{0.2i}{X} \text{ cgs lines / cm}^2$$

Then the voltage induced in the loop is:

$$e_d = \frac{d\phi_d}{dt} \cdot 10^{-8} \text{ volts}$$

$$= \left(0.2\, I_m \cos\theta\right)\left(ln \frac{X'_1}{X_1}\right) 2\pi f\, S 10^{-8} \qquad (2)$$

$$(i = I_m \sin\theta)$$

$$E_d = \frac{0.4\, S\pi f}{\sqrt{2}} \cdot 10^{-8}\, I_m\, ln \frac{X'_1}{X_1} \text{ volts effective (open circuit)} \qquad (3)$$

Where I_m is the crest value of the sinusoidal current in conductor A, f is the frequency, and S is the length of the loop in centimeters.

The current in the loop D-D′ is:

$$I_d = \frac{E_d}{Z_d} = \frac{E_d}{\sqrt{R^2_L + 2\pi f L^2_s}} \text{ amperes effective}$$

Where L_s is the self-inductance of the loop.

When:

$$I_d R_L = I_d (2\pi f L_s) = 0.707 E_d,$$

the power delivered to the resistance R_L is maximum.

The self-inductance of the loop D-D′ is (neglecting ground reflections):

$$L_s = \frac{\phi_s}{I_d} \cdot 10^{-8} \text{ henrys / cm}$$

Where:

$$\phi_s = 0.2 I_d \left[\int_{r_d}^{b} \frac{1}{X'} dX' + \int_{0}^{b-r_d} \frac{1}{b-X'} dX' \right]$$

$$= 0.2 I_d \left[\ln X' \Big|_{r_d}^{b} - \ln(b-X) \Big|_{0}^{b-r_d} \right]$$

$$= 0.2 I_d \left[\ln \frac{b}{r_d} - \ln \frac{r_d}{b} \right]$$

$$= 0.4 I_d \ln \frac{b}{r_d}$$

lines per centimeter length of loop,

where r_d is the radius of conductors D and D′. (5)

Hence, when $\frac{S}{b}$ is large (and considering only flux external to the conductors):

$$L_s = 0.4 \ln \frac{b}{r_d} \cdot 10^{-8} \text{ henrys / loop cm} \quad (6)$$

Where the length of the loop is not great relative to its breadth, an extra term must be added to Equation 6 to care for the inductance of the end connections. Then, approximately, for low frequencies:

$$L_{s1} = 0.40 \left[s\left(2.303 \log \frac{b}{r_d} - \frac{b}{s} + 0.25\right) + b\left(2.303 \log \frac{s}{r_d} - \frac{s}{b} + 0.25\right) \right] 10^{-8} \text{ henrys} \quad (7)$$

The exact equation for the inductance of a rectangle in free space is [1]:

$$L_{s2} = 0.921 \left[(S + b) \log \frac{2Sb}{r_d} - S \log (S + g) - b \log (b + g) \right] 10^{-8} + 0.40 \left[\mu\delta (S + b) + 2 (g + r_d) - 2 (S + b) \right] 10^{-8} \text{ henrys} \quad (8)$$

Where:

$g = (S^2 + b^2)^{\frac{1}{2}}$

$\mu\delta = 0.25$ for low frequencies in air.

2. **Influence of ground reflections.** Equations 1, 3, 5, 6, 7, and 8 apply strictly only when the conductors are suspended above a ground plane of relatively poor longitudinal conductivity; that is, when the ground currents resulting from magnetic flux penetration are negligible. This condition is generally true in practice. If the earth, or reference plane, is perfectly conducting, however, no flux penetration can exist, and reflection occurs from the earth surface. This reflection, in its influence on the flux at point X produced by the current in A, can be simulated by the image conductor A carrying the current I in the opposite direction, the whole system being immersed in free space.

Then:

$$\theta'_d = S \int_{X_1}^{X'_1} \frac{0.2i}{X} dX + S \int_{X'_2}^{X_2} \frac{0.2i}{X} dX = 0.2i\, S \ln \frac{X'_1 X_2}{X_1 X'_2} \quad (9)$$

Equation 9 indicates that if h_2 and h_3 are small compared to h_1, ϕ_d' approaches two times ϕ_d. Also, if the perfectly conducting ground is far removed, X_2 approaches X_2' and Equation 1 obtains.

The loop voltage given by Equation 3 now becomes:

$$E'_d = (0.4\pi f SI \ln \frac{X'_1 X_2}{X_1 X'_2}) 10^{-8} \text{ volts effective} \quad (10)$$

This is the open-circuit voltage of the loop when conductor A is carrying effective current I.

The self-inductance of the loop is also influenced by its proximity to the conducting ground plane. This influence can be simulated by an image loop D-D′ carrying the current I_d in the opposite direction. The effect is again one of magnetic flux reflections.

The self-inductance of a loop, the plane of which is normal to the ground plane, is then:

$$L'_s = \frac{\phi'_s}{I_d} \cdot 10^{-8} \text{ henrys / cm} \tag{11}$$

Where:

$$\phi'_s = 0.2 I_d \left[\int_{r_d}^{b} \frac{1}{X} dX' + \int_{0}^{b-r_d} \frac{1}{b - X'} dX' - \int_{2h_3}^{2h_3+b} \frac{1}{X''} dX'' + \int_{2h_3+b}^{2h_3+2b} \frac{1}{X'''} dX''' \right]$$

$$\phi'_s = 0.2 I_d \left[ln \frac{b}{r_d} - ln \frac{r_d}{b} - ln \frac{2h_3 + b}{2h_3} + ln \frac{2h_3 + 2b}{2h_3 + b} \right]$$

$$= 0.461 \; I_d \log \left[\left(\frac{b}{r_d}\right)^2 \left(\frac{4h_3(h_3 + b)}{(2h_3 + b)^2} \right) \right]$$

lines per cm length of loop (12)

Then, from Equations 11 and 12 (considering only flux external to conductors before reflection):

$$L'_s = 0.461 \log \left[\left(\frac{b}{r_d}\right)^2 \left(\frac{4h_3(h_3 + b)}{(2h_3 + b)^2} \right) \right] 10^{-8}$$

henrys per loop cm. (13)

If the plane of the loop is not normal to the ground plane, Equation 13 becomes:

$$L'_s = 0.461 \log \left[\left(\frac{b}{r_d}\right)^2 \left(\frac{4h_2h_3}{d_2^2 + (h_2 + h_3)^2} \right) \right] 10^{-8} \tag{14}$$

where d_2 is the distance between the vertical projections on the ground plane of the two sides of the loop D-D′.

Unless otherwise noted, the above equations for induced voltage and self-inductance apply with good accuracy only when h_1, h_2, and b are small relative to S and S′.

Equations 7 and 8 only, include the influence of the internal flux of the conductors.

3. **Loop end effects.** When the loop is short relative to its breadth b, an end fringing-effect term must be *subtracted from* Equations 13 and 14. This term is, approximately:

$$L_{ee} = 0.4b \frac{\log \left[\left(\frac{b}{r_d}\right)^2 \left(\frac{4h_3(h_3 + b)}{(2h_3 + b)^2} \right) \right]}{\log \left(\frac{b}{r_d}\right)^2} \cdot 10^{-8} \text{ henrys} \qquad (15)$$

Under the same conditions an additional term must be *added* to these same equations to care for the inductance of the end connections. When the quantities b/r_d and s'/r_d are large, this term is approximately [2]:

$$L_e = \left[b(0.921 \log \frac{S'}{r_d} + 0.1) - 0.4S' \right] 10^{-8} \text{ henrys} \qquad (16)$$

The sum of Equations 13 or 14 and 16, minus 15, gives a total inductance that is a slight amount too small. A closer approach to the exact value might be obtained by using the average of the above sum and the value given by Equation 8.

4. **Maximum power.** The resistance for maximum power abstraction is, from (2a):

$$R_{Lm} = 2\pi f L_{st}$$

$$(I_d E_R = \text{max.}) \qquad (17)$$

where: $L_{st} = SL_s$, the total self-inductance of the loop.

Also, since the negative self-inductance drop is one component of the total voltage induced in the loop:

$$I_d R_{Lm} = 0.707 \ E_d$$

$$I_d = \frac{0.707 \ E_d}{R_{Lm}} \qquad (18)$$

The power P_{Lm} dissipated in the resistor is:

$$I_d^2 R_{Lm} = \frac{0.5 \ E_d^2}{R_{Lm}} \text{ watts}$$

$$= \frac{1}{4R_{Lm}} \left[0.4S\pi f I_m \ln \frac{X'_1}{X_1} \right]^2 10^{-16}$$

$$= \frac{1}{2R_{Lm}} \left[0.4S\pi f I \ln \frac{X'_1}{X_2} \right]^2 10^{-16} \qquad (19)$$

Then, from Equations 6 and 17:

$$P_{Lm} = \frac{0.723\, S\, f\, (I \log \frac{X'_1}{X_1})^2}{\log \frac{b}{r_d}} \cdot 10^{-8} \text{ watts} \qquad (20)$$

for the maximum dissipation condition.

When the conductors are near a perfectly conducting plane, from Equations 10, 14, and 17, Equation 20 becomes:

$$P'_{Lm} = \frac{1.45\, f\, S\, I^2 (\log \frac{X'_1 X_2}{X_1 X'_2})^2}{\log \left[(\frac{b}{r_d})^2 (\frac{4h_2h_3}{d^2_2 + (h_2 + h_3)^2}) \right]} \cdot 10^{-8} \text{ watts} \qquad (21)$$

For any total self-inductance L_{st} of the pick-up loop D-D' having length S' parallel to A, Equation 21 becomes:

$$P'_{Lm} = \frac{0.667\, f\, S'^2 I^2 (\log \frac{X'_1 X_2}{X_1 X'_2})^2}{L_{st}} \cdot 10^{-16} \text{ watts} \qquad (22)$$

5. **Electric induction.** Consider the circuit of Figure 53. With switch S_w open, the voltage induced electrically on conductor B by the potential E on conductor A is:

$$E_b = E \frac{C_{ab}}{C_b + C_{ab}} \qquad (23)$$

This potential is independent of frequency. In the following analysis, the effective values of C_{ab} and C_b, for switch S_w open and closed, will be determined.

From the theory of the potential[3] it can be shown that:

$$E_b = E \frac{\log \frac{X_2}{X_1}}{\log \frac{2h_1}{r}} \qquad (24)$$

From Equation 23:

$$C_{ab} = \frac{E_b C_b}{E - E_b} \qquad (25)$$

The only dielectric flux emanating from B is that which enters B from A. If X_1 is large relative to h_2, and h_2 large relative to r_b, the total flux leaving B is:

$$\psi b = 2r_b D \text{ coulombs} \tag{26}$$

where r_b is the radius of conductor B and D is the flux density at B. This statement is true only when the potential of B is equal to its space potential due to A.

The field of A is then relatively undisturbed by the presence of B. The same flux both enters and leaves B.

The effective capacitance of B to ground is then:

$$C_b = \frac{\psi_b}{Eb} \text{ farads} \tag{27}$$

From the theory of the potential:

$$D = \frac{2\,h_1\psi}{2\pi\,X_1X_2} \text{ coulombs / cm}^2 \tag{28}$$

Where:

$$\psi = C_a E = \frac{2.41E}{\log\frac{2h_1}{r}} \cdot 10^{-13} \text{ coulombs} \tag{29}$$

= total flux per cm from A to ground (neglecting end effect).

Then:

$$D = \frac{4.82\,h_1\,E}{2\pi\,X_1X_2\log\frac{2h_1}{r}} \cdot 10^{-13} \tag{30}$$

Equations 26 and 30 substituted in 27 give:

$$C_b = \frac{1.53\,r_b\,h_1E}{E_b\,X_1X_2\log\frac{2h_1}{r}} \cdot 10^{-13} \text{ farads / cm} \tag{31}$$

From Equation 24:

$$C_b = \frac{1.53\,r_b\,h_1}{X_1X_2\log\frac{X_2}{X_1}} \cdot 10^{-13} \text{ farads / cm} \tag{32}$$

Equation 31 substituted in 25 gives:

$$C_{ab} = \frac{1.53\, r_b\, h_1 E}{(E - E_b)\, X_1 X_2 \log \frac{2h_1}{r}} \cdot 10^{-13} \text{ farads / cm} \tag{33}$$

From Equation 24:

$$C_{ab} = \frac{1.53\, r_b\, h_1}{X_1 X_2 \log \frac{2h_1 X_1}{r X_2}} \cdot 10^{-13} \text{ farads / cm} \tag{34}$$

Where:

$$X_1 = [(h_1 - h_3)^2 + d^2]^{\frac{1}{2}} \tag{35}$$

$$X_2 = [(h_1 - h_2)^2 + d^2]^{\frac{1}{2}} \tag{36}$$

The effective capacitances C_b and C_{ab} remain essentially constant, when X_1 is large compared to h_2 and E is large compared to E_b, for small changes of the potential of B from its space potential due to A. It can be shown that for this condition, the maximum energy abstraction from A, by the resistance R connected to B, occurs when:

$$R_c = \frac{1}{2\pi f\, (C_{ab} + C_b)} \text{ ohms} \tag{37}$$

For $C_b \gg C_{ab}$, $R_c \cong X_{cb}$ and the current in R_c is equal to that in C_b. The voltage drop across R_c is then 70.7 per cent of the space potential of B.

The current in the resistor is:

$$I_{Rc} = \frac{E}{\left[R^2_c \left(1 + \frac{C_b}{C_{ab}}\right)^2 + \left(\frac{1}{2\pi f C_{ab}}\right)^2\right]^{\frac{1}{2}}} \text{ amp.} \tag{38}$$

The maximum power is:

$$P_{cm} = I^2_{Rc} R_c$$

$$= \frac{E^2}{2\pi f\, (C_{ab} + C_b)\left[R^2_c \left(1 + \frac{C_b}{C_{ab}}\right)^2 + \left(\frac{1}{2\pi f C_{ab}}\right)^2\right]}$$

watts (39)

Then, from Equations 37 and 39:

$$P_{cm} = \frac{2\pi f C^2_{ab} E^2}{2\, (C_{ab} + C_b)} \text{ watts} \tag{40}$$

Equation 40 indicates that the maximum power available is proportional to the square of the voltage on A and to the square of the length S′ of the pick-up conductor B.

6. **Relative induction magnitudes.** If the only current flowing in conductor A is that due to its capacitance to ground, assuming this current to be led away transversely through the ground plane and assuming a "nominal π"; that is, one-half the "charging" current fed in at each end of A, the approximate current active in magnetic induction (Equations 3, 10, 20, and 21) is:

$$I = \frac{E}{2X_{ca}} = \frac{2\pi f C_a E}{2} \text{ amperes} \tag{41}$$

where C_a is capacitance to ground of conductor A, is:

$$C_a = \frac{2.41}{\log \frac{2h_1}{r}} \cdot 10^{-13} \text{ farads / cm} \tag{42}$$

Where X_1 and X'_1 are large relative to h_2 and h_3.

Then, when $\frac{S}{h_1}$ is large:

$$I = \frac{7.57\, fE}{\log \frac{2h_1}{r}} \cdot 10^{-13} \text{ amperes / cm} \tag{43}$$

The voltage of magnetic induction from charging current is then, from Equations 43 and 3:

$$E_d = \frac{2.19\, S^2 f^2 E \log \frac{X'_1}{X_1}}{\log \frac{2h_1}{r}} \cdot 10^{-20} \text{ volts} \tag{44}$$

In the presence of a perfectly conducting ground plane, Equation 43 substituted in 10:

$$E'_d = \frac{2.19\, S^2 f^2 E \log \frac{X'_1 X_2}{X_1 X_2}}{\log \frac{2h_1}{r}} \cdot 10^{-20} \text{ volts} \tag{45}$$

The maximum power from magnetic induction due to charging current from Equations 43 and 20 is:

$$P_{Lm} = \frac{4.14\, S^3 f^3 E^2 (\log \frac{X'_1}{X_1})^2}{\log \frac{b}{r_d} (\log \frac{2h_1}{r})^2} \cdot 10^{-33} \text{ watts} \qquad (46)$$

In the presence of a perfectly conducting plane, from Equations 43 and 21:

$$P'_{Lm} = \frac{8.28\, S^3 f^3 E^2 (\log \frac{X'_1 X_2}{X_1 X'_2})^2}{(\log \frac{2h_1}{r})^2 \log \left[(\frac{b}{r_d})^2 (\frac{4h_2h_3}{d^2_2 + (h_2 + h_3)^2}) \right]} \cdot 10^{-33} \text{ watts} \qquad (47)$$

Equations 44, 45, 46, and 47 apply to full-length loops where S/h_1 is so large as to make end effects negligible.

For *loops of fractional length* S' the current in A, which is effective in inducing voltage in the loop D-D', is very nearly:

$$I' = 2\pi f\, C'_a\, E \qquad (48)$$

where C'_a is the capacitance to ground of A over a length of $(S - \frac{S'}{2})$ cm. Hence:

$$C'_a = \frac{2.41 (S - \frac{S'}{2})}{\log \frac{2h_1}{r}} \cdot 10^{-13} \text{ farads} \qquad (49)$$

Then:

$$I' = \frac{1.51\, f\, E (S - \frac{S'}{2})}{\log \frac{2h_1}{r}} \cdot 10^{-12} \text{ amp.} \qquad (50)$$

The voltage of magnetic induction due to charging current (Equation 45) then becomes:

$$E'_d = \frac{4.37\, f^2 E\, S' (S - \frac{S'}{2}) \log \frac{X'_1 X_2}{X_1 X'_2}}{\log \frac{2h_1}{r}} \cdot 10^{-20} \text{ volts} \qquad (51)$$

The maximum power of magnetic induction due to charging current (Equation 47) for a loop of fractional length S′ is, from Equations 50 and 21:

$$P'_{Lm} = \frac{3.31\, f^3 E^2 S' \left(S - \frac{S'}{2}\right)^2 \left(\log \frac{X'_1 X_2}{X_1 X'_2}\right)^2}{\left(\log \frac{2h_1}{r}\right)^2 \log \left[\left(\frac{b}{r_d}\right)^2 \left(\frac{4h_2 h_3}{d^2_2 + (h_2 + h_3)^2}\right)\right]} \cdot 10^{-32} \text{ watts} \qquad (52)$$

Equation 52 indicates that the maximum resistance power is a function of the cube of the frequency, the square of the voltage on A, the length of the pick-up loop S′, and the square of the quantity (S — 0.5 S′).

Equation 52 applies to pick-up loops in which the ratio of length S′ to breadth b is so great as to make end effects negligible. For any total self-inductance L_{st} of the loop D-D′ having length S′ parallel to A, Equation 52 becomes:

$$P'_{Lm} = \frac{1.52\, f^3 S'^2 E^2 \left(S - \frac{S'}{2}\right)^2 \left(\log \frac{X'_1 X_2}{X_1 X'_2}\right)^2}{L_{st} \left(\log \frac{2h_1}{r}\right)^2} \cdot 10^{-40} \text{ watts} \qquad (53)$$

7. NUMERICAL EXAMPLES

Example I (Voltage)

Full-length loop, magnetic

Assume full-length pick-up loop (Figure 52) receiving voltage and power inductively due to the charging current to ground flowing in the inducing conductor.

Let:

$h_1 = 1{,}100$ cm	$E = 100{,}000$ V
$h_2 = 100$ cm	$S = 10{,}000$ cm
$h_3 = 10$ cm	$r = 0.5$ cm
$X_1 = 1{,}000$ cm	$r_b = r_d = 10$ cm
$X'_1 = 1{,}090$ cm	$b = 90$ cm
$X_2 = 1{,}200$ cm	$d = 0$
$X'_2 = 1{,}110$ cm	$f = 100$ cps

Assume further: Ground-plane conductivity: infinite.

Then, from Equation 45:

$$E'_d = \frac{2.19 \times 10^8 \times 10^4 \times 10^5 \log \frac{131 \times 10^4}{111 \times 10^4}}{\log \frac{2{,}200}{0.5}} \cdot 10^{-20}$$

$$= 4.33 \times 10^{-5} \text{ volts} \qquad (54)$$

If the frequency is raised to 10^6 cps, Equation 54 becomes:

$$E'_d = 4.33 \times 10^3 \text{ volts} \tag{55}$$

Full-length conductor, electric

If the loop is replaced by a single conductor of height h_1, the voltage of electric induction (Equation 24), is:

$$E_b = 10^5 \frac{\log \frac{1{,}200}{1{,}000}}{\log \frac{2{,}200}{0.5}}$$

$$= 2.175 \times 10^3 \text{ volts} \tag{56}$$

Hence, if in (55) the frequency is reduced to:

$$\left[\frac{2.175}{4.33}\right]^{\frac{1}{2}} 10^6 = 7.08 \times 10^5 \text{ cps}$$

the induced voltages are identical.

Short pick-up loop, magnetic and electric

If the inducing conductor is of length S but the length of the loop is reduced to 100 cm = S', (Figure 52) the voltage of electric induction remains unchanged but that of magnetic induction becomes, from equation (51):

$$E'_d = \frac{4.37 \times 10^4 \times 10^5 \times 10^2 \times 9.95 \times 10^3 \log \frac{131 \times 10^4}{111 \times 10^4}}{\log \frac{2{,}200}{0.5}} \cdot 10^{-20}$$

$$= 8.59 \times 10^{-7} \text{ volts} \tag{57}$$

At 10^6 cps, Equation 57 becomes:

$$E'_d = 85.9 \text{ volts} \tag{58}$$

To obtain the same voltage from Equation 57 as from electric induction, Equation 56, the frequency must be raised to:

$$f' = \left[\frac{2.175 \times 10^3}{85.9}\right]^{\frac{1}{2}} \cdot 10^6$$

$$= 5.03 \times 10^6 \text{ cps} \tag{59}$$

Example II (Maximum Power)

Full-length loop, magnetic

Assume same conditions and circuit dimension as those given under Example I.

Then, from Equation 47, the maximum power that can be obtained from the pick-up loop is:

$$P'_{Lm} = \frac{8.28 \times 10^{12} \times 10^{6} \times 10^{10} \times \left[\log \frac{131 \times 10^{4}}{111 \times 10^{4}}\right]^2}{\left[\log \frac{2{,}200}{0.5}\right]^2 \log\left[\left(\frac{90}{1}\right)^2 \cdot \frac{4 \times 10^{2} 10}{(10^2 + 10)^2}\right]} \cdot 10^{-33}$$

$$= \frac{4.28}{13.26 \times 3.428} \cdot 10^{-7}$$

$$= 9.4 \times 10^{-9} \text{ watts} \tag{60}$$

If the frequency is raised to 10^6 cps, (60) becomes:

$$P'_{Lm} = 9.4 \times 10^{3} \text{ watts} \tag{61}$$

Full-length conductor, electric

If the loop is replaced by a single conductor of height h_1 and length S, the maximum power of electric induction, Equation 40, is:

$$P_{em} = \frac{6.28 \times 10^{2} C^{2}_{ab} \times 10^{10}}{2\,(C_{ab} + C_b)} \text{ watts} \tag{62}$$

From Equation 34:

$$C_{ab} = \frac{1.53 \times 1.0 \times 1.1 \times 10^{3} \times 10^{4}}{1.2 \times 10^{6} \log \frac{2.2 \times 10^{6}}{6 \times 10^{2}}} \cdot 10^{-13}$$

$$= 3.93 \times 10^{-13} \text{ farads} \tag{63}$$

From Equation 32:

$$C_b = \frac{1.53 \times 1.0 \times 1.1 \times 10^{3} \times 10^{4}}{1.2 \times 10^{6} \log \frac{1{,}200}{1{,}000}} \cdot 10^{-13}$$

$$= 17.7 \times 10^{-12} \text{ farads} \tag{64}$$

Then, from Equations 62, 63, and 64:

$$P_{em} = \frac{6.28 \times 15.5}{36.2} \cdot 10^{-2}$$

$$= 2.69 \times 10^{-2} \text{ watts} \tag{65}$$

If the frequency is raised to 10^6 cps, Equation 65 becomes:

$$P'_{cm} = \frac{10^6}{10^2} \cdot 2.69 \times 10^{-2}$$

$$= 269 \text{ watts} \tag{66}$$

The frequency f' for equal maximum power by both types of induction can be obtained as follows:

$$\frac{f'}{100} \times 2.69 \times 10^{-2} = (\frac{f'}{100})^3 \times 9.4 \times 10^{-9}$$

$$2.69 \times 10^{-4} f' = 9.4 \times 10^{-15} f'^3$$

$$f'^3 = \frac{2.69 \times 10^{-4} f'}{9.4 \times 10^{-15}}$$

$$f'^2 = 2.86 \times 10^{10}$$

$$f' = 1.69 \times 10^5 \text{ cps} \tag{67}$$

Short pick-up loop, magnetic

If the inducing conductor remains of length S but the loop is shortened to 100 cm = S' (Figure 52) the maximum power that can be obtained by induction due to charging current in the inducing conductor is, from Equation 53:

$$P'_{Lm} = \frac{1.52 \times 10^6 \times 10^4 \times 10^{10} \times 9.9 \times 10^7 \times 5.17 \times 10^{-3}}{L_{st} \times 13.26} \cdot 10^{-40}$$

watts (68)

From Equations 13, 15, and 16:

$$L_{st} = \left[46.1 \log (8{,}100 \times 0.33) - 32 \right] 10^{-8}$$

$$+ \left[90 (0.921 \log 100 + 0.1) - 40 \right] 10^{-8} h$$

$$= 2.61 \times 10^{-6} h \tag{69}$$

Then, from Equations 68 and 69:

$$P'_{Lm} = 2.25 \times 10^{-10} \text{ watts} \tag{70}$$

For a frequency of 10^6 cps, Equation 70 becomes:

$$P'_{Lm} = (\frac{10^6}{10^2})^3 \times 2.25 \times 10^{-10}$$

$$= 225 \text{ watts} \tag{71}$$

Short pick-up conductor, electric

If the short loop is replaced by a conductor of length S′ and height h_1, the maximum power that can be transferred is, from Equation 40:

$$P_{em} = \frac{6.28 \times 10^2 \times C^2_{ab} \times 10^{10}}{2\,(C_{ab} + C_b)} \text{ watts} \tag{72}$$

From Equation 63: ($S' = S \times 10^{-2}$)

$$C_{ab} = 3.93 \times 10^{-13} \times 10^{-2}$$
$$= 3.93 \times 10^{-15} \text{ farads} \tag{73}$$

And from Equation 64:

$$C_b = 17.7 \times 10^{-14} \text{ farads} \tag{74}$$

Then from Equations 72, 73, and 74:

$$P_{em} = \frac{6.28 \times 10^2 \times 15.5 \times 10^{-30} \times 10^{10}}{2 \times 18.1 \times 10^{-14}} \text{ watts}$$
$$= 2.69 \times 10^{-4} \text{ watts} \tag{75}$$

If the frequency is raised to 10^6 cps, Equation 75 becomes:

$$P'_{em} = \frac{10^6}{10^2} \times 2.69 \times 10^{-4} \text{ watts}$$
$$= 2.69 \text{ watts} \tag{76}$$

The frequency f′ for equal maximum power by both types of induction is again obtained as in Equation 67 and is:

$$f' = 1.09 \times 10^5 \text{ cps} \tag{77}$$

Short inducing conductor and short loop

As long as the inducing conductor remains substantially longer than the pick-up conductor, the voltage and maximum power of electric induction remain unchanged. The voltage and power of magnetic induction depend greatly upon the current in the inducing conductor, however, and hence upon its length, the factor that determines its capacitance to ground.

If the length S is reduced to 400 cm with S′ unchanged at 100 cm, neglecting end effects, the maximum power is from Equations 53 and 70:

$$P_{Lm} = \frac{(400 - \frac{100}{2})^2}{(10{,}000 - \frac{100}{2})^2} \times 2.25 \times 10^{-10} \text{ watts}$$
$$= 2.8 \times 10^{-13} \text{ watts} \tag{78}$$

The frequency f′ for equal power by both types of induction is now, as in Equation 67:

$$f' = 3.11 \times 10^6 \text{ cps} \tag{79}$$

Thus a very high frequency is now necessary to obtain equal induction powers. A similar condition exists in the voltages.

From Equations 51 and 57:

$$E'_d = \frac{400 - \frac{100}{2}}{10{,}000 - \frac{100}{2}} \times 8.59 \times 10^{-7} \text{ volts}$$

$$= 3.02 \times 10^{-8} \text{ volts} \tag{80}$$

The frequency f′ for equal voltages by both types of induction is, as in Equation 59:

$$f' = \left(\frac{2.175 \times 10^3}{3.02}\right)^{\frac{1}{3}} 10^6$$

$$= 26.8 \times 10^6 \text{ cps} \tag{81}$$

XXI. APPENDIX III-A

The Approximate Variation with Distance of the Potential Induced Electrically in Space by an Elevated, Charged Disc

From Equation 10, Appendix III, for long, straight conductors:

$$E_b = E \frac{\log \frac{X_2}{X_1}}{\log \frac{2h_1}{r}} \text{ volts} \tag{1}$$

If the conductor is curved into a circle to form the edge of a disc of major radius R, the dielectric flux remains essentially unchanged in the transverse plane, but diverges in the horizontal plane according to:

$$\psi_h = \frac{R}{d} \psi \tag{2}$$

Where ψ is the flux at the induction point from a straight conductor and d is the horizontal distance from the center of the disc to this point,

Then, approximately:

$$E_b = E \frac{\log \frac{X_2}{X_1}}{\log \frac{2h_1}{r}} \cdot \frac{R}{d} \tag{3}$$

Let: $X_1 = d = 450$ cm

$h_1 = 120$ cm

$X_2 = (4h^2_1 + X^2_1)^{\frac{1}{2}} = 510$ cm

$R = 20$ cm

$r = 0.5$ cm

Then, from Equation 3:

$$E_b = E \frac{\log \frac{510}{450}}{\log \frac{240}{0.5}} \times \frac{20}{450} = 8.8 \times 10^{-4} E \tag{4}$$

For $d' = 900$ cm

$X'_2 = 932$ cm:

$$E'_b = E \frac{\log \frac{932}{900}}{\log \frac{240}{0.5}} \cdot \frac{20}{900} = 1.24 \times 10^{-4} E \tag{5}$$

For $d'' = 1{,}800$ cm

$X''_2 = 1{,}819$ cm:

$$E''_b = 1.78 \times 10^{-5} E \tag{6}$$

For $d''' = 225$ cm

$X'''_2 = 329$ cm:

$$E''' = 5.52 \times 10^{-3} E \tag{7}$$

It will be observed that in each case, reducing the distance fifty per cent increased the induction voltage approximately seven times. Hence, within the range chosen, the electric induction pick-up from a concentrated source would be expected to vary inversely as approximately the 2.8 power of the distance. Experimental tests gave an exponent of approximately 3.2.

XXII. APPENDIX IV

Electromagnetic Radiation and Induction

The magnetic potential at a point P in space is:

$$F = \frac{M}{d} = \frac{i\Delta L}{d} \sin\theta \text{ gilberts,} \tag{1}$$

Where M is the magnetic pole strength, d is the distance from the pole to point P, i is the current flowing in the elemental conductor, ΔL, and θ is the angle between the axis of the conductor and the line joining P and the center of ΔL.

The magnetic field intensity at P is the rate of change of F with respect to d and is:

$$\Delta H = \frac{d(F)}{dd} = -\frac{i\Delta L}{d^2} \sin\theta \text{ oersteds.} \tag{2}$$

When the alternating frequency of i is great and distance d is appreciable, there is a definite lag between the current i and the magnetic potential at P. Then:

$$F = \frac{I \sin 2\pi f \left(t - \frac{d}{v}\right)}{d} \Delta L \sin\theta \text{ gilberts} \tag{3}$$

and $$\Delta H = \frac{d(F)}{dd}$$

$$\Delta H = -\frac{I\Delta L \sin\theta}{d^2}\left[\frac{2\pi fd}{v} \cos 2\pi f \left(t - \frac{d}{v}\right)\right] - \frac{I\Delta L \sin\theta}{d^2}\left[\sin 2\pi f \left(t - \frac{d}{v}\right)\right]$$

$$= \text{lines per square cm in air} \tag{4}$$

The first term of Equation 4 is the radiation term and is dependent on the current and the frequency, and inversely on the distance and the velocity v of wave propagation. It reduces to:

$$\Delta H_r = \frac{2\pi fI\Delta L \sin\theta}{vd} \cos 2\pi f \left(t - \frac{d}{v}\right) \tag{5}$$

The second term is the induction term and is independent of frequency. The velocity term enters only in the phase-position factor and distance enters as the inverse square. It is:

$$\Delta Hi = -\frac{I\Delta L \sin\theta}{d^2} \sin 2\pi f \left(t - \frac{d}{v}\right) \tag{6}$$

Integration of $I\Delta L$ over the entire conductor (area under curve of maximum current distribution along radiator, abampere-centimeters), since $H = B$ in space, (assuming all current elements in phase), gives:

$$B_r = -\frac{2\pi f \int_o^L IdL}{vd} \sin\theta \cos 2\pi f\left(t - \frac{d}{v}\right) \tag{7}$$

and

$$B_i = -\frac{\int_o^L IdL}{d^2} \sin\theta \sin 2\pi f\left(t - \frac{d}{v}\right) \tag{8}$$

The voltage induced by the radiation field in a conductor parallel to the radiator and in such a position that a line joining centers of radiator and conductor is normal to both, in free space is:

$$E_r = 10^{-8} v \frac{B_r}{10}$$

$$= \frac{6.28f \int_o^L I_e dL}{d} \cdot 10^{-7} \text{ volts, effective, per meter} \tag{9}$$

Where: f = cps

I_e = effective antenna current in element L, amperes

d = distance in centimeters.

The induction voltage corresponding to Equation 9 can be obtained as follows:

The "induction" flux per centimeter length passing the conductor, or space, from zero to crest of sinusoidal wave induces the voltage per $\frac{1}{4}$ cycle (crest to zero) and is,

$$\phi_i = \int_d^{\frac{\lambda}{4}+d} B_i\, dx \tag{10}$$

$$\lambda = \frac{v}{f} \text{ cm}$$

The average voltage during this $\frac{1}{4}$ cycle is

$$e_a = 4\phi_i f \cdot 10^{-8}$$

The effective voltage is

$$E_i = \frac{\pi}{2\sqrt{2}} e_a \text{ volts per cm} \tag{11}$$

Equation 8 substituted in 10 gives

$$\phi_1 = -\frac{\int_0^L I_m\,dL}{10}\sin\theta\int_d^{\frac{\lambda}{4}+d}\frac{\sin 2\pi f\left(t-\frac{x}{v}\right)}{x^2}\,dx \qquad (10a)$$

$$v = 3\times 10^{10}\ \text{cm / sec}$$

This equation can be integrated by the sine series.

If the inducting conductor is long compared to distance d and if the current is uniform, Equation 10a becomes

$$\phi_1 = 0.2I_m\int_d^{\frac{\lambda}{4}+d}\frac{\sin 2\pi f\left(t-\frac{x}{v}\right)}{x}\,dx \qquad (10b)$$

The voltage induced in a loop of n turns, A sq cm area, in a line normal to the center of the radiator and lying in the plane of the radiator is (sides of loop in close proximity compared to λ) :

$$E_r = NA\frac{d(B_r)}{dt}\cdot 10^{-8} \qquad (12)$$

$$= NA\,4\pi^2f^2\frac{\int_0^L IdL}{vd}\sin 2\pi f\left(t-\frac{d}{v}\right)10^{-8}$$

$$= 1.31\ NA\ f^2\frac{\int_0^L I_e dL}{d}\cdot 10^{-18} \qquad (13)$$

volts effective from radiation

Also:

$$E_1 = 6.28\ NA\ f\frac{\int_0^L I_e dL}{d^2}\cdot 10^{-9} \qquad (14)$$

volts effective from induction

For a half-wave dipole in free space, with sinusoidal current distribution, the radiation term Equation 9 reduces to:

$$E_r = \frac{60\,I_e}{d}\ \text{volts per cm} \qquad (15)$$

Where: I_e = effective current at antinode, amperes,
and d = distance in centimeters.

XXIII. APPENDIX V. TABLES 1 TO 16, INCLUSIVE

Table 1. RADIO COMPASS CALIBRATION ON PORTLAND RANGE AT WASHOUGAL, WASHINGTON
Boeing 247-D No. 365; belly loop, shielded. Reference standard, gyro compass.

Gyro compass (—90°)	Radio compass	Correction
	Degrees	*Degrees*
60	153	—3
70	162	—2
80	174	—4
90	182	—2
100	194	—4
110	198	+2
120	207	+3
130	218	+2
140	229	+1
150	238	+2
160	251	—1
170	264	—4
180	277	—7
250	342	—2
260	349	+1
270	356	+4
280	9	+1
290	18	+2
300	27	+3
310	32	+8
320	45	+5
330	60	0
340	70	0
350	82	—2
360	96	—6

Table 2. AIRPLANE DISCHARGE CHARACTERISTICS, GROUND TESTS
Discharge electrode: Vertical rod 0.25 in. diameter pointed, 11 in. from concrete floor.
Polarity of ship: Negative.
Background signal: Local signal generator, 0.5.
Series discharge resistance: R = 0.
Barometer, 29.8 in.; Temperature, 60°F.; Humidity, 66%.

	Antenna of Radio Receiver			
	Lower "V"		Lower Loop, Shielded	
Kilovolts ship to ground (nominal)	Point discharge current Mu a	Relative radio noise	Point discharge current Mu a	Relative radio noise
....	8	2.40	.....	.....
30	9	2.30	9	0.51
31	10	1.80	10	0.50
32	10	1.60	10	0.51
33	11	2.20	11	0.55
34	12	3.70	12	0.50
35	13	4.50	13	0.50
36	14	2.30	14	0.70
37	15	1.40	15	0.53
38	16	1.10	16	0.56
39	16	0.90	17	0.51
40	18	0.71	18	0.50
50	30	0.52	29	0.50
60	46	0.53	44	0.50
70	64	0.55	64	0.50
80	84	0.65	85	0.50
90	110	0.90	110	0.50

Table 3. AIRPLANE DISCHARGE CHARACTERISTICS, GROUND TESTS

Discharge electrode: Vertical wire 7.5 in. long, 0.007 in. diameter, 3 in. from concrete floor.
Polarity of ship: Negative.
Background signal: Local signal generator, 0.5.
Series discharge resistance: R = 0 and R = 28 megohms.
Antenna of radio receiver: Lower "V".
Barometer, 29.8 in.; Temperature, 60°F.; Humidity, 66%.

Kilovolts ship to ground (nominal)	R = 0		R = 28 megohms	
	Point discharge current Mu a	Relative radio noise	Point discharge current Mu a	Relative radio noise
30	58.0	5.1	52	0.8
40	114.0	5.4	98	1.1
50	184.0	5.6	152	1.5
60	260.0	6.0	210	1.9
70	340.0	6.3	280	2.1
80	460.0	6.5	360	2.4
90	580.0	6.7	460	2.6
	50.0*	4.7	.....	.....
	40.0*	4.5	.....	.....
	30.0*	3.6	.....	.....
	20.0*	2.8	.....	.....
	15.0*	2.2	.....	.....
	10.0*	1.7	.....	.....
	6.5*	4.0	.....	.....
	5.0*	1.8	.....	.....

*Decaying.

Table 4. AIRPLANE DISCHARGE CHARACTERISTICS, GROUND TESTS

Discharge electrode: Vertical wire 7.5 in. long, 0.007 in. diameter, 3 in. from concrete floor.
Polarity of ship: Negative.
Background signal: Local signal generator, 0.5.
Series discharge resistance: R = 0 and R = 28 megohms.
Antenna of radio receiver: Lower loop, shielded.
Barometer, 29.8 in.; Temperature, 60°F.; Humidity, 66 %.

Kilovolts ship to ground (nominal)	R = 0		R = 28 megohms	
	Point discharge current Mu a	Relative radio noise	Point discharge current Mu a	Relative radio noise
30	60	0.61	52	0.50
40	118	0.80	96	0.50
50	188	1.10	157	0.50
60	260	1.20	210	0.50
70	340	1.40	280	0.50
80	440	1.65	360	0.50
90	560	1.80	460	0.51
	40*	0.55	.....	.....

*Decaying.

Table 5. AIRPLANE DISCHARGE CHARACTERISTICS, GROUND TESTS

Discharge electrode: Vertical wire 7.5 in. long, 0.007 in. diameter, 7.5 in. from concrete floor.
Polarity of ship: Positive.
Background signal: Local signal generator, 0.5.
Series discharge resistance: R = 0 and R = 28 megohms.
Antenna of radio receiver: Lower "V".
Barometer, 29.8 in.; Temperature, 60°F.; Humidity, 61%.

Kilovolts ship to ground (nominal)	R = 0		R = 28 megohms	
	Point discharge current Mu a	Relative radio noise	Point discharge current Mu a	Relative radio noise
30	14	0.50	15	0.5
40	28	0.54	30	0.5
50	52	0.58	51	0.9
60	80	0.59	76	1.1
70	110	0.60	104	1.5
75	127	6.20	.....	.....
80	143	7.00	134	1.8
85	164	8.50	151	2.0
90	186	9.00	166	2.3
	75*	5.00	50*	0.8
	60*	4.00	32*	0.7
	35*	3.00	21*	0.6
	22*	2.00	.....	.....
	14*	1.00	.....	.....

*Decaying.

Table 6. AIRPLANE DISCHARGE CHARACTERISTICS, GROUND TESTS

Discharge electrode: Vertical wire 7.5 in. long, 0.007 in. diameter, 7.5 in. from concrete floor.
Polarity of ship: Positive.
Background signal: Local signal generator, 0.5.
Series discharge resistance: Lower loop, shielded.
Barometer, 29.8 in.; Temperature, 60°F.; Humidity, 61%.

Kilovolts ship to ground (nominal)	R = 0		R = 28 megohms	
	Point discharge current Mu a	Relative radio noise	Point discharge current Mu a	Relative radio noise
30	15	0.5	14	0.5
40	30	0.5	30	0.5
50	52	0.5	50	0.5
60	77	0.5	74	0.5
70	108	0.5	105	0.5
75	122	0.8	.....	.....
80	145	0.9	136	0.5
85	160	1.1	150	0.5
90	180	1.2	163	0.5
	100*	0.7	.....	.....
	84*	0.6	.....	.....

*Decaying.

Table 7. HIGH-VOLTAGE DIRECT-CURRENT POINT DISCHARGE CHARACTERISTICS

Electrodes: 30-degree conical point to plane.
Spacing: 10.2 centimeters.
Polarity: Positive.
Temperature: Dry bulb: 22.3°C.; Wet bulb: 18.0°C.
Barometer: 740.4 mm. mercury.

Voltage KV DC	Current Mu a	Relative radio noise*	Type discharge
9.5	0.5	3.3	2′
11.0	1.0	3.3	2′
14.2	2.5	3.3	2′
18.5	5.0	3.3	2′
21.5	7.5	6.0	2′
24.6	10.0	13.0	2′
26.8	12.5	17.0	2′
38.5	15.0	29.0	2′
30.5	17.5	39.0	2′
32.3	20.0	52.0	2′
34.0	22.5	68.0	2′
35.4	25.0	82.0	2′
37.5	28.0	105.0	2′
38.6	30.0	123.0	2′
40.0	32.2	143.0	2′
41.5	35.0	159.0	2′
43.0	37.5	182.0	2′
44.5	40.0	200.0	2′

*Radio gain 0.307.

Table 8. HIGH-VOLTAGE DIRECT-CURRENT POINT DISCHARGE CHARACTERISTICS

Electrodes: 30-degree conical point to plane.
Spacing: 10.2 centimeters.
Polarity: Negative.
Temperature: Dry bulb: 22.3°C.; Wet bulb: 18.0°C.
Barometer: 740.4 mm. mercury.

Voltage KV DC	Current Mu a	Relative radio noise*	Type discharge
7.0	0.5	0	1′
9.0	1.0	0+	1′
12.0	2.5	1.5	1′
15.9	5.0	2.5	1′
19.5	7.5	3.5	1′
21.6	10.0	4.5	1′
24.0	12.5	4.0	1′
25.9	15.0	5.0	1′
27.5	17.5	3.5	1′
28.8	20.0	3–30	1′
30.4	22.5	2.0	1′
31.4	24.5	10–40	1′
33.2	27.5	1.0	1′
35.0	30.0	1.0	1′
36.5	32.5	1.0	1,
37.8	35.0	1.0	1′
39.0	37.5	30–150	1′
40.0	39.5	6.0	1′
41.2	42.5	10–100	1′
42.3	45.0	5.0	1′
43.8	48.5	2.0	1′
44.7	50.0	2.0	1′

*Radio gain 0.603.

Table 9. HIGH-VOLTAGE DIRECT-CURRENT POINT DISCHARGE CHARACTERISTICS

Electrodes: 45-degree conical point to plane.
Spacing: 10.2 centimeters.
Polarity: Positive.
Temperature: Dry bulb: 22.6°C.; Wet bulb: 18.0°C.
Barometer: 747.6 mm. mercury.

Voltage KV DC	Current Mu a	Relative radio noise*	Type discharge
12.0	0.5	3.0	3′
12.5	1.0	6.5	3′
14.5	2.5	16.0	3′
18.0	5.0	23.0	3′
21.6	7.5	24.5	3′
24.5	10.0	36.0	2′
26.5	12.5	52.0	2′
28.5	15.0	65.0	2′
30.0	17.5	85.0	2′
32.0	20.0	101.0	2′
34.0	22.6	124.0	2′
35.5	25.0	140.0	2′
37.0	27.5	153.0	2′
38.5	30.0	169.0	2′
40.0	32.5	182.0	2′
41.5	35.0	195.0	2′
43.0	38.0	208.0	2′
43.7	40.0	218.0	2′

*Radio gain 0.307.

Table 10. HIGH-VOLTAGE DIRECT-CURRENT POINT DISCHARGE CHARACTERISTICS

Electrodes: 45-degree conical point to plane.
Spacing: 10.2 centimeters.
Polarity: Negative.
Temperature: Dry bulb: 22.6°C.; Wet bulb: 18.0°C.
Barometer: 747.6 mm. mercury.

Voltage KV DC	Current Mu a	Relative radio noise*	Type discharge
12.5	0.5	1.0	1′
13.6	1.0	3.5	1′
15.6	2.5	8.3	1′
18.5	5.0	12.4	1′
21.2	7.5	15.7	1′
24.0	10.0	16.6	1′
26.0	13.0	16.6	1′
27.5	15.0	15.7	1′
28.5	17.5	12.4	1′
30.0	20.0	15.0	1′
31.5	22.5	16.0	1′
33.0	25.0	16.0	1′
34.6	27.5	8.2	1′
36.0	30.0	50.0	1′
37.5	32.5	8.5	1′
38.0	34.2	167.0	1′
38.5	35.0	1.5	1′
40.0	37.5	4.0	1′
41.0	40.0	100.0	1′
44.0	45.2	7.0	1′
44.5	48.0	5.0	1′

*Radio gain 0.603.

Table 11. HIGH-VOLTAGE DIRECT-CURRENT POINT DISCHARGE CHARACTERISTICS

Electrodes: 60-degree conical point to plane.
Spacing: 10.2 centimeters.
Polarity: Positive.
Temperature: Dry bulb: 23.0°C.; Wet bulb: 18.4°C.
Barometer: 757.1 mm. mercury.

Voltage KV DC	Current Mu a	Relative radio noise*	Type discharge
10.0	0.1	0	3
13.5	1.4	15.5	3
15.5	2.8	34.0	3
22.3	7.3	53.0	3
28.1	14.5	75.0	3
32.5	19.7	90.0	3
35.8	24.5	96.0	3
38.3	30.6	97.0	3
40.5	33.0	97.0	3

*Radio gain 0.307.

Table 12. HIGH-VOLTAGE DIRECT-CURRENT POINT DISCHARGE CHARACTERISTICS

Electrodes: 60-degree conical point to plane.
Spacing: 10.2 centimeters.
Polarity: Negative.
Temperature: Dry bulb: 23.0°C.; Wet bulb: 18.4°C.
Barometer: 757.1 mm. mercury.

Voltage KV DC	Current Mu a	Relative radio noise*	Type discharge
10.0	0.1	0	1′
15.5	2.0	5.5	1′
22.3	7.8	16.5	1′
28.1	17.5	25.0	1′
32.5	23.8	30.0	1′
35.8	28.8	30.0	1′
38.3	35.0	30.0	1′
40.5	37.3	40.0	1′

*Radio gain 0.603.

Table 13. HIGH-VOLTAGE DIRECT-CURRENT POINT DISCHARGE CHARACTERISTICS

Electrodes: Sharp, slender point to plane.
Spacing: 10.2 centimeters.
Polarity: Positive.
Temperature: Dry bulb: 23.8°C.; Wet bulb: 18.2°C.
Barometer: 745.1 mm. mercury.

Voltage KV DC	Current Mu a	Relative radio noise*	Type discharge
7.0	0.5	0	1
8.8	1.0	0	1
11.2	2.0	0	1
13.5	3.0	0	1
16.5	5.0	0	1
19.7	7.5	0	1
23.2	10.0	0	1
26.0	12.5	0	1
28.0	15.0	0	1
29.8	17.5	0	1
31.5	20.0	0	1
34.8	25.0	0	1
37.0	30.0	0	1
40.5	35.0	0	1
43.6	40.0	0	1

*Radio gain 1.75.

Table 14. HIGH-VOLTAGE DIRECT-CURRENT POINT DISCHARGE CHARACTERISTICS

Electrodes: Sharp, slender point to plane.
Spacing: 10.2 centimeters.
Polarity: Negative.
Temperature: Dry bulb: 23.8°C.; Wet bulb: 18.2°C.
Barometer: 745.1 mm. mercury.

Voltage KV DC	Current Mu a	Relative radio noise*	Type discharge
4.5	0.5	0	1
6.8	1.0	0	1
9.8	2.0	0	1
11.0	3.0	0	1
12.7	4.0	0+	1
14.2	5.0	0	1
16.5	7.0	1	1
18.7	9.0	5	1
20.0	10.0	2	1
22.7	12.5	0+	1
24.8	15.0	0	1
26.5	17.5	0	1
28.0	20.0	0	1
29.5	22.3	0	1
30.7	25.0	0	1
32.2	27.6	0	1
33.8	30.0	0	1
35.4	33.0	0	1
36.5	35.0	0	1
39.0	40.0	0	1
40.7	44.0	0	1
41.3	45.0	0	1
43.0	50.0	0	1
45.1	55.0	0	1

*Radio gain 1.75.

Table 15. DUDDELL OSCILLOGRAPH AMPLITUDE RESPONSE CHECK

Frequency	Duddell oscillograph	Cathode-ray oscillograph	Ratio: Duddell to C. R. response
60	4.50	2.45	1.90
H.F.*	2.00	1.00	.....
60	1.75	1.35	1.07
H.F.*	1.60	1.15	.....
60	1.75	1.25	0.97
H.F.*	3.65	2.70	.....

*DC corona discharge from 60° conical point—various voltages.

Table 16. HIGH-VOLTAGE DIRECT-CURRENT POINT DISCHARGE CHARACTERISTICS

Influence of Series Resistance and Inductance on Induced Radio Interference.

Electrodes: 50-degree conical point to plane.
Spacing: 10.2 centimeters.
Polarity: Positive.
Temperature: Dry bulb: 22.4°C.; Wet bulb: 18.1°C.
Barometer: 745.0 mm. mercury.

Voltage KV DC	Current Mu a	Relative radio noise	Discharge resistance and inductance
16.8	3.9	42.3	R = 0, L = 0
27.9	13.5	71.0	
33.5	21.0	89.0	
41.0	33.5	119.0	
16.6	3.7	11.1	R = 2 megohms L = 0
27.9	13.5	22.2	
33.7	21.0	34.5	
41.2	33.5	55.5	
16.8	4.0	4.4	R = 2 megohms L = 37.2 mh
28.0	13.5	9.4	
33.7	21.0	14.4	
41.2	33.5	26.6	

PUBLICATIONS OF THE ENGINEERING EXPERIMENT STATION

Bulletins—

No. 1. Preliminary Report on the Control of Stream Pollution in Oregon, by C. V. Langton and H. S. Rogers. 1929.
Fifteen cents.

No. 2. A Sanitary Survey of the Willamette Valley, by H. S. Rogers, C. A. Mockmore, and C. D. Adams. 1930.
Forty cents.

No. 3. The Properties of Cement-Sawdust Mortars, Plain, and with Various Admixtures, by S. H. Graf and R. H. Johnson. 1930.
Twenty cents.

No. 4. Interpretation of Exhaust Gas Analyses, by S. H. Graf, G. W. Gleeson, and W. H. Paul. 1934.
Twenty-five cents.

No. 5. Boiler-Water Troubles and Treatments with Special Reference to Problems in Western Oregon, by R. E. Summers. 1935.
Twenty-five cents.

No. 6. A Sanitary Survey of the Willamette River from Sellwood Bridge to the Columbia, by G. W. Gleeson. 1936.
Twenty-five cents.

No. 7. Industrial and Domestic Wastes of the Willamette Valley, by G. W. Gleeson and F. Merryfield. 1936.
Fifty cents.

No. 8. An Investigation of Some Oregon Sands with a Statistical Study of the Predictive Values of Tests, by C. E. Thomas and S. H. Graf. 1937.
Fifty cents.

No. 9. Preservative Treatments of Fence Posts.
1938 Progress Report on the Post Farm, by T. J. Starker, 1938.
Twenty-five cents.

No. 10. Precipitation-Static Radio Interference Phenomena Originating on Aircraft, by E. C. Starr. 1939.
Seventy-five cents.

Circulars—

No. 1. A Discussion of the Properties and Economics of Fuels Used in Oregon, by C. E. Thomas and G. D. Keerins. 1929.
Twenty-five cents.

No. 2. Adjustment of Automotive Carburetors for Economy, by S. H. Graf and G. W. Gleeson. 1930.
None available.

No. 3. Elements of Refrigeration for Small Commercial Plants, by W. H. Martin. 1935.
None available.

No. 4. Some Engineering Aspects of Locker and Home Cold-Storage Plants, by W. H. Martin. 1938.
Twenty cents.

Reprints—

No. 1. Methods of Live Line Insulator Testing and Results of Tests with Different Instruments, by F. O. McMillan. Reprinted from 1927 Proc. N. W. Elec. Lt. and Power Assoc.
Twenty cents.

No. 2. Some Anomalies of Siliceous Matter in Boiler Water Chemistry, by R. E. Summers. Reprinted from Jan. 1935, Combustion.
Ten cents.

No. 3. Asphalt Emulsion Treatment Prevents Radio Interference, by F. O. McMillan. Reprinted from Jan. 1935, Electrical West.
None available.

No. 4. Some Characteristics of A-C Conductor Corona, by F. O. McMillan. Reprinted from Mar. 1935, Electrical Engineering.
Ten cents.

No. 5. A Radio Interference Measuring Instrument, by F. O. McMillan and H. G. Barnett. Reprinted from Aug. 1935, Electrical Engineering.
Ten cents.

No. 6. Water-Gas Reaction Apparently Controls Engine Exhaust Gas Composition, by G. W. Gleeson and W. H. Paul. Reprinted from Feb. 1936, National Petroleum News.
Ten cents.

No. 7. Steam Generation by Burning Wood, by R. E. Summers. Reprinted from April 1936, Heating and Ventilating.
Ten cents.

No. 8. The Piezo Electric Engine Indicator, by W. H. Paul and K. R. Eldredge. Reprinted from Nov. 1935, Oregon State Technical Record.
Ten cents.
No. 9. Humidity and Low Temperatures, by W. H. Martin and E. C. Willey. Reprinted from Feb. 1937, Power Plant Engineering.
None available.
No. 10. Heat Transfer Efficiency of Range Units, by W. J. Walsh. Reprinted from Aug. 1937, Electrical Engineering.
None available.
No. 11. Design of Concrete Mixtures, by I. F. Waterman. Reprinted from Nov. 1937, Concrete.
None available.
No. 12. Water-wise Refrigeration, by W. H. Martin and R. E. Summers. Reprinted from July 1938, Power.
Ten cents.
No. 13. Polarity Limits of the Sphere Gap, by F. O. McMillan. Reprinted from Vol. 58, A.I.E.E. Transactions, Mar. 1939.
Ten cents.
No. 14. Influence of Utensils on Heat Transfer, by W. G. Short. Reprinted from Nov., 1938, Electrical Engineering.
Ten cents.
No. 15. Corrosion and Self-Protection of Metals, by R. E. Summers. Reprinted from Sept. and Oct., 1938, Industrial Power.
Ten cents.
No. 16. Monocoque Fuselage Circular Ring Analysis, by B. F. Ruffner. Reprinted from Jan., 1939, Journal of the Aeronautical Sciences.
Ten cents.
No. 17. The Photoelastic Method as an Aid in Stress Analysis and Structural Design, by B. F. Ruffner. Reprinted from Apr., 1939, Aero Digest.
Ten cents.

Research Papers—

(Published as indicated. Not available from the Station.)

No. 1. Electric Fish Screens, by F. O. McMillan. Bulletin of the U. S. Bureau of Fisheries, vol. 44, 1928. Also in pamphlet form, U. S. Bureau of Fisheries, Document No. 1042.
No. 2. Water Control of Dry Mixed Concrete, by G. W. Gleeson. Concrete Products, December 1929.
No. 3. High-voltage Gaseous Conductor Lamps, by F. O. McMillan and E. C. Starr. Trans. American Institute of Electrical Engineers, vol. 48, no. 1, pp. 11-18, 1929.
No. 4. The Influence of Polarity in High-voltage Discharges, by F. O. McMillan and E. C. Starr. Trans. American Institute of Electrical Engineers, vol. 50, no. 1, pp. 23-35, 1931.
No. 5. Progress Report on Radio Interference from High-voltage Transmission Lines—Pin and Pedestal Type Insulators, by F. O. McMillan. Trans. 8th annual general meeting, Engineering Section, Northwest Electric Light and Power Assoc., 1931.
No. 6. Aggregate Grading for Tamped Concrete Pipe, by G. W. Gleeson. Concrete, June 1932. Rock Products, 1932. Concrete Products, June 1932 and May-June 1934.
No. 7. Water Control of Dry Mixed Concrete, by G. W. Gleeson. Concrete Products, September 1932, and Rock Products, November 1932.
No. 8. Litharge and Glycerine Mortars, by G. W. Gleeson. Paper Trade Journal, October 13, 1932.
No. 9. Radio Interference from Insulator Corona, by F. O. McMillan. Trans. American Institute of Electrical Engineers, vol. 51, no. 2, pp. 385-391, 1932.
No. 10. The Coordination of High-voltage Transmission Lines with Radio, by F. O. McMillan. Trans. 9th annual general meeting, Engineering Section, Northwest Electric Light and Power Assoc., 1932.
No. 11. Asphalt Emulsion Reduces Insulator Radio Troubles, by F. O. McMillan. Electrical World, vol. 102, no. 6, August 5, 1933.
No. 12. Silicon, a Major Constituent of Boiler Scales in Western Oregon, by R. E. Summers and C. S. Keevil. Paper presented at annual meeting, American Society of Mechanical Engineers, 1933. Abstracts published in Mechanical Engineering, vol. 55, p. 720, November 1933; Power, vol. 77, p. 687, mid-Dec., 1933; and Power Plant Engineering, vol. 37, p. 519, December 1933, and vol. 38, p. 219, May 1934.
No. 13. Study of the Frequency of Fuel Knock Noises, by W. H. Paul and A. L. Albert. National Petroleum News, August 9, 1933.
No. 14. The Pollutional Character of Flax Retting Wastes, by G. W. Gleeson, F. Merryfield, and E. F. Howard. Sewage Works Journal, May 1934.
No. 15. Siliceous Scales in Boilers of Western Oregon and Washington, by R. E. Summers and C. S. Keevil. The Timberman, vol. 35, p. 30, May 1934.

No. 16. How Much Phosphate? by R. E. Summers. Power, vol. 78, p. 452, August 1934.
No. 17. The Carbon Dioxide-Hydrogen Ratio in the Products of Combustion from Automotive Engines, by G. W. Gleeson and W. H. Paul. National Petroleum News, September 15, 1934.
No. 18. Exhaust Gas Analysis, by G. W. Gleeson and W. H. Paul. Parts I, II, and III. National Petroleum News, September 26, October 3 and 10, 1934.
No. 19. Simplified Measurements of Sound Absorption, by A. L. Albert and T. B. Wagner. Electrical Engineering, vol. 53, no. 8, p. 1160, August 1934.
No. 20. Treatment and Recovery of Sulfite Waste, by F. Merryfield. Civil Engineering, June 1936.
No. 21. Industrial Wastes in the Willamette Valley, by F. Merryfield. Civil Engineering, October 1936.
No. 22. Flow Characteristics in Elbow Draft-Tubes, by C. A. Mockmore. Proc. American Society of Civil Engineers, vol. 63, no. 2, pp. 251-286, Feb. 1937.
No. 23. Some Simple Experiments Dealing with Rates of Solution, by G. W. Gleeson. Journal of Chemical Education, vol. 15, no. 4, April 1938.
No. 24. Heat Transfer Coefficient in Boiling Refrigerant, by W. H. Martin. Refrigerating Engineering, vol. 36, no. 3, September 1938.
No. 25. Kiln Drying Guaranteed Moisture Content Spruce Lumber, by Glenn Voorhies. West Coast Lumberman, vol. 66, no. 1, January 1939.
No. 26. Steam Demand in Drying Douglas Fir Lumber, by Glenn Voorhies. The Timberman, vol. 40, no. 4, February 1939.

THE ENGINEERING EXPERIMENT STATION STAFF

R. H. DEARBORN, Dean and Director of Engineering.
S. H. GRAF, Director of Engineering Research.
A. L. ALBERT, Communication Engineering.
F. A. EVEREST, Radio Engineering.
G. W. GLEESON, Chemical Engineering.
BURDETTE GLENN, Highway Engineering.
J. R. GRIFFITH, Structural Engineering.
E. G. MASON, Forestry.
F. O. McMILLAN, Electrical Engineering.
W. H. MARTIN, Mechanical Engineering.
FRED MERRYFIELD, Sanitary Engineering.
C. A. MOCKMORE, Civil and Hydraulic Engineering.
W. H. PAUL, Automotive Engineering.
B. F. RUFFNER, Aeronautical Engineering.
F. S. STARR, Electrical Engineering.
C. E. THOMAS, Engineering Materials.
GLENN VOORHIES, Wood Products.

Technical Counselors

R. L. BALDOCK, State Highway Engineer, Salem.
R. G. DIECK, Consulting Civil Engineer, Portland.
C. V. LANGTON, Professor of Hygiene, Oregon State College.
PAUL B. MCKEE, President, Portland Gas and Coke Company, Portland.
J. H. POLHEMUS, Executive Vice President, Portland Electric Power Company.
J. C. H. LEE, Colonel, Corps of Engineers, Division Engineer, North Pacific Division, Portland.
J. C. STEVENS, Consulting Civil and Hydraulic Engineer, Portland.
C. E. STRICKLIN, State Engineer, Salem.

Oregon State College

Corvallis

RESIDENT INSTRUCTION

Liberal Arts and Sciences
- The Lower Division (Junior Certificate)
- School of Science (B.A., B.S., M.A., M.S., Ph.D. degrees)

The Professional and Technical Curricula
- School of Agriculture (B.S., M.S., Ph.D. degrees)
- School of Education (B.A., B.S., B.S. in Ed., M.A., M.S., Ed.M., Ed.D. degrees)
- School of Engineering and Industrial Arts (B.S., M.S., Ch.E., C.E., E.E., M.E. degrees)
- School of Forestry (B.S., M.S., M.F., F.E. degrees)
- School of Home Economics (B.A., B.S., M.A., M.S. degrees)
- School of Pharmacy (B.S., M.S. degrees)
- Secretarial Science (B.S.S. degree)

The Graduate Division (M.A., M.S., Ed.M., M.F., Ch.E., C.E., E.E., F.E., M.E., Ed.D., Ph.D. degrees)

The Summer Sessions

The Short Courses

RESEARCH AND EXPERIMENTATION

The General Research Council

The Agricultural Experiment Station—
- The Central Station, Corvallis
- The Union, Moro, Hermiston, Talent, Burns, Astoria, Hood River, Pendleton, Medford, and Squaw Butte Branch Stations

The Engineering Experiment Station, Corvallis

EXTENSION

Federal Cooperative Extension (Agriculture and Home Economics)

General Extension Division